# Investigating novel therapies for brain tumors - the roles of MCT4, cellular senescence, and arsenic trioxide treatment

**by**

**Kah Suan Lim**

A dissertation submitted to the Johns Hopkins University

in conformity with the requirements of the degree of

Doctor of Philosophy

Baltimore, MD

October 2013

## ABSTRACT

My studies focused on characterizing signaling and metabolic pathways involved in the pathobiology of brain tumors in order to develop improved therapies. One project was centered on investigating oncogenic KIAA1549-BRAF fusion induced senescence as a growth suppressive mechanism in pilocytic astrocytoma. We found that loss of expression of tumor suppressor $p16^{INK4a}$ lead to significantly decreased survival in pilocytic astrocytoma patients. Another major focus was on metabolic targeting in glioblastoma cells. We found that the monocarboxylate exporter MCT4 was specifically upregulated under hypoxic conditions in glioblastoma cells, and its overexpression was significantly linked to survival. Silencing MCT4 in glioblastoma neurospheres led to decreased growth *in vitro* and *in vivo*, inhibition of clonogenic capacity, and reductions in CD133-positive stem-like tumor cells. This was partially due to an induction of apoptosis. Interestingly, we found that this apoptotic induction and growth inhibition was not due to lack of lactate export, but instead, due to an inhibition of the HIF response, highlighting the importance of aberrant metabolic regulation in cancer. Finally, we investigated the possibility of targeting Notch and Hedgehog signaling simultaneously in glioblastoma neurospheres using arsenic trioxide. We found that aberrant Notch and Hedgehog pathway signaling was decreased following arsenic trioxide treatment, and this decrease was accompanied by decreased neurosphere growth and proliferation, decreased clonogenic capacity, decreased CD133-positive cells, and increased apoptosis. These studies thus identify mechanisms by which several hallmarks of cancer are altered in brain tumors, and our preclinical data suggest some potential therapeutic applications. However, it is important to note that targeting only one or two hallmark changes in

cancer often leads to therapeutic resistance, and multimodal therapies will likely be necessary if we are to cure aggressive brain tumors.

**Thesis Advisors and Readers:**

Charles G. Eberhart, MD, PhD, Professor of Pathology, Ophthalmology and Oncology, Johns Hopkins University School of Medicine

Eli E. Bar, PhD, Assistant Professor of Medicine and Pathology, Johns Hopkins University School of Medicine

**Thesis Committee:**

Gregory Riggins, MD, PhD, Professor of Neurosurgery and Oncology, Irving J. Sherman Research Professor, Johns Hopkins University School of Medicine

Gregg L. Semenza, MD, PhD, Professor of Pediatrics, Medicine, Oncology, Radiation Oncology, Biological Chemistry, Director, Vascular Program, Institute for Cell Engineering, Johns Hopkins University School of Medicine

## ACKNOWLEDGEMENTS

Graduate school had been an amazing five and a half years, full of ups and downs, but its an experience I will never trade for anything else. It would have been impossible for me to make it to the end without the incredible support of friends, co-workers and mentors, and for that I am extremely grateful.

First of all, I have to thank my undergraduate research mentors Axel for giving me the opportunity to work in his lab where I had my first exposure to research, and Han Kiat for teaching me various experimental techniques and for encouraging me to apply to graduate school in Hopkins. I am also very grateful to Margaret Lee and Al Njoo, for their generosity and kindness, for without their support, I would not have been able to get here.

I also have to thank the amazing support staff in Pathobiology and Neuropathology, Wilhelmena, Nancy, Tracie, Elaine, Argie and Carole for making the journey to Johns Hopkins smooth, and for making the administrative part of graduate school relatively stress-free; Dr. Rose and Dr. Gabrielson for taking such great care of the students, keeping track of both our academic and personal wellbeing.

My thesis committee members, Charles, Eli, Dr. David Berman, Dr. Chi Dang, Dr. Gregg Semenza and Dr. Greg Riggins, have also been greatly helpful in providing suggestions and scientific recommendations for my thesis, and without them, this work could never have been completed.

My fellow labmates in the Eberhart lab, past and present, had always been a great source of support and companionship. In particular, labmates I have spent long hours in

the lab with, Mike Coonfield, Kah Jing, Ann, Qian, Sam, Allison, Will, Sama, Karisa, Harpreet and Laura, together, they have made long hours in the tissue culture room and unpacking delivery boxes a lot more fun. Another constant presence in the lab, Barb Reiss, has been very helpful in all sorts of lab and thesis related administrative work, and being able to hear her signature laughter in the morning always gives a bright start to the day.

My mentors in graduate school, Charles and Eli, had been incredible sources of knowledge and support, always giving me suggestions for my projects and being respectful and encouraging towards my ideas. More importantly, they have taught me about integrity in research and humility and patience towards others. Through their selfless mentorship over the years, my scientific knowledge and thinking has matured greatly, and I am now ready to move on to the next stage of my career in academia.

Last but not least, I have to thank my family, and my boyfriend Weijie. They have been very supportive and encouraging throughout this journey. It had been a difficult decision, moving halfway across the globe to pursue my dreams, and without my family being so understanding and encouraging, I would not have been able to do it. Weijie had been a great source of support and companionship for the past three years, and going through graduate school with him by my side had made everything a lot more manageable and less stressful. And for that, I am very grateful.

Graduate school had been a steep learning curve, but also an incredible experience. I am extremely fortunate to have to love and support of so many people, and it is through their help that I am where I am today. This thesis is an acknowledgement to everything they had done to help me get here.

**TABLE OF CONTENTS**

## LIST OF FIGURES

## LIST OF TABLES

# Chapter 1: Introduction

According to the National Library of Medicine, “Cancer is the uncontrolled growth of abnormal cells in the body.” The earliest known existence of cancer had been documented in a dinosaur, a fossilized extraskeletal osteosarcoma in the brain. While it is unknown if the dinosaur had died directly from the brain tumor, it had caused severe debilitation from multiple broken bones that were thought to have resulted from the tumor affecting mobility. In humans, the first recorded documentation of cancer came from the ancient Egyptians, about 4500 years ago, by a physician called Imhotep. Due to the lack of knowledge of cellular existence then, it was thought that cancer resulted from a fluid, or humor, imbalance.

In the past century, knowledge about this deadly disease has increased tremendously. Our understanding of cancer as a disease has been summarized in a seminal review, "Hallmarks of Cancer" by Douglas Hanahan and Robert Weinberg(Hanahan and Weinberg). In it, some of the classical characteristics of cancer listed include sustaining proliferative signaling, evading growth suppressors, activating invasion and metastasis, enabling replicative immortality, inducing angiogenesis, evading cell death, deregulated cellular energetic and avoiding immune destruction.

Sustained proliferative signaling is one of the most important characteristic of tumor cells. In normal cells, proliferation is governed by strict and precise control of growth signals and different stages of the cell cycle. In contrast, in tumor cells, one or more of these signals and cell cycle processes are dysregulated, leading to uncontrolled proliferation. Some of the commonly aberrant pathways include developmental pathways such as Notch and Hedgehog. As a result, Notch and Hedgehog targeting is an attractive

therapeutic target in cancer(Fan, Khaki et al. ; Hu, Zheng et al. ; Wang, Wakeman et al. ; Purow, Haque et al. 2005; Shih and Holland 2006; Bar, Chaudhry et al. 2007; Clement, Sanchez et al. 2007; Ehtesham, Sarangi et al. 2007; Kanamori, Kawaguchi et al. 2007; Zhang, Zheng et al. 2008; Sarangi, Valadez et al. 2009).

The flip side to the coin is that too much oncogenic signaling can sometimes lead to cellular senescence. It had been demonstrated that some oncogenes upregulating proliferative signaling lead to a burst of proliferative activity in cells, then tumor suppressive mechanisms get activated and induce cellular senescence. Thus, there is likely a delicate balance in the levels of proliferative signaling that allows tumorigenesis without activating cellular tumor suppressive defence systems. It had also been found that in some tumors with activated oncogenes, the tumor suppressors that commonly get activated in response to upregulation of proliferative signaling had been silenced or lost, highlighting another mechanism by which tumor cells evade cellular growth control.

In addition to the 6 original hallmarks of cancer identified by Hanahan and Weinberg in their first "Hallmarks of Cancer" review, 2 emerging hallmarks and 2 enabling characteristics for tumorigenesis were added in this update(Hanahan and Weinberg). One of the emerging hallmarks highlighted in the review by Hanahan and Weinberg is deregulated cellular energetics. In response to the increased cellular proliferation in tumors, energetic requirements are also dramatically reprogrammed. Energetic pathways within the cells, such as glycolysis and the Citric Acid Cycle, are important in generating cellular building blocks such as phospholipids and amino acids, in addition to producing ATP. While under aerobic conditions in normal cells, carbon from glucose typically goes through glycolysis, the Citric Acid Cycle and finally oxidative phosphorylation in order

to generate ATP, in tumor cells, carbon gets shunted from glycolysis and the Citric Acid Cycle into pathways generating cellular building blocks. This creates a paradoxical aerobic glycolytic phenomenon that had first been described by Otto Warburg(Warburg, Wind et al. 1927; Warburg 1956; Warburg 1956). Clearly, cancer cells have an arsenal of adaptive metabolic changes that they have evolved to enable this aerobic glycolysis, allowing them to have unfettered proliferation.

In the next few sections, we will be discussing subsets of some of these tumorigenic mechanisms reviewed by Hanahan and Weinberg, specifically oncogene-induced senescence in the context of pediatric low-grade gliomas, targeting aberrant metabolic signaling in high-grade glioblastoma, and co-targeting of developmental pathways Notch and Hedgehog in glioblastoma stem-like cells.

### 1.1 Oncogene-induced senescence

Oncogenes are hyperactivated variants of proto-oncogenes, thought to result in uncontrolled cellular proliferation and ultimately, cancer. Recent findings by a few different groups however, disputed this. Manuel Serrano, Scott Lowe and colleagues had found that when they attempted to transform fibroblasts using oncogenic Ras alone, instead of becoming immortalized, the fibroblasts senesced. This was accompanied by overexpression of tumor suppressors p53 and $p16^{INK4a}$. When they silenced the tumor suppressors together with adding oncogenic Ras, the cells became immortalized(Serrano, Lin et al. 1997). Chrysiis Michaloglou, Daniel Peeper and colleagues had a similar observation where they introduced oncogenic $BRAF^{V600E}$ into human melanocytes and found that the cells exhibited signs of senescence. They also found that the oncogenic $BRAF^{V600E}$, frequently found in melanoma tumors, was also found in benign naevi, and

these naevi express senescence markers(Michaloglou, Vredeveld et al. 2005). The model that was put forth based on these observations describes the first oncogenic hit giving rise to dramatic induction of proliferative signaling, resulting in a proliferative burst. However, this quickly turns on growth inhibitory mechanisms controlled by tumor suppressors such as p53 and $p16^{INK4a}$, and upregulation of these tumor suppressors in turn lead to cellular senescence. Since this senescent phenotype is independent of telomere shortening, seen in replicative senescence, it was termed oncogene-induced senescence.

Pilocytic astrocytomas the most common pediatric brain tumors. They are low grade, with indolent growth, however significant morbidity results from its location and age of onset. In 2008, several groups including ours identified a novel oncogenic BRAF fusion gene in pediatric pilocytic astrocytomas(Bar, Lin et al. 2008; Jones, Kocialkowski et al. 2008; Sievert, Jackson et al. 2009). It was found that a fusion gene involving both BRAF and KIAA1549 resulted in the formation of a chimeric protein where the regulatory portion of BRAF is replaced by KIAA1549 leading to constitutive activation. In addition to the KIAA1549-BRAF fusion, which consists of half or more of all pilocytic astrocytoma tumors, other MAPK pathway activating mutations in BRAF and RAS had also been identified in pilocytic astrocytomas, including $BRAF^{V600E}$. It is thus believed that MAPK pathway hyperactivation might be important in pilocytic astrocytoma pathogenesis.

Interestingly, pilocytic astrocytoma tumors can be very indolent and sometimes even spontaneously regress(Sakai, Miyahara et al. ; Gunny, Hayward et al. 2005). This led us to draw parallels between pilocytic astrocytoma that have the oncogenic MAPK pathway

activating mutations and benign naevi with oncogenic $BRAF^{V600E}$ mutation. We wondered if the slow growth of pilocytic astrocytoma tumors could be due to oncogene-induced senescence. To test this, we attempted to clone the 7kb KIAA1549-BRAF fusion and transduce normal human astrocytes with it. Unfortunately, we found that the fusion protein was expressed at extremely low levels even when coupled to a CMV promoter in 293T cells. Additionally, due to the length of the fusion gene, we had trouble packaging it into a lentiviral construct for viral transduction of normal human astrocytes.

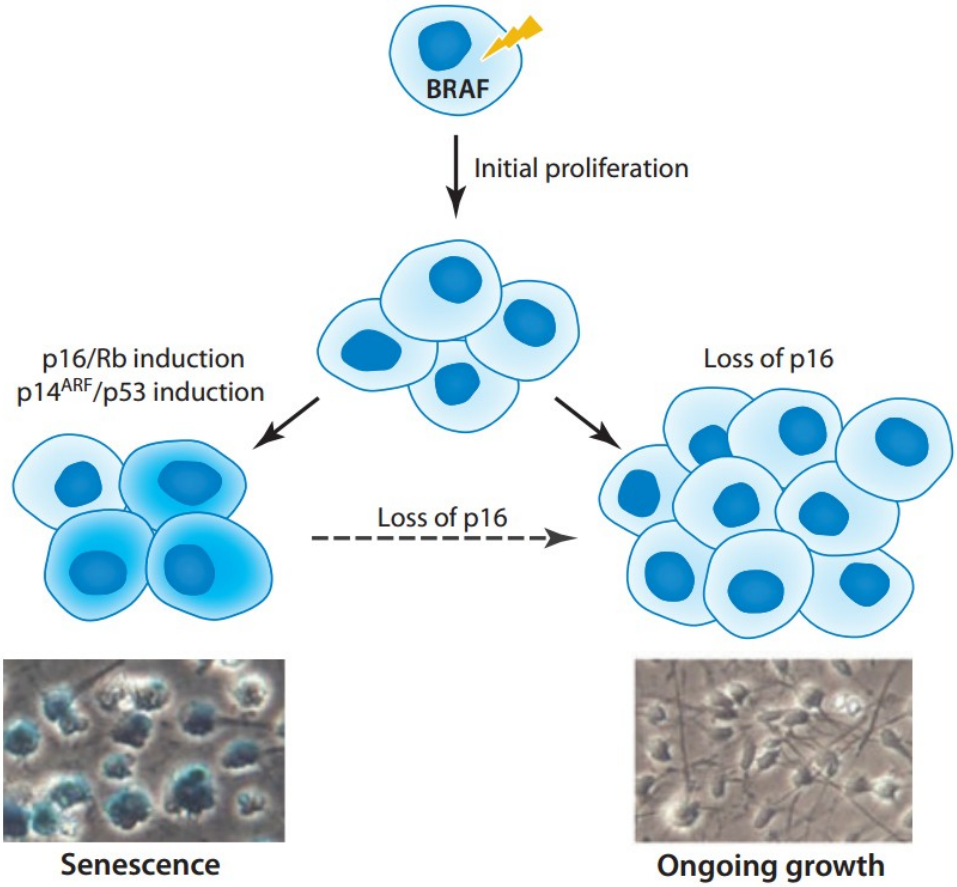


**Figure 1-1. Schematic showing different growth characteristics of pilocytic astrocytoma cells with or without $p16^{INK4a}$**

After BRAF is mutated, there is an initial proliferation followed by oncogene-induced senescence (bottom left picture). If $p16^{INK4a}$ is lost, cells do not senesce and growth continues (bottom right picture).

As a result, we utilized 2 other model systems to investigate this: 1. Short term cultures of pilocytic astrocytomas using freshly resected tumors mechanically dissociated into single cells. 2. Normal fetal astrocytic neurospheres transduced with $BRAF^{V600E}$ viral construct, another activating BRAF mutation that had been identified in ~5% of pilocytic astrocytomas. We saw that in both model systems, senescence-associated beta-galactosidase staining was intense compared to control. We also found that in patients with primary pilocytic astrocytoma tumors, the majority had $p16^{INK4a}$ overexpression, another marker of oncogene-induced senescence, and in the few patients whose tumors do not express $p16^{INK4a}$, survival was significantly lower. We thus came up with a model for pilocytic astrocytoma pathogenesis where the initial hit activating MAPK pathway results in a proliferative burst, giving rise to pilocytic astrocytoma tumors, but p53 and $p16^{INK4a}$ quickly get upregulated, resulting in senescence. In the rare occasion that $p16^{INK4a}$ is lost or silenced, growth continues, resulting in more aggressive tumors (Figure 1 and Chapter 2).

## 1.2 Metabolic deregulation in cancer

### *1.2.1 Aerobic glycolysis*

Otto Warburg first described the aerobic glycolysis that is now a well-accepted trademark of cancer cells in 1930. It was thus termed the Warburg Effect. While preferentially utilizing glycolysis instead of oxidative phosphorylation for ATP generation might appear to be counterintuitive, as the proportion of ATP molecules produced per molecule of glucose is much lower in glycolysis alone compared to oxidative phosphorylation, aerobic glycolysis had in fact been observed in other proliferative phenotypes such as

during embryogenesis. This suggests that aerobic glycolysis might be advantageous to rapidly proliferating cells. One widely accepted hypothesis states that while glycolysis might be energetically inefficient, intermediates of glycolysis feed into several pathways that generate cellular building blocks such as nucleosides and lipids(Potter 1958; Vander Heiden, Cantley et al. 2009). As a result, upregulating glycolysis is actually advantageous to rapidly proliferating cells as it provides cells with the materials required for growth.

### *1.2.2 Hypoxic metabolism in tumors*

In addition to aerobic glycolysis, many aggressive tumors harbor hypoxic regions. It had been found that hypoxic metabolism is advantageous to tumor growth, potentially due to the upregulation of glycolysis, similar to the Warburg Effect. In addition, several groups including ours had found that many different types of tumors including glioblastomas thrive under a hypoxic environment and are highly addicted to HIF1alpha for survival(Bar, Lin et al. ; Wong, Gilkes et al. ; Wong, Zhang et al. ; Heddleston, Li et al. 2009; Li, Bao et al. 2009; Pistollato, Chen et al. 2009; Soeda, Park et al. 2009). While this might appear to be counterintuitive, our group also found that hypoxia induces a stem-like phenotype in glioblastoma neurosphere cells, making them significantly more clonogenic *in vitro*, with larger and more numerous clones, and more aggressive *in vivo*. This stem-like phenotype is mediated by HIF1alpha and downregulation of HIF1alpha inhibited tumor growth and stem-like characteristic. HIF1alpha is thus an important microenvironmental mediator in tumors and an attractive therapeutic target. In fact, recent data obtained from studies in breast and glioblastoma tumor xenografts suggest that the reason why anti-angiogenic agents fail to work in certain tumor types could be due to the increase in intratumoral hypoxia leading to both increased stemness and

induction of cytoprotective autophagy(Conley, Gheordunescu et al. ; Hu, DeLay et al.). This also underscores the importance of fully understanding tumor biology in drug design.

Following our finding that HIF1alpha mediates hypoxic tumor cell survival and stem-like characteristics in tumors, we performed a microarray screen looking at genes that are specifically upregulated by hypoxia to identify downstream targets of HIF1alpha important for glioblastoma cell survival. We identified MCT4 (monocarboxylate transporter 4), as one of the top upregulated genes under hypoxia. We found that MCT4 is overexpressed in aggressive tumors and correlated with decreased survival. Using loss of function studies, we found that MCT4 is important in glioblastoma cell survival both *in vivo* and *in vitro* and depletion of MCT4 led to loss of stem-like characteristics in glioblastoma cells. Interestingly, we found that HIF1alpha signaling was downregulated following MCT4 inhibition, potentially via a feedback mechanism. This can potentially explain why MCT4 silencing lead to inhibition of growth and stemness, since HIF1alpha signaling is involved in the growth and stemness of glioblastoma cells as we had previously established.

## 1.3 Proliferative signaling mediated by Notch and Hedgehog signaling

### *1.3.1 Notch and Hedgehog signaling mediates growth and stem-like characteristics in tumor cells*

Notch and Hedgehog signaling pathways are important for embryogenesis and developmental patterning, but are usually not present in terminally differentiated cells.

Notch and Hedgehog signaling had been found to be aberrantly activated in the stem-like cells of several tumor types including glioblastomas, suggesting that activation of these developmental signaling pathways in differentiated cells might allow them to revert back to a stem-like state(Berman, Karhadkar et al. 2003; Pasca di Magliano and Hebrok 2003; Thayer, di Magliano et al. 2003; Liu, Dontu et al. 2006; Peacock, Wang et al. 2007; Shih Ie and Wang 2007; Zhang, Zheng et al. 2008). Our group and others had found that when Notch or Hedgehog signaling is silenced, glioblastoma cell growth is inhibited. However, we also found that when Notch signaling is inhibited in glioblastoma cells, Hedgehog pathway proteins are upregulated, suggesting that there might be some redundancy in developmental pathway signaling during tumorigenesis(Schreck, Taylor et al.). As a result, therapeutic targeting of either pathway alone had been met with limited success.

### *1.3.2 Co-targeting of Notch and Hedgehog signaling in glioblastoma cells*

Arsenic trioxide (ATO), a drug that is FDA approved to treat a form of leukemia known as acute promyelocytic leukemia, had been found separately to inhibit Notch and Hedgehog signaling in several different tumor types including gliomas(Kim, Aftab et al. ; Zhen, Zhao et al. ; Chen, Zhu et al. 1996; Shen, Chen et al. 1997). ATO as a therapeutic agent might therefore be superior to single-pathway targeting agents in preventing resistance. We were thus interested in using ATO to target both Notch and Hedgehog signaling in glioblastoma.

We found that when we treated glioblastoma tumor cells with ATO, cell growth was significantly inhibited. In addition, we found that apoptosis was induced and proliferation decreased, pointing to possible cellular mechanisms of growth inhibition. We found that

both Notch and Hedgehog pathway targets were decreased following ATO treatment, indicating an inhibition of both pathways by ATO. Importantly, we also observed an inhibition of stem-like characteristics following ATO treatment, including a decrease in the percentage of CD133-positive cells and a decrease in the number and size of colonies formed when a clonogenic assay was performed. This decrease in stem-like characteristics is congruent with the role of Notch and Hedgehog pathways in maintaining the stem-like potential in tumor cells, and might explain the mechanistic reason behind growth inhibition following ATO treatment (Chapter 5).

From the above examples, we can see that following decades of extensive research by cancer researchers, several hallmarks of cancer had been identified, and all of them are important for tumorigenesis and survival of tumor cells. Different tumor types exhibit different levels of sensitivity to targeting each of these hallmarks, and in each of the following chapters, we will describe in detail how we investigated oncogene-induced senescence in the context of pediatric low-grade astrocytomas, targeted deregulated energetic signaling in high-grade glioblastoma, and co-targeted Notch and Hedgehog signaling pathways in glioblastomas using ATO.

# Chapter 2: BRAF Activation Induces Transformation and then Senescence in Human Neural Stem Cells: A Pilocytic Astrocytoma Model

Eric H. Raabe[1*], Kah Suan Lim[2], Julia M. Kim[3], Alan Meeker[2], Xing Gang Mao[2], Guido Nikkhah[4], Jarek Maciaczyk[5], Ulf Kahlert[4], Deepali Jain[2], Eli Bar[2], Kenneth J. Cohen[1], Charles G. Eberhart[2*]

**Authors' Affiliations:**

[1] Division of Pediatric Oncology [2] Department of Pathology [3] Department of Pediatrics and Adolescent Medicine Johns Hopkins University School of Medicine 720 Rutland Ave - Ross Building 558 Baltimore, MD 21205

[4] Department of Stereotactic and Functional Neurosurgery [5] Department of General Neurosurgery Neurocenter University Hospital Freiburg Breisacher Str. 64 D – 79106 Freiburg, Germany

**Financial Support:**

CGE: PLGA Foundation, Children's Cancer Foundation, Pilocytic/Pilomyxoid Astrocytoma Fund, Lauren's First and Goal EHR: St. Baldrick's Foundation Fellowship JM and GN: Comprehensive Cancer Center Freiburg

**Acknowledgement:** We thank Donata Maciaczyk for her excellent technical support

*** Corresponding Authors**

Charles Eberhart 720 Rutland Ave – Ross Bldg 558 Baltimore, MD 21205 ceberha@jhmi.edu

Eric Raabe 720 Rutland Ave – Ross Bldg 558 Baltimore, MD 21205 eraabe2@jhmi.edu

Statement of Translational Relevance

BRAF and the MAPK signaling cascade are active in the majority of pilocytic astrocytoma, but the oncogenic effects of these hallmark molecular changes are poorly understood. Using neurospheres derived from normal human fetal cortex, we found that early increases in anchorage-independent growth after BRAF activation were followed by proliferation arrest and induction of cellular senescence. We also detected the senescence markers acidic beta-galactosidase and $p16^{INK4a}$ in pilocytic astrocytoma samples. Patients whose tumors lacked $p16^{INK4a}$ protein had significantly shorter survival. Immunohistochemical analysis of $p16^{INK4a}$ may therefore aid in therapeutic stratification. The findings presented here suggest that the indolent growth of pilocytic astrocytoma may be due to oncogene-induced senescence, similar to what is observed in melanocytic nevi. Failure to induce senescence, or the tumor's escape from senescence, may result in more aggressive tumor biology. Understanding the regulation of oncogene-induced senescence may help develop more effective treatments for pediatric low-grade gliomas.

**Abstract**

**Purpose:** BRAF is frequently activated by gene fusion or point mutation in pilocytic astrocytoma, the most common pediatric brain tumor. We investigated the functional effect of constitutive BRAF activation in normal human neural stem and progenitor cells to determine its role in tumor induction in the brain.

**Experimental Design:** The constitutively active $BRAF^{V600E}$ allele was introduced into human neurospheres, and its effects on MAPK signaling, proliferation, soft agarose colony formation, stem cell phenotype and induction of cellular senescence were assayed. Immunohistochemistry was used to examine $p16^{INK4a}$ levels in pilocytic astrocytoma.

**Results:** $BRAF^{V600E}$ expression initially strongly promoted colony formation, but did not lead to significantly increased proliferation. $BRAF^{V600E}$ expressing cells subsequently stopped proliferating and induced markers of oncogene-induced senescence including acidic beta-galactosidase, PAI-1 and $p16^{INK4a}$, while controls did not. Onset of senescence was associated with decreased expression of neural stem cell markers, including SOX2. Primary pilocytic astrocytoma cultures also showed induction of acidic beta-galactosidase activity. Immunohistochemical examination of 66 pilocytic astrocytomas revealed $p16^{INK4a}$ immunoreactivity in the majority of cases, but patients with tumors negative for $p16^{INK4a}$ had significantly shorter overall survival.

**Conclusions:** BRAF activation in human neural stem and progenitor cells initially promotes clonogenic growth in soft agarose, suggesting partial cellular transformation, but oncogene-induced senescence subsequently limits proliferation. Induction of senescence by BRAF may help explain the low grade pathobiology of pilocytic

astrocytoma, while worse clinical outcomes associated with tumors lacking p16$^{INK4a}$ expression could reflect failure to induce senescence or an escape from oncogene-induced senescence.

## 2.1 Introduction

Pilocytic astrocytoma is the most common childhood brain tumor (1). It often follows an indolent course, with waxing and waning growth kinetics and some cases of spontaneous regression reported (2, 3). Tumors frequently respond to treatment with chemo or radiation therapy, but they can re-grow after a period of quiescence, requiring further therapy (2, 4). Several laboratories have identified constitutive activation of the RAS/RAF pathway as the primary molecular alteration in pilocytic astrocytoma (5-11). The most common alteration is a tandem duplication at chromosome 7q34 involving BRAF, an upstream regulator of the MAP kinase pathway. In most cases, the regulatory domain of BRAF is lost, and the catalytic domain is fused to KIAA1549, causing constitutive activation of downstream signaling, as measured by ERK activation (8, 12). A subset of pilocytic astrocytoma lacking the KIAA1549:BRAF fusion instead contain mutations at BRAF codon 600 resulting in a single amino acid substitution ($BRAF^{V600E}$) that also constitutively activates the kinase (6, 7, 9, 10, 12, 13). Finally, point mutations in KRAS, fusions involving RAF1 or small insertions activating BRAF have been identified in rare cases (5, 7, 11, 14).

Activation of BRAF in melanocytic nevi and melanoma has been associated with a process known as “oncogene-induced senescence”, in which an inciting oncogenic stimulus also limits neoplastic growth via induction of cellular senescence (15). The mechanisms by which BRAF activation leads to transformation of neural cells into pilocytic astrocytomas are not yet clear, but their often indolent growth pattern suggests that oncogene-induced senescence may play a role. To address this, we used human neural stem and progenitor cells isolated from first trimester fetal autopsy specimens and

grown in long-term culture (16, 17) to examine the effects of BRAF activation on cells from which pilocytic astrocytoma are thought to arise (18). We found that expression of $BRAF^{V600E}$ in neurospheres derived from cerebral cortex initially promoted colony formation in soft agar, but the cells subsequently became senescent, with increased expression of acidic beta-galactosidase, PAI-1 and $p16^{INK4a}$. This suggests that growth of pilocytic astrocytoma may be regulated in part by the induction of senescence.

## 2.2 Methods

Neurosphere cell culture

Cells were obtained from first trimester human fetal autopsy specimens in concordance with German law and Ethics Board evaluation. The study was also approved by the Johns Hopkins Institutional Review Board. Cells from cerebral cortex were microdissected and processed as described previously (19), then passaged in neurosphere media (30% Ham's F12 media, 70 % DMEM, 5% B27 reagent (Invitrogen), 1% L-glutamine, 1% antibiotic-antimycotic, 5 micrograms/ml heparin, 20 ng/ml FGF, and 20 ng/ml EGF. Cells were split at high density after incubation with Accutase (Sigma-Aldrich) and gentle trituration.

DNA constructs and viral infection

The construct encoding $BRAF^{V600E}$ was purchased from Addgene (Cambridge, MA) (Addgene plasmid 15269) (20). The $BRAF^{V600E}$ cDNA was subcloned into the lentiviral vector pWPI (Addgene plasmid 12254 – constructed originated by Didier Trono). Lentiviral particles were produced by transfecting 293T cells with VSVG envelope plasmid, delta 8.9 gag/pol plasmid and the plasmid of interest, as described previously, (21) using Fugene (Roche) per the manufacturer's instructions. After 24 hours, the media was changed to FGF/EGF neurosphere media, and supernatants were collected at 48 and 72 hours. These supernatants were pooled and passed through a 0.45 micron filter, then frozen at -80 C until needed. Human neural stem and progenitor cells growing as neurospheres were triturated to small sphere size, and then incubated with lentiviral supernatants in the presence of Polybrene for 24 hours. After approximately one week in

culture, spheres were able to be identified, and they were then individually placed into wells of a 24-well plate. Spheres were visually scored for GFP-positivity. Control cells were infected with pWPI empty vector, which constitutively expresses GFP. These cells were found to proliferate and behave identically to uninfected parental cells, and both parental and GFP cells were used as controls.

Establishment of pilocytic astrocytoma primary culture

Pilocytic astrocytoma primary cultures were established following the protocol previously described for primary glioblastoma cultures (22, 23). Freshly resected pilocytic astrocytoma tumors were placed into basal medium and dissected into 1 $mm^3$ sections. Tumor sections were then placed in papain solution (Sigma-Aldrich) and incubated at 37 degrees for 15 minutes. Dissociated tissue was passed through a Pasteur pipette several times then centrifuged and washed once with 10% serum-containing DMEM/F12. Cells were then plated in serum-containing DMEM/F12 media in tissue culture flasks.

Assays of cell proliferation, senescence and telomere length

BrdU assays were performed as described previously (24). Cells were cytospun on to positively charged slides. After washing cells once with PBS, they were fixed with 4% paraformaldehyde for 15 minutes, permeabilized with 0.1% Triton/PBS, denatured with 0.1N HCl, washed in PBST, and then blocked with 5% normal goat serum/PBST or 5% BSA/PBST, and incubated with the appropriate primary antibody. Anti-BrdU antibody was used as per the manufacturer's directions (Sigma B2531) at 1:100 dilution. After

washing three times with PBST, cells were incubated for 45 minutes in the dark with the appropriate Cy-2 or Cy-3 conjugated secondary antibody (Jackson Immunoresearch). Cells were counterstained with DAPI and mounted with anti-fade (Vectastain) and visualized as described below.

Acidic beta-galactosidase staining was performed as per the manufacturer's instructions (Cell Signaling Technology kit #9860). Human neurosphere cells were plated on Matrigel-coated 24-well plates and incubated at 37°C for 48 hours to allow cells to extend processes prior to staining. Cells were then washed with PBS and fixed with fixing solution. After 15 min, fixative was removed and cells were washed twice with PBS then incubated with staining solution. After staining, cells were washed with PBS and covered with 70% glycerol and photographed by inverted light microscopy.

Fluorescent In-Situ Hybridization (FISH) determination of telomere length in GFP compared to $BRAF^{V600E}$ infected cells was performed as previously described using cytospun cells (25).

Western blotting

Western blotting was performed as described (24). Antibodies were used as per the manufacturer's instructions and were as follows: BRAF (Santa Cruz # SC-1660), $p16^{INK4a}$ (Santa Cruz #SC-56330), SOX-2 (Santa Cruz #SC-17320), OLIG2 (Millipore AB9610), NESTIN (Millipore MAB 5326), GAPDH (Research Diagnostics #10R-G109a), ERK (Cell Signaling Technologies #9102), phospho-ERK (Cell Signaling Technologies #4376). Blots that have had intervening lanes removed are clearly marked with a white vertical line.

Colony formation in soft agarose

A 2X concentration of the neurosphere media was prepared and mixed 1:1 with 1 percent melted agarose (Invitrogen) in water to make bottom agar, which was used to coat each well of a 6-well plate. Cells were incubated in Accutase (Sigma) and triturated by pipetting through a P1000 pipette to single cell density and placed into the top agarose media/soft agarose mixture (0.5 %) and immediately plated into 6-well plates at a density of 20,000 cells/well in 1.5ml of agarose. After the agarose polymerized, 2 ml of normal growth media was placed into each well. Media was changed every 7 days, and the cultures were incubated for 4 to 6 weeks. Colonies were visualized by staining with 0.005% cresyl violet in PBS for three hours at room temperature. Colonies greater than 50 microns in diameter were scanned and counted using MCID Elite software (Cambridge, England, UK).

Clinical specimens

Pilocytic astrocytoma and control tissues were obtained from the Johns Hopkins University School of Medicine Department of Pathology, with institutional review board approval. All cases from 1990 to 2009 were reviewed in order to confirm the diagnosis of pilocytic astrocytoma, and to determine if sufficient material was still present in the paraffin block to use in the construction of a tissue microarray. All cases which met these criteria (a total of 77) were included in the study. One older case (from 1988) and two grade two pediatric infiltrating astrocytomas were included in the array to yield a total of 80 tumors, but the infiltrating astrocytomas were not included in the analyses described in this paper. Tumor classification and cellularity were independently confirmed by two

neuropathologists (DJ and CGE). No tumors were of the pilomyxoid variant. The tissue array was constructed as previously described (26) with 4 cores 0.6 mm in diameter taken from each tumor. Consistent with recently published reports, for purposes of data analysis tumor location in the hypothalamus, optic chiasm, thalamus, and brainstem was designated as unfavorable, while all other locations including cerebellum/posterior fossa, cerebral cortex, spinal cord, optic nerve and fornix were considered favorable (27, 28). Of the 78 tumor samples, 66 were from primary tumor resections and had sufficient material to be scored for $p16^{INK4a}$ immunohistochemistry.

Immunohistochemistry

Sections from the pilocytic astrocytoma microarray were stained in the Johns Hopkins Hospital Pathology Department Central Laboratory according to standard clinical protocols using prediluted $p16^{INK4a}$ antibody (MTM Laboratories, Westborough, MA, Catalog #: CMA802) and p53 antibody (Ventana, Catalog #: 760-2542, Roche, Tucson, AZ). Only tumors with two or more evaluable cores were scored, and staining was classified using the following scale: strong (>50% of tumor cells showing immunoreactivity), moderate (between 10% and 50% of tumor cells showing immunoreactivity), weak (up to 10% of tumor cells showing immunoreactivity), and negative (no tumor cells showing immunoreactivity).

Statistical Analysis

Statistical tests for laboratory experiments were performed using GraphPad Prism (GraphPad Software, San Diego California USA) or Excel (Microsoft). All tests were two

sided unless otherwise indicated, and p values less than 0.05 were considered significant. Error bars in all graphs represent standard error of the mean, unless otherwise indicated. Stata 11 (StataCorp, College Station, TX) was used for the descriptive and multivariate clinical analyses. Baseline characteristics of study patients and their tumors were evaluated according to $p16^{INK4a}$ expression status. P-values were calculated with the use of Fisher's exact test for race, location, extent of resection, and therapy, chi-square test for sex, and t-test with unequal variance for age and follow-up time. Spearman's correlation tests were performed to determine correlation between covariates. An initial bivariate analysis with Fisher's exact test was performed to estimate the association between $p16^{INK4a}$ expression status and mortality. We then conducted a survival analysis using the Kaplan-Meier estimator, and the log-rank test was used to compare survival distributions across groups. A univariate and multivariate Cox proportional-hazards regression analysis was performed with overall survival as the dependent variable. Risk factors including age, sex, race, extent of resection, location of tumor, and therapy modality were considered for final model selection. The proportional hazards assumption was evaluated using complementary log-log plots and Schoenfeld residual plots.

## 2.3 Results

### *2.3.1 Expression of constitutively active BRAF$^{V600E}$ activates the MAPK pathway in neural stem and progenitor cells and promotes soft agar colony formation*

Normal neurospheres derived from developing human brain express markers for neural stem cells such as SOX2, OLIG2, NESTIN and have the capability to differentiate into neurons, astrocytes and oligodendroglia *in vitro* and *in vivo* (16, 17). To test the hypothesis that activation of BRAF would lead to transformation of human neural stem and progenitor cells, we infected neurospheres derived from human fetal cerebral cortex with a lentiviral construct containing constitutively active BRAF$^{V600E}$. Bulk cultures and subclones derived from single neurospheres including BRAF$^{V600E}$ #1, #2 and #4 expressed high levels of BRAF as compared to controls (Figure 1A). Cells transduced with BRAF$^{V600E}$ also showed activation of downstream signaling, as evidenced by increased levels of phospho-ERK (Figure 1A). These experiments were repeated with cortical neural stem cells isolated from an additional brain with similar results (Supplementary Figure S1A).

Expression of BRAF$^{V600E}$ did not lead to a dramatic increase in cell proliferation (Figure 1B), with a non-significant 2% increase in the percentage of cells incorporating BrdU as compared to vector infected controls (control =11% BrdU positive, BRAF$^{V600E}$ = 13% BrdU positive, p=0.33, *t*-test). To test the hypothesis that expression of constitutively active BRAF leads to transformation of neural stem and progenitor cells, early passage BRAF$^{V600E}$ transduced neurospheres were placed into soft agarose. After approximately

six weeks in culture, $BRAF^{V600E}$ expressing cells formed a significantly larger number of colonies in soft agarose compared to control cells (Figure 1C, D, $p < 0.001$, *t*-test). Interestingly, constitutively active BRAF was almost as effective in promoting growth in soft agar as the potent oncogenic combination of SV40 large T antigen and hTERT (Figure 1D).

### *2.3.2 $BRAF^{V600E}$ expression promotes senescence in human cortical neurospheres*

Although their initial proliferation rate was equal to that of control cells, after approximately five passages in culture, the $BRAF^{V600E}$ transduced cells showed significantly decreased proliferation compared to controls (Figure 2A, B, $p < 0.05$). Proliferation eventually completely ceased over the next few passages, though the cells appeared viable by light microscopy. In concert with this decreased growth, both the nuclear diameter and overall size of the cells growing in suspension increased, a change similar to the phenotype previously associated with oncogene-induced senescence (15). In contrast, at the point that the $BRAF^{V600E}$ expressing cells could no longer be passaged, GFP- transduced control cultures were still proliferating and had no change in their morphology (Figure 2A, Supplementary figure S2).

To test the hypothesis that these cells had undergone oncogene-induced senescence, we performed acidic beta-galactosidase staining, which has been associated with the senescent phenotype in numerous studies (15, 29). We observed diffuse acidic beta-galactosidase staining in $BRAF^{V600E}$ transduced cells, a 35-fold increase in percentage as compared to control cultures transduced with the same vector only expressing GFP (Figure 2C, D). A human glioblastoma neurosphere culture (JHH-

GBM10) grown in the same media did not express acidic beta-galactosidase (Figure 2D), indicating that it was not a non-specific effect of oncogenic transformation.

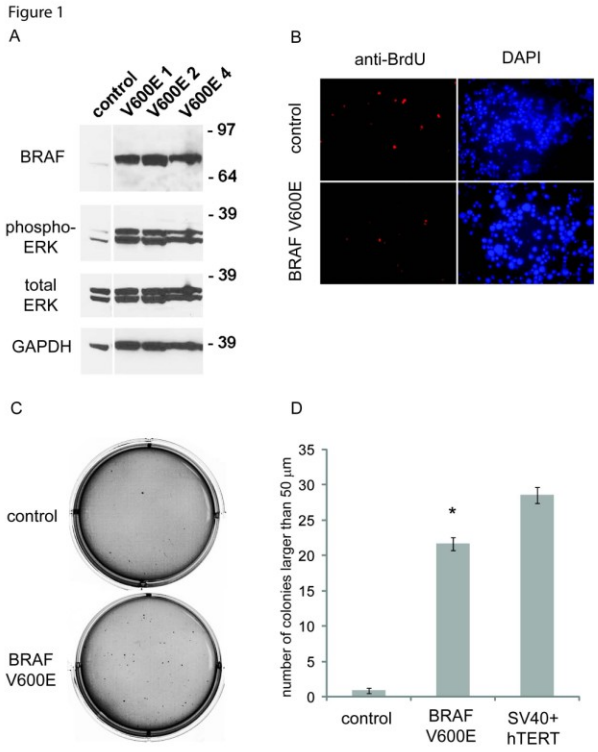


**Figure 2-1: ERK activation, cellular proliferation, and colony formation in soft agarose following BRAF$^{V600E}$ transduction.**

Western blot showing that normal human neural stem and progenitor cells transduced with BRAF$^{V600E}$ lentivirus express higher levels of activated phospho-ERK compared to control neurospheres. V600E 1-3 represent separate subclones transduced with BRAF$^{V600E}$. B. Proliferation as measured by BrdU incorporation is initially similar between control cells (top) and BRAF$^{V600E}$ infected cells (bottom), with 11% of control cells BrdU positive and 13% of BRAF$^{V600E}$ cells BrdU positive, p=0.33, Student's t-test. C. Soft agarose experiment, showing that control cells (top) do not form large numbers of colonies compared to BRAF$^{V600E}$ transduced cells. D. Quantification of soft agarose colony formation, including SV40 Large T Antigen and hTERT transduced cells as positive control. BRAF$^{V600E}$ infected cells show statistically significant increase in colony formation, compared to control cortex neurosphere cells. Asterisk indicates $p<0.0001$, control versus BRAF$^{V600E}$ infected cells, Student's t-test.

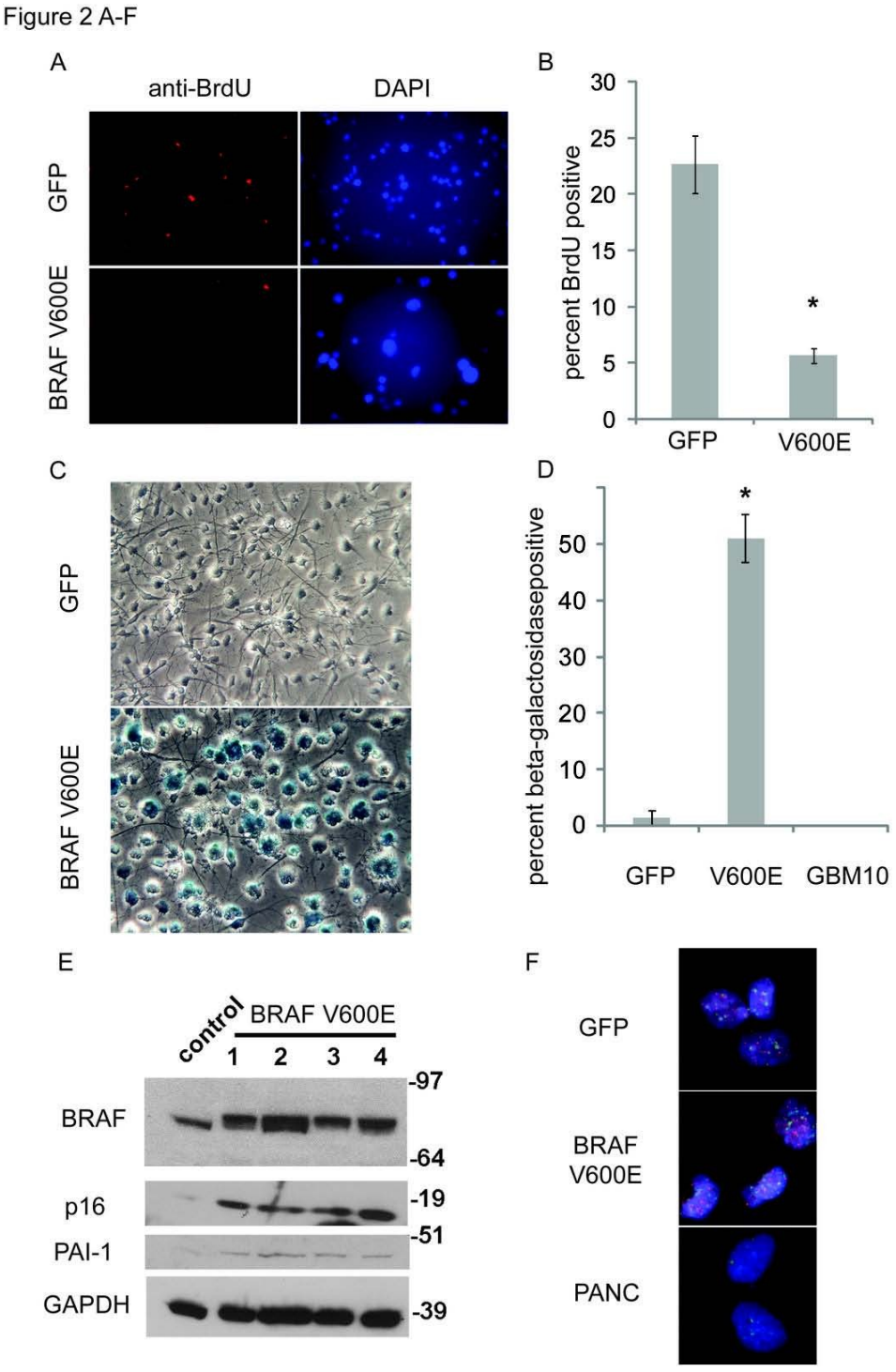


A.

**Figure 2-2: BRAF$^{V600E}$ expressing cells upregulate senescence markers and show decreased proliferation after several passages.**

A. Immunofluorescence 20X photomicrographs of BrdU (red) and DAPI (blue) stained GFP control and $BRAF^{V600E}$ expressing neural stem and progenitor cells. After five passages, $BRAF^{V600E}$ expressing neurosphere cells show increased nuclear size (DAPI) and decreased proliferation as measured by BrdU incorporation (bottom panels) compared to control neurospheres (top panels). B. Quantification of BrdU positivity, showing percentage of BrdU positive cells. Asterisk indicates $p < 0.05$, GFP versus $BRAF^{V600E}$ infected cells, Student's *t*-test. C. Bright field 20X photomicrographs of acidic beta-galactosidase activity in control GFP and $BRAF^{V600E}$ infected neurosphere cells. Cells have been plated on an adherent substrate to allow for improved visualization of acidic beta-galactosidase staining. Blue staining, indicating increased acidic beta-galactosidase activity, is increased in $BRAF^{V600E}$ transduced cells, which also become enlarged when compared to GFP expressing controls. D. Quantification of acidic beta-galactosidase activity, comparing the mean percentage of beta-galactosidase positive cells in GFP control and $BRAF^{V600E}$ transduced neural stem and progenitor cells. Asterisk indicates $p < 0.005$ GFP versus $BRAF^{V600E}$ infected cells, Student's *t*-test. E. Western blot showing increased $p16^{INK4a}$ and PAI-1 expression in late passage $BRAF^{V600E}$ expressing cells compared to controls. Senescent markers $p16^{INK4a}$ and PAI-1 are induced in late passage $BRAF^{V600E}$ expressing neurosphere cells compared to control neurosphere cells. $BRAF^{V600E}$ 1-4 represent subclones isolated from the bulk infected culture. Molecular weight markers are located at the right of the blot. F. Fluorescent in situ hybridization analysis reveals similar telomere length in GFP control and $BRAF^{V600E}$ expressing neurosphere cells. Fluorescent 100X photomicrographs of FISH-stained nuclei from similar passage GFP and $BRAF^{V600E}$ neurospheres. At this passage, $BRAF^{V600E}$ transduced cells were highly senescent, while GFP-expressing neurospheres continued to proliferate normally. Telomeres are labeled red, and centromeres are labeled green. Nuclei are counterstained with DAPI. PANC is a pancreatic carcinoma cell line with shortened telomeres and corresponding decreased red telomere signal.

To further confirm the induction of oncogene-induced senescence following BRAF activation, we analyzed two additional markers in protein lysates. Immunoblotting showed increased expression of the senescence associated markers $p16^{INK4a}$ (15) and PAI-1 (30) in $BRAF^{V600E}$ transduced cells as compared to controls (Figure 2E, supplementary figure S1B,C).

The passage number of the cultures used in these studies was below the threshold at which senescence due to telomere shortening generally occurs. However, to confirm that the senescent phenotype we observed was not due to effects on telomeres, we assessed their length using FISH as previously described (25). This revealed similar telomere lengths (red fluorescence signal) between control proliferating GFP expressing control cells and senescent $BRAF^{V600E}$ transduced cells, with no sign of overall shortening in either culture (Figure 2F). A pancreatic carcinoma cell line (PANC), which is known to have shortened telomeres, exhibited reduced red fluorescence. Quantification of the telomere length showed that $BRAF^{V600E}$ transduced cells did not have shorter telomeres than GFP-transduced cells at the same passage number – in fact their telomeres were somewhat longer (Figure S3).

### *2.3.3 Lack of expression of the senescence marker $p16^{INK4a}$ in pilocytic astrocytoma is associated with shorter survival*

Examination of a tissue microarray containing 66 evaluable pilocytic astrocytomas showed that while 9 cases (14%) lacked $p16^{INK4a}$ protein (Figure 3A), the majority (86%)

exhibited weak, moderate or strong immunoreactivity for this senescence marker (Figure 3B,C,D). Table 1 summarizes the characteristics of the 66 tumors with evaluable $p16^{INK4a}$ staining. Most of the characteristics of the patients with $p16^{INK4a}$ negative tumors, including those commonly associated with outcome, were similar to those with $p16^{INK4a}$ positive tumors (location, time of follow-up, extent of resection, and need for additional therapy). There was a significant difference in the sex of the patients, with $p16^{INK4a}$ negative patients being more likely to be female than $p16^{INK4a}$ positive patients. There was a trend toward increasing age in the $p16^{INK4a}$ negative patients, but this was not statistically significant.

Descriptive examination of characteristics of patients in this cohort regardless of $p16^{INK4a}$ staining showed positive Spearman's rank correlation coefficients between extent of resection and location of tumor (rho=0.7, $p<0.001$), extent of resection and therapy modality (rho=0.59, $p<0.001$), and location of tumor and therapy modality (rho=0.41, $p<0.001$), indicating high correlation between these variables. These correlations are similar to previously reported in low grade gliomas (27, 28).

We also examined expression of TP53, another marker of senescence. TP53 staining was much less intense, and was detected in only 18 of 78 (23%) pilocytic astrocytoma samples (Figure 3E, F). However, TP53 immunoreactivity correlated significantly with that of $p16^{INK4a}$ in the 66 cases in which both could be scored (Spearman rho = 0.45, p = 0.0001). $p16^{INK4a}$ protein expression also correlated with outcome, with bivariate analysis revealing that 33 percent (n=3) of $p16^{INK4a}$ negative patients died, compared to 3.6

percent (n=2) of $p16^{INK4a}$ positive patients (Fisher's exact test, p=0.02). Patients with tumors which were negative for $p16^{INK4a}$ also had significantly shorter overall survival when Kaplan Meier survival curves were compared using the log-rank test (p = 0.0002; (Figure 3G). Univariate Cox proportional-hazards regression analysis revealed that the relative risk of death was 13 times greater for patients with $p16^{INK4a}$ negative tumors versus $p16^{INK4a}$ positive status (hazard ratio=13.0, 95% CI: 2.1 to 80.5, p=0.006). In multivariate analysis we attempted to adjust for tumor location, type of resection, and therapy modality, which were highly correlated, but comparison groups only included 0 or 1 death, so it was not possible to control for these predictors given the small sample size.

### *2.3.4 Primary cultures of KIAA1549:BRAF fusion containing pilocytic astrocytoma express markers of senescence*

To further determine if pediatric pilocytic astrocytoma undergoes oncogene-induced senescence, we examined the senescence marker acidic beta-galactosidase in low passage primary pilocytic astrocytoma cultures established from freshly resected tumors. In two separate cultures which were derived from tumors harboring KIAA1549:BRAF fusions, we observed expression of the senescence marker in over half of the cells at low passage. Representative images are shown in (Figure 3H-I) and compared to control normal human fibroblasts.

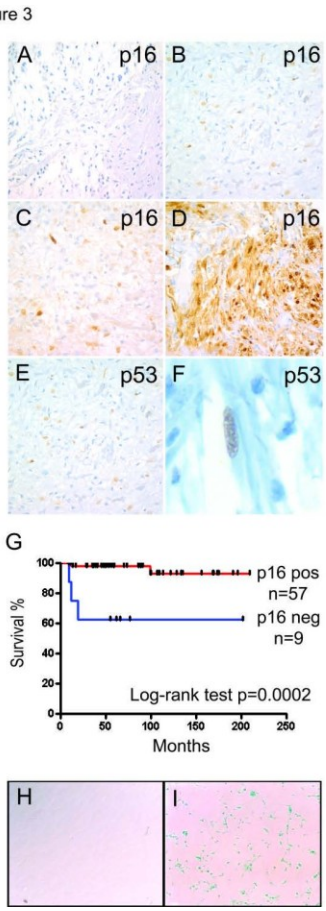


**Figure 2-3: Pilocytic astrocytoma cells express markers of senescence *in vivo* and *in vitro*.**

Photomicrographs showing p16$^{INK4a}$ immunohistochemical staining in pilocytic astrocytoma specimens. A. negative; B. weak; C. moderate; and D. strong p16$^{INK4a}$ immunohistochemical staining in pilocytic astrocytomas. E, F. Immunohistochemical staining for p53 was largely negative, with only rare tumors showing scattered weakly staining cells F. Digitally expanded higher power view showing nuclear p53 staining in elongated tumor cell. (Original magnification 40X for A-F). G. Log rank analysis of Kaplan-Meier curves showed significantly shorter overall survival in patients whose tumors were p16$^{INK4a}$ immunonegative (p = 0.0002). H, I. Acidic beta-galactosidase stain of an early-passage representative primary pilocytic astrocytoma culture. Bright field photomicrograph (10X power) showing prominent acidic beta-galactosidase activity in

primary pilocytic astrocytoma cells after three passages in culture (I), while human fibroblasts of equal density (H) do not stain after 10 passages.

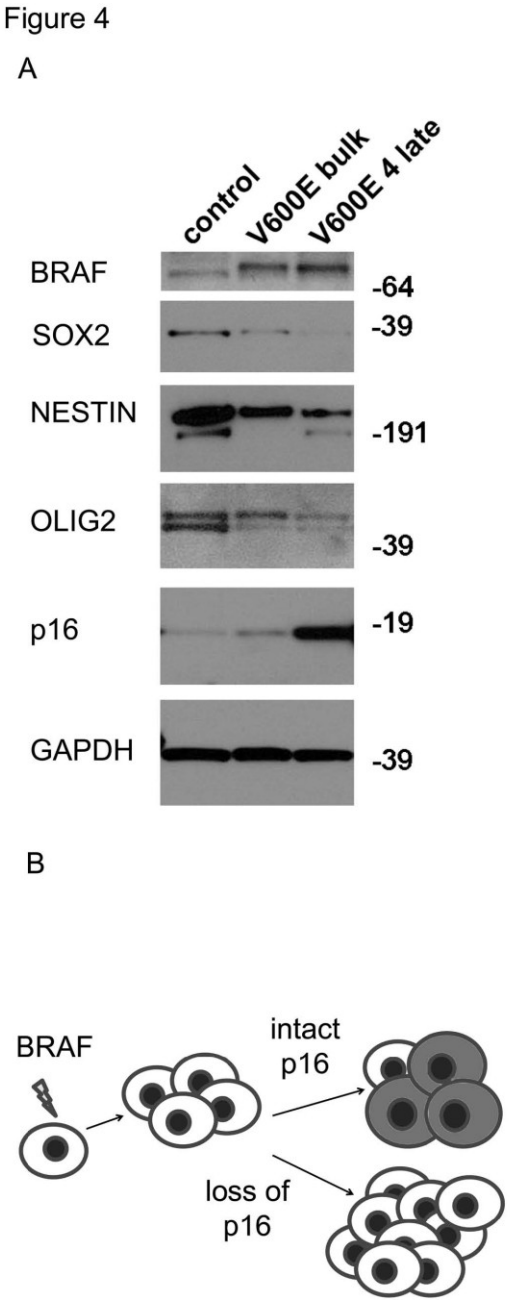


**Figure 2-4: Onset of senescence in BRAF$^{V600E}$-expressing neurospheres corresponds to decreased expression of neural stem cell markers.**

A. Western blot showing decreased expression of neural stem cell markers in late passage neurospheres (V600E #4), compared to the early passage bulk culture infected with constitutively active BRAF. B. Model for formation of pilocytic astrocytoma. BRAF

activation promotes initial transformation, but the induction of senescence (indicated by shaded cells) limits growth unless $p16^{INK4a}$ is deleted or silenced.

| Total | | $p16^{INK4a}$ positive | $p16^{INK4a}$ negative | p value* |
|---|---|---|---|---|
| Patients in cohort | 66 | 57 | 9 | |
| Mean Age ± SD (range) | 14±12 (0.5-52 yrs) | 12±10 (0.5-52 yrs) | 25±17 (9-51 yrs) | 0.06 |
| Sex | | | | |
| Male (%) | 40 (60.6%) | 38 (66.7%) | 2 (22.2%) | 0.01* |
| Female (%) | 26 (39.3%) | 19 (33.3%) | 7 (77.8%) | |
| Race | | | | |
| White | 55 (83.3%) | 46 (80.7%) | 9 (100%) | 0.80 |
| Black | 7 (10.6%) | 7 (12.3%) | 0 (0%) | |
| Other | 4 (6.1%) | 4 (7%) | 0 (0%) | |
| Mean follow-up (months) ± SD (range) | 71±55 (1-209) | 73±54 (1-209) | 56±62 (1-202) | 0.40 |
| Location [a] | | | | |
| Favorable | 40 (60.6%) | 33 (57.9%) | 7 (77.8%) | 0.50 |
| Unfavorable | 26 (39.4%) | 24 (42.1%) | 2 (22.2%) | |
| Extent of resection | | | | |
| Gross total | 31 (47%) | 26 (45.6%) | 5 (55.6%) | 0.70 |
| Subtotal Therapy b | 35 (53%) | 31 (54.3%) | 4 (44.4%) | |
| Initial surgery only | 37 (56.1%) | 32 (56.1%) | 5 (55.6%) | 1.0 |
| Additional therapy* | 29 (43.9%) | 25 (43.9%) | 4 (44.4%) | |
| Radiation | 18 (62.1%) | 15 (60%) | 3 (75%) | 0.70 |
| Repeat surgery | 24 (82.8%) | 21 (84%) | 3 (75%) | 1.0 |
| Chemotherapy | 7 (24.1%) | 6 (24%) | 1 (25%) | 1.0 |
| Outcome | | | | |
| Alive | 61 (92.4%) | 55 (96.5%) | 6 (66.7%) | 0.02* |
| Died of disease | 5 (7.6%) | 2 (3.5%) | 3 (33.3%) | |

**Table 2-1.** Characteristics of study patients and their tumors, according to $p16^{INK4a}$ status

[a] Unfavorable location was defined as a tumor located in the optic chiasm, thalamus, midbrain, or brain stem. All other locations were considered favorable.

[b] Patients receiving additional therapy may have received more than one modality. Percentages associated with each modality are of the total receiving additional therapy.

*P-values were calculated using Fisher's exact test for race, location, extent of resection, therapy and outcome; chi-square test for sex; and t-test with unequal variance for age and follow up. Asterisk indicates statistically significant value of $p<0.05$.

### *2.3.5 Induction of senescence is associated with downregulation of neural stem cell markers, including SOX2*

The neural stem cell and somatic cell reprogramming factor SOX2 is associated with the repression of $p16^{INK4a}$-mediated senescence in multiple cell systems (31, 32). To investigate the mechanism behind the induction of senescence in $BRAF^{V600E}$ transduced cells, we examined the expression of SOX2 and other markers of neural stem cells in neurospheres which had undergone senescence. Compared to GFP-control infected cells, high expression of $BRAF^{V600E}$ led over time to decreased expression of the neural stem cell markers SOX2, OLIG2, and NESTIN (Figure 4A). Expression of $p16^{INK4a}$ increased as neural stem cell marker expression decreased. The experiment was repeated in cortex-derived neurospheres from another brain, with similar loss of SOX2 expression in late passage neurospheres (Supplementary figure S1 B, C). While $BRAF^{V600E}$ expressing neurospheres at early passage expressed SOX2 at levels comparable to GFP infected controls (Figure S1 B), after five passages, at the time when cells were exhibiting increased expression of senescent markers, the same $BRAF^{V600E}$ neurosphere subclone expressed less SOX2 than similar-passage GFP neurospheres (Figure S1 C).

## 2.4 Discussion

Genetic alterations activating the RAS/RAF pathway, including $BRAF^{V600E}$, are a hallmark of pediatric pilocytic astrocytomas. We hypothesized that introducing $BRAF^{V600E}$ into human neural stem and progenitor cells would lead to cellular transformation similar to that seen in pilocytic astrocytoma or other pediatric gliomas. Interestingly, while there is no significant proliferative advantage to expression of $BRAF^{V600E}$ in these neurospheres, neural stem and progenitor cells did show increased colony formation in soft agar, indicating that expression of $BRAF^{V600E}$ was sufficient to promote some aspects of oncogenic transformation. This is similar to results previously reported for activating mutations in BRAF in non-stem cells (10). However, within several passages of BRAF activation, proliferation slowed in these cells, and they subsequently stopped growing entirely.

Activation of BRAF by V600E substitution is a hallmark of melanoma, but also of benign melanocytic nevi. In the latter, oncogene-induced senescence is thought to limit the tumorgenicity of $BRAF^{V600E}$ (15). The cessation of proliferation of our $BRAF^{V600E}$ expressing cells in culture led us to investigate whether a similar cellular senescence phenotype might also operate in neural cells. $BRAF^{V600E}$ expressing human fetal cortical neurosphere cells show increased acidic beta-galactosidase expression compared to controls, and have increased expression of the senescence-associated markers PAI-1 and $p16^{INK4a}$. In primary human pilocytic astrocytomas, $p16^{INK4a}$ expression was identified using immunohistochemistry in 86 percent of the tumors on a tissue microarray containing 66 evaluable samples. Even in intensely stained tumors, there were piloid

tumor cells without $p16^{INK4a}$ induction, suggesting that not all cells are uniformly senescent. This heterogeneity of $p16^{INK4a}$ expression may explain continued growth in a tumor that is also expressing markers of senescence.

*CDKN2A* locus deletion (encoding $p16^{INK4a}$ and $p19^{ARF}$) has been reported in pediatric low grade astrocytoma, and is associated with higher grade pediatric gliomas (27, 33, 34). Deletion of the locus is often associated with expression of activating mutations in BRAF in these tumors. Recently, homozygous deletions affecting $p16^{INK4a}$ were found selectively in more aggressive "anaplastic" pilocytic astrocytoma (35). Consistent with this, we find that loss of $p16^{INK4a}$ protein expression is associated in univariate analysis with worse outcomes in the pilocytic astrocytoma patients represented on our tissue microarray. This worse outcome could not be explained by location of the tumor, because unfavorable locations (e.g. hypothalamus optic chiasm/thalamus/brainstem) and subtotal resections were not overrepresented in the $p16^{INK4a}$ negative cohort (Table 1). A multivariate analysis was hampered by the relatively small size of our patient sample, and the low number of deaths within the cohort. These data reveal the potential of $p16^{INK4a}$ expression status as a predictor of survival, although future studies with greater numbers of patients are clearly needed to further explore this association. If validated in larger cohorts, $p16^{INK4a}$ immunostaining may provide a tool for risk stratification in pilocytic astrocytoma. It also suggests that tumors in which cellular senescence does not occur (or tumors which escape from senescence) will behave in a more aggressive fashion. Senescence due to telomere shortening has been investigated previously in pediatric low grade gliomas (36). In our studies, we measured telomere length in senescent $BRAF^{V600E}$

expressing neurospheres, and showed that they were longer than those of non-senescent, control GFP neurospheres of the same passage number. In our model system, shortened telomeres do not account for the senescence phenotype, although it is possible this plays a role *in vivo* in pilocytic astrocytoma.

Loss of stem cell markers in our system was also temporally associated with the induction of senescence. SOX2 is a neural stem cell factor critical in somatic cell reprogramming and induced pluripotency. One of the functions of SOX2 is to suppress $p16^{INK4a}$ induced cellular senescence (31, 32). In our model system, we observe downregulation of SOX2 associated with the induction of senescence, consistent with this previously reported role. We also observe downregulation of other neural stem cell markers, such as OLIG2 and NESTIN, suggesting this phenomenon may not be causally related to SOX2, but rather to depletion of stem cells in the culture.

In summary, we show that introduction of constitutively active $BRAF^{V600E}$ into human cortical stem and progenitor cells initially promotes clonogenic growth in soft agar, but ultimately results in dramatically reduced proliferation and arrested growth of the culture. Because this coincides with the induction of senescent markers, it strongly suggests that "oncogene-induced senescence" similar to that seen in melanocytic cells can occur in neural tissues, and this may explain the often indolent growth of pilocytic astrocytoma. Furthermore, examination of $p16^{INK4a}$ expression in primary tumors suggests that escape from this process may underlie aggressive tumor growth. Further investigation of oncogene-induced senescence pathways may therefore provide new therapeutic opportunities in pilocytic astrocytoma.

## Supplementary Figures

### Supplementary figure 2-S1:

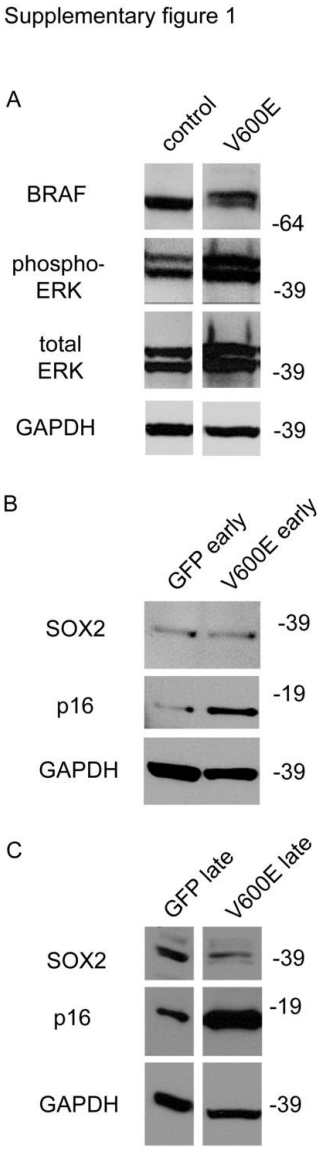


**Cortex BRAF$^{V600E}$-expressing neurospheres derived from a second source show high level activation of the MEK/ERK pathway and subsequent induction of p16$^{INK4a}$ and decreased expression of neural stem cell markers.**

A. Western blot showing activation of phospho-ERK in BRAF$^{V600E}$ transduced cortical neural stem and progenitor cells compared to control neurosphere cells. B. Western blot showing equivalent expression of SOX2 in early passage GFP and BRAF$^{V600E}$ transduced

neurospheres. There is some moderate upreguation of $p16^{INK4a}$ in these early passage $BRAF^{V600E}$ transduced cells. C. Western blot showing decreased expression of SOX2 and substantial upregulation of $p16^{INK4a}$ in late (5th passage) $BRAF^{V600E}$ expressing neurospheres compared to equivalent passage GFP expressing neurospheres.

**Supplementary figure 2-S2:**

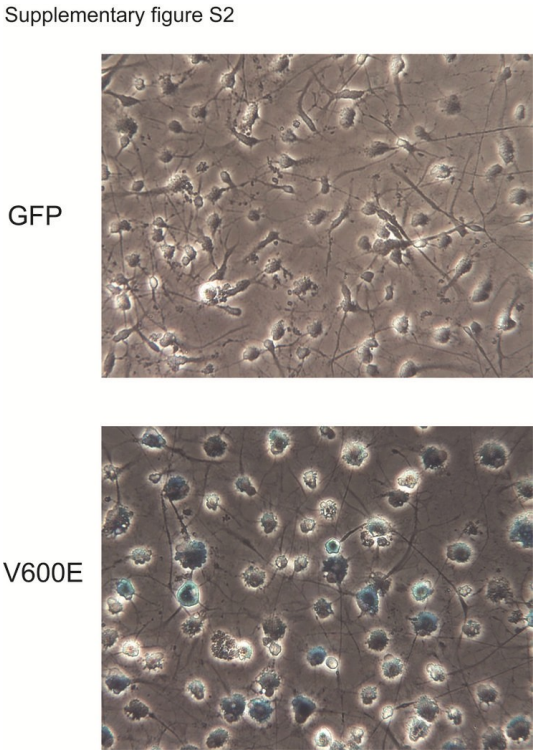


**Expanded view of senescent $BRAF^{V600E}$ –expressing cells compared to GFP-expressing cells**

Photomicrograph (20X magnification) showing GFP and $BRAF^{V600E}$ transduced neural stem cells stained with acidic beta-galactosidase (blue pigment) as a marker of senescence. The $BRAF^{V600E}$ cells are positive for acidic beta-galactosidase and are substantially enlarged compared to control GFP cells.

**Supplementary figure 2-S3:**

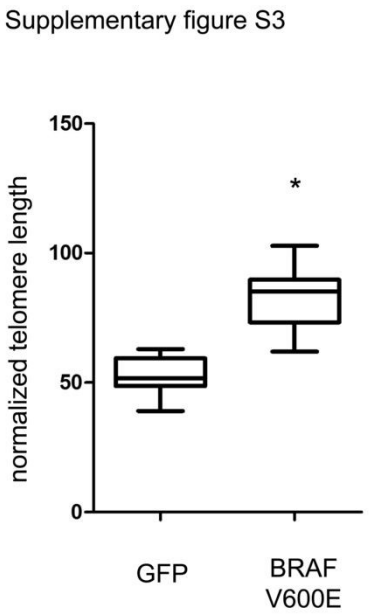


**Quantification of telomere length in GFP versus BRAF$^{V600E}$ expressing neural stem and progenitor cells.**

Box and whisker plot showing the distribution and mean of the DAPI normalized total telomere content in BRAF$^{V600E}$ expressing neurospheres, compared to equivalent passage GFP expressing neurospheres. At this passage, BRAF$^{V600E}$ transduced cells were highly senescent, while GFP-expressing neurospheres continued to proliferate normally. The BRAF$^{V600E}$ transduced neurospheres have more telomere content than GFP transduced controls ($p<0.0001$, Student's *t*-test). This difference may be due to the clonal derivation of BRAF$^{V600E}$ expressing and GFP expressing neurosphere cells from populations of neural stem cells, as described in the materials and methods.

# Chapter 3: Pathological and Molecular Advances in Pediatric Low Grade Astrocytoma

Fausto J. Rodriguez[1], Kah Suan Lim[1], Daniel Bowers[2] and Charles G. Eberhart[1]

Johns Hopkins University School of Medicine, Department of Pathology[1]

University of Texas Southwestern Medical School, Department of Pediatrics[2]

Keywords: Pilocytic astrocytoma, BRAF, NF1, RAF1,

Contact Information:

Charles G. Eberhart

Division of Neuropathology

720 Rutland Ave – Ross Building 558

Baltimore, MD 21205

ceberha@jhmi.edu

**ABSTRACT**

Pediatric low grade astrocytomas are the commonest brain tumors in children. They sometimes have similar microscopic and clinical features, making accurate diagnosis difficult. For patients whose tumors are in locations that do not permit full resection, or those with an intrinsically aggressive biology, more effective therapies are required. Until recently, little was known about the molecular changes that drive the initiation and growth of pilocytic and other low grade astrocytomas beyond the association of a minority of cases, primarily in the optic nerve, with neurofibromatosis type 1. Over the last several years, a wide range of studies have implicated the *BRAF* oncogene and other members of this signaling cascade in their pathobiology. In this review, we attempt to summarize this rapidly developing field, and discuss the potential for translating our growing molecular knowledge into improved diagnostic and prognostic biomarkers and new targeted therapies.

## 3.1 CLINICAL AND DEMOGRAPHIC FEATURES

Pediatric low grade astrocytomas (PLGA) arise throughout the central nervous system (CNS), but are found most often in the cerebellum, followed by the cerebrum and deep midline structures, optic pathways, brainstem and spinal cord (Sievert and Fisher 2009). According to 2012 CBTRUS data, pilocytic astrocytoma (PA) are the second most common brain tumor (after embryonal neoplasms) in the 0-4 year age group, the commonest tumors in children 5-14 years of age, and the second most common tumors (after pituitary neoplasms) in 15-19 year-olds (http://www.cbtrus.org). A graphical representation of primary pediatric brain tumor diagnoses based on current CBTRUS data

is shown in Figure 1. Most non-infiltrative PLGA (i.e. pilocytic/pilomyxoid astrocytoma, pleomorphic xanthoastrocytoma, subependymal giant cell astrocytoma) show variable contrast enhancement on imaging studies, while infiltrating diffuse low grade astrocytomas are generally non-enhancing.

Outcomes for this group of tumors are good overall, but vary depending on the extent of surgical resection and histopathological classification. In one large institutional series of children with low grade astrocytomas, 5 year overall survival (OS) was 96% for PA patients and 48% for diffuse astrocytoma patients (Fisher, Tihan et al. 2008). Gross total resection has consistently been strongly prognostic of long-term survival, but can often only be achieved when tumors are localized to the cerebellum or superficial cerebrum (Pollack, Claassen et al. 1995; Pencalet, Maixner et al. 1999; Fernandez, Figarella-Branger et al. 2003). It has also been suggested that PA behave in a more aggressive fashion when arising in adults (Stuer, Vilz et al. 2007).

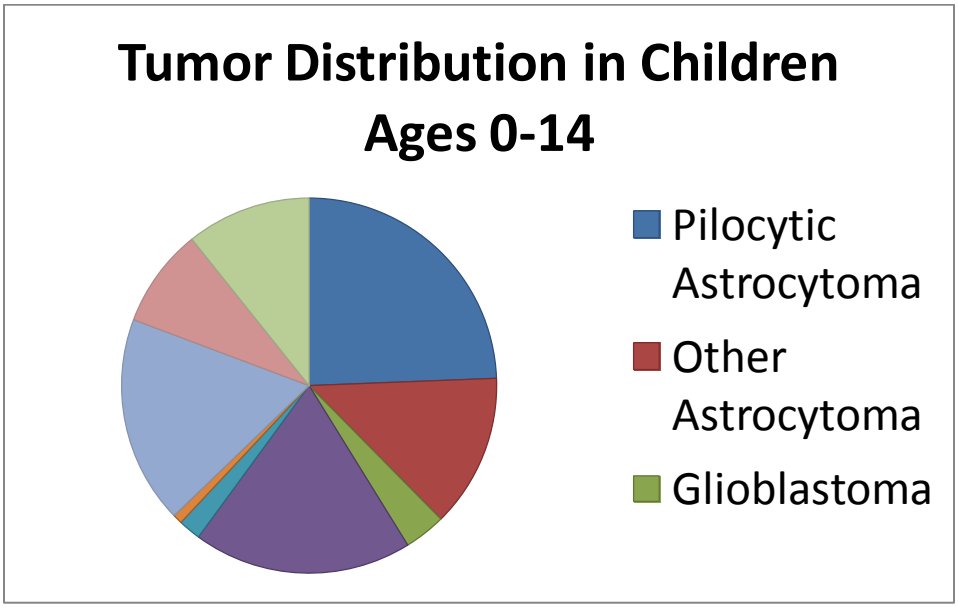


**Figure 3-1** – Primary CNS tumor distribution in children ages 0-14 based on CBTRUS data.

## 3.2 HISTOLOGICAL CLASSIFICATION

### *3.2.1 Pilocytic Astrocytoma (WHO Grade I)*

PA are generally characterized by a biphasic growth pattern including both compacted bipolar cells (Figure 2A) and regions with microcysts and more loosely textured cells (Figure 2B). Characteristic elements include Rosenthal fibers and eosinophilic granular bodies (Figure 2A,B). Oligodendroglial-appearing cells are often encountered in PA, and in some cases can comprise a significant portion of the tumor (Takei, Yogeswaren et al. 2008), making diagnosis difficult in small samples. Most lesions are cytologically bland, although some atypia can be present. Mitotic figures are only present in the minority of cases, and the lack of infiltration, as well as the presence of more specific features such as eosinophilic granular bodies, allows most cases to be differentiated from high grade astrocytomas (Louis, Ohgaki et al. 2007).

A number of potential histological and immunohistochemical prognostic markers have been investigated. It has been suggested that tumors with an elevated Ki67 proliferation index are associated with worse progression-free survival (Dirven, Koudstaal et al. 1998; Bowers, Gargan et al. 2003), although in other studies proliferation was not prognostic (Fisher, Naumova et al. 2002; Tibbetts, Emnett et al. 2009; Horbinski, Nikiforova et al. 2012). Anaplastic features, including cytological atypia, hypercellularity, high mitotic activity, and necrosis, can also portend worse outcomes (Rodriguez, Scheithauer et al. 2010). It has been suggested that morphological or immunohistochemical evidence of oligodendroglial differentiation may also predict aggressive behavior in PA patients (Takei, Yogeswaren et al. 2008; Tibbetts, Emnett et al. 2009).

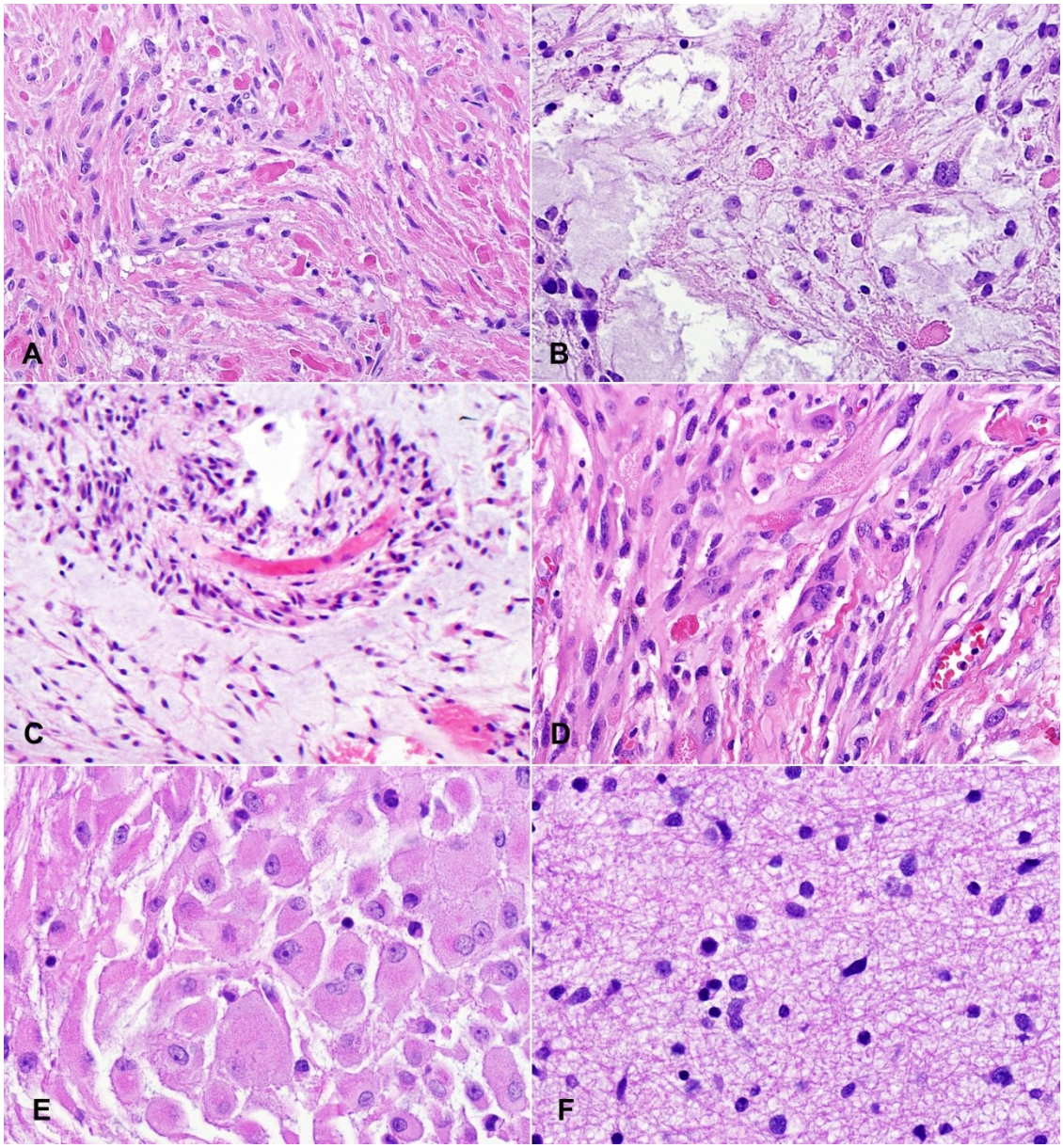


**Figure 3-2 –** Histopathological features of PLGA. (A) PA with compacted glial cells and Rosenthal fibers (arrow). (B) Microcysts (asterisks) and eosinophilic granular bodies (EGB, arrow) in a looser region of a PA. (C) Pilomyxoid astrocytoma comprised of monomorphous cells with a pronounced perivascular growth pattern. (D) Spindled, pleomorphic cells in a PXA. (E) Enlarged ganglion-cell like elements in a SEGA. (F) Diffuse astrocytoma are only modestly hypercellular with scattered atypical cells.

### *3.2.2 Pilomyxoid Astrocytoma (WHO Grade II)*

Pilomyxoid astrocytomas are comprised of monomorphous bipolar cells, often arrayed around vessels, with a mucoid background matrix, and lack Rosenthal fibers and eosinophilic granular bodies (Figure 2C). Referred to in early reports as "infantile" pilocytic astrocytomas, their distinct microscopic features and more aggressive clinical behavior were highlighted in 1999 by Tihan and colleagues (Tihan, Fisher et al. 1999), leading to their recognition as a potentially distinct variant in the 2007 WHO classification (Louis, Ohgaki et al. 2007). They are often found in hypothalamus, optic chiasm, and around the third ventricle, although other sites can also be involved. Recently, transitional tumors with mixed pilocytic and pilomyxoid features have been described, as well as cases in which a pilomyxoid astrocytoma "matured" into a classic pilocytic astrocytoma over time (Johnson, Eberhart et al. 2010), suggesting that these lesions represent part of a spectrum rather than completely distinct entities.

### *3.2.3 Pleomorphic Xanthoastrocytoma (PXA, WHO Grade II)*

PXA generally show greater cellularity and atypia than other entities discussed in this review, and can sometimes be misdiagnosed as high grade glioma. They occur most frequently in teenagers and young adults, often involve superficial cortex and meninges, and can contain lipidized "xanthomatous" astrocytes (Louis, Ohgaki et al. 2007). Eosinophilic granular bodies as well as spindled and pleomorphic glial elements are all common, and the tumors frequently attract a lymphocytic infiltrate and contain abundant extracellular reticulin (Figure 2D).

### *3.2.4 Subependymal Giant Cell Astrocytoma (SEGA, WHO Grade I)*

These benign tumors are tightly associated with the autosomal dominant inherited condition tuberous sclerosis, and arise almost exclusively in the walls of the lateral ventricles (Louis, Ohgaki et al. 2007). Spindled, gemistocytic and ganglion-cell like elements can be present, with the latter cells representing the most characteristic finding (Figure 2E). Immunohistochemical and ultrastructural studies have shown mixed glial and neuronal differentiation in tumor cells (Sharma, Ralte et al. 2004; Jozwiak, Jozwiak et al. 2005; Buccoliero, Franchi et al. 2009), and despite their designation as an "astrocytoma" these are probably best regarded as mixed glial-neuronal neoplasms.

### *3.2.5 Diffuse Astrocytoma (WHO Grade II)*

Infiltrating fibrillary astrocytomas in children are morphologically similar to their WHO grade II counterparts in adults. They are characterized by modest cellularity, diffuse infiltration of normal brain elements, and a lack of significant mitotic activity, vascular proliferation or necrosis (Figure 2F) (Louis, Ohgaki et al. 2007). Because of their ability to spread diffusely, these tumors are difficult to completely resect and have worse outcomes than PA in children (Fisher, Tihan et al. 2008). As in adults, they can progress to high grade glioma, although this often does not occur.

### *3.2.6 Diagnostic Difficulties in PLGA*

Tumors which are difficult to classify are unfortunately all too often encountered among the spectrum of PLGA. In one institutional study of 278 consecutive PLGA resected between 1965 and 1996, 75 cases (27%) did not clearly fit into a WHO

diagnostic category. A more recent review of 1,670 pediatric brain tumors of all types diagnosed at our institution between 2003 and 2008 identified 302 cases which could not be classified, and 7 of the 10 most common problems with diagnosis involved low grade gliomas (personal communication, Peter Burger). In some cases diagnostic dilemmas arise due to small biopsies, but in others they reflect inability of the current scheme to fit a heterogeneous spectrum of lesions. Molecular studies have the potential to help with these problematic issues, and as described below are beginning to shed light on some diagnostic difficulties.

### 3.3 MOLECULAR ADVANCES

Aside from PA arising in NF1 patients, and SEGA in children and young adults with tuberous sclerosis, for many years little was known about the molecular underpinnings of PLGA. Sporadic PA do not inactivate *NF1*, and generally lack changes to the oncogenes and tumor suppressors altered in adult diffuse astrocytomas (Cheng, Pang et al. 2000; Louis, Ohgaki et al. 2007). Early cytogenetic studies of PA were notable for a lack of detectable chromosomal alterations, with largely normal karyotypes in the more than 100 cases initially studied (Louis, Ohgaki et al. 2007). Mutations in *IDH1* have been identified in the majority of low grade gliomas in adults, but interestingly are almost never detected in pediatric low or high grade glioma, and when present have mostly been reported in children at least 14 years old (Paugh, Qu et al. 2010; Pollack, Hamilton et al. 2011; Buccoliero, Castiglione et al. 2012). This suggests that adolescents with *IDH1*-mutant tumors may represent the youngest patients with "adult" gliomas. Over the last few years, however, it has become clear that most non-syndromic PLGA harbor genomic alterations which affect the function of BRAF, and that mitogen

activated protein kinase (MAPK) represents the dominant genetically altered pathway in these tumors (Figure 3).

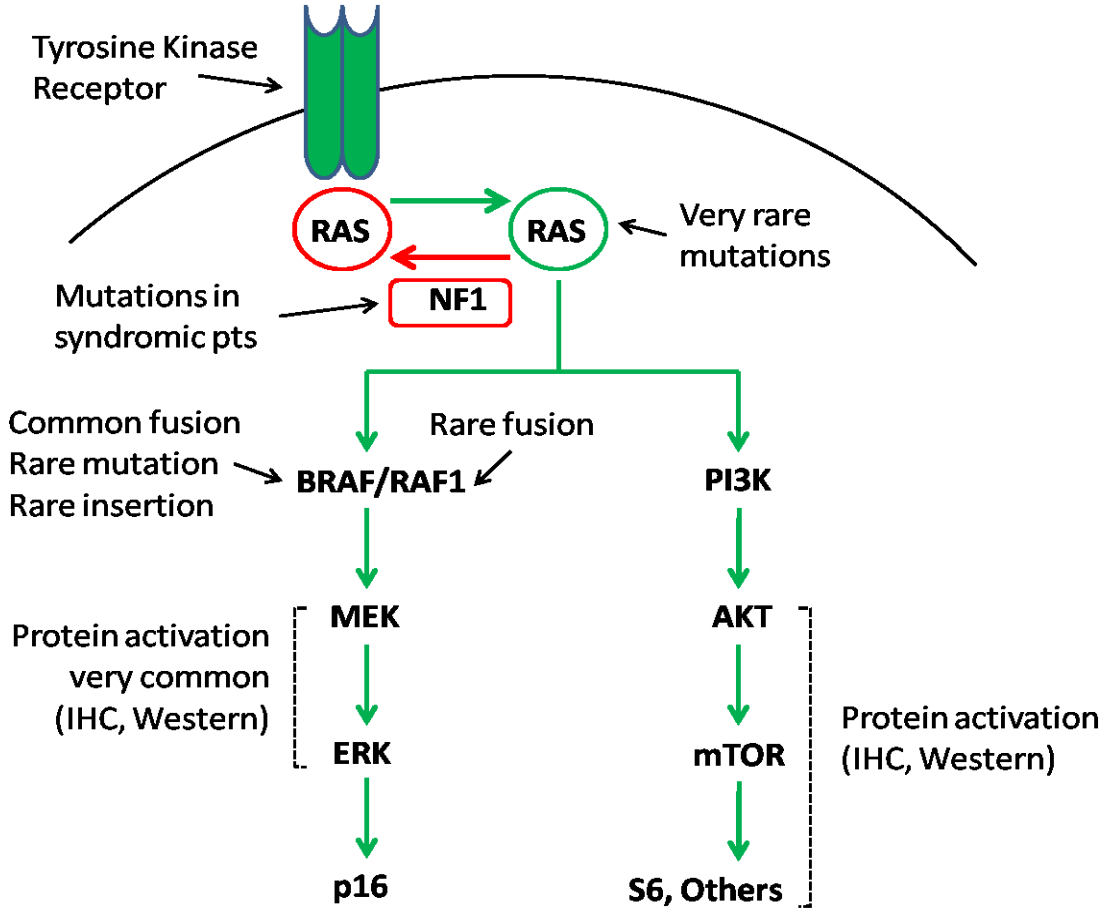


**Figure 3-3** – Signaling pathways commonly activated in PLGA.

### *3.3.1 BRAF Fusions and MAPK Activation in PLGA*

In 2008, five different groups identified gains at 7q34 approximately 2 megabases in size in most PLGA using array-based comparative genomic hybridization (Figure 4A) (Bar, Lin et al. 2008; Deshmukh, Yeh et al. 2008; Jones, Kocialkowski et al. 2008; Pfister, Janzarik et al. 2008; Sievert, Jackson et al. 2009). Fluorescent in situ hybridization (FISH) and other molecular analyses showed that these represented

segmental duplications in the region (Figure 4B) (Pfister, Janzarik et al. 2008; Sievert, Jackson et al. 2009). In these initial studies, between 53% and 77% of the PLGA examined (mostly PA) contained the duplication at 7q34, with relatively few other chromosomal alterations detected, suggesting this represented the dominant change in PA.

In two of the papers, the authors demonstrated that 7q34 duplication resulted in expression of a novel fusion transcript between the *KIAA1549* locus and *BRAF* that included the *BRAF* kinase domain but lacked the inhibitory N-terminal regulatory region of this oncogene (Figure 4C) (Jones, Kocialkowski et al. 2008; Sievert, Jackson et al. 2009). The fusion showed constitutive kinase activity and was able to transform NIH 3T3 cells (Jones, Kocialkowski et al. 2008). BRAF is known to induce signaling in the MAPK pathway, and activated targets including phosphorylated MEK (pMEK) and/or ERK (pERK) (Figure 4D) were identified in the majority of PLGA specimens examined in these initial studies (Bar, Lin et al. 2008; Pfister, Janzarik et al. 2008; Sievert, Jackson et al. 2009).

A large number of additional reports have confirmed these exciting findings and firmly establish *KIAA1549:BRAF* duplication/fusion as the commonest genetic change in PA (Forshew, Tatevossian et al. 2009; Jacob, Albrecht et al. 2009; Korshunov, Meyer et al. 2009; Yu, Deshmukh et al. 2009; Horbinski, Hamilton et al. 2010; Lawson, Tatevossian et al. 2010; Cin, Meyer et al. 2011; Tian, Rich et al. 2011; Lin, Rodriguez et al. 2012; Tihan, Ersen et al. 2012). Specific breakpoints between *KIAA1549* and *BRAF* can vary, but all lead to loss of the BRAF autoregulatory domain (Figure 5). In one recent study of 106 pediatric low grade brain tumors, five types of *KIAA1549:BRAF* gene fusions were

identified, involving exons 1-16/9-18 (49%), 1-15/9-18 (35%), 1-16/11-18 (8%), 1-15/11-18 (6%) and 1-17/10-18 (1%) (Lin, Rodriguez et al. 2012). In this study the 1-16/11-18 fusion was limited to infratentorial sites, and the 1-15/11-18 fusion to supratentorial locations, but it will be necessary to examine larger numbers of cases before firm conclusions can be drawn regarding associations between fusion genotype and tumor phenotype. Genetic mapping of the breakpoints involved have highlighted enrichment for microhomologous DNA sequences, suggesting microhomology-mediated break-induced replication as a possible mechanism for the rearrangements (Lawson, Hindley et al. 2011).

The NF1 gene product acts to inhibit RAS and BRAF activity, and the discovery of fusions activating BRAF therefore links syndromic and sporadic PA to the same oncogenic signaling cascade (Figure 3). Some patients with Noonan syndrome, in which MAPK signaling is activated by mutations in PTPN11, SOS1 and KRAS, have also been reported to have PA (Sanford, Bowman et al. 1999; Fryssira, Leventopoulos et al. 2008; Schuettpelz, McDonald et al. 2009), providing further support for the central role of this pathway. A rare rosette forming glioneuronal tumor of the posterior fossa demonstrating strong pERK immunoreactivity has also been reported in a case of Noonan syndrome (Karafin, Jallo et al. 2011).

Novel genetic mechanisms driving activation of the MAPK pathway in PLGA continue to be discovered. Two groups identified oncogenic fusions between *SRGAP3* and *RAF1* predicted to give rise to unregulated kinase activity similar to that seen with KIAA1549:BRAF (Figure 5) (Forshew, Tatevossian et al. 2009; Jones, Kocialkowski et al. 2009). Rare 3 base pair insertions at position 599 have also been described in PA

(Jones, Kocialkowski et al. 2009; Yu, Deshmukh et al. 2009; Eisenhardt, Olbrich et al. 2010; Schindler, Capper et al. 2011). This insertion ($BRAF^{insT}$) results in duplication of a threonine residue, and results in over 6-fold increases in kinase activity *in vitro* (Eisenhardt, Olbrich et al. 2010). An interstitial deletion causing fusions between *FAM131B* and *BRAF* has also been identified (Cin, Meyer et al. 2011). However, both the *SRGAP3* and *FAM131B* fusions and the $BRAF^{insT}$ are much less common than *KIAA1549:BRAF* fusions in PLGA.

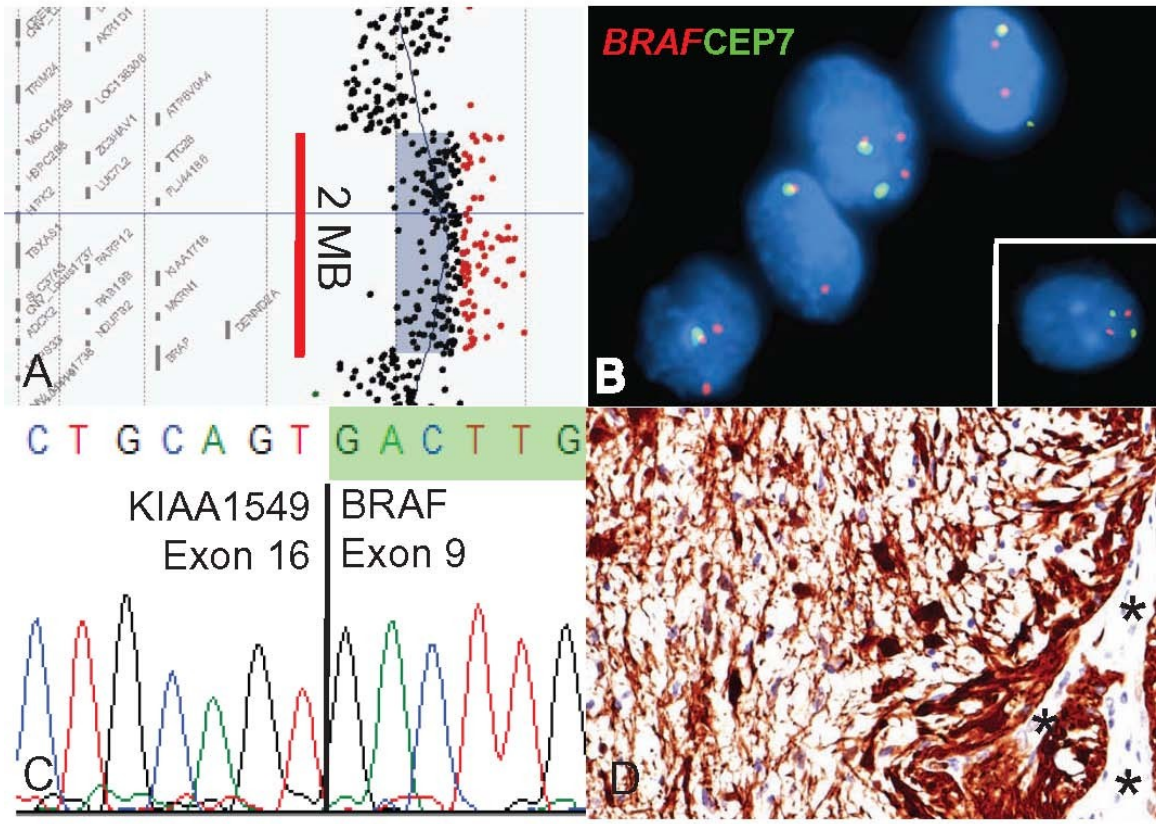


**Figure 3-4** – Molecular alterations involving *BRAF*. (A) Segmental gains at 7q34 approximately 2 megabases in size are commonly identified in PA using array CGH. (B) FISH reveals duplication in this region, with and extra copy of the region encoding BRAF. A normal control is shown in the inset. (C) Sequencing of a *KIAA1549:BRAF* fusion product between exons 16 and 9 of the two genes. (D) PA contain abundant active phospho-ERK. Normal vessels serve as an internal negative control (asterisks).

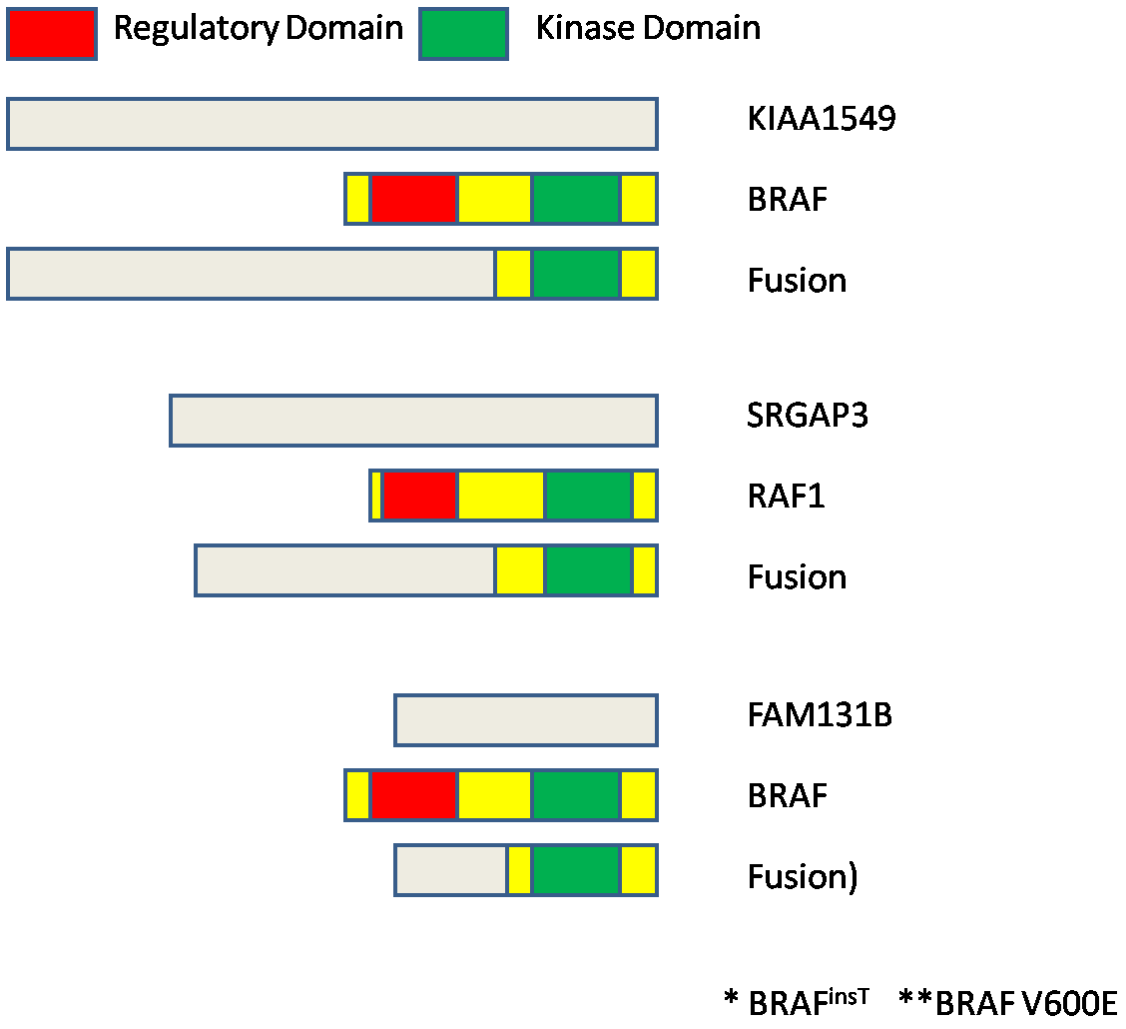


**Figure 3-5** – Mechanisms of BRAF and RAF1 activation in PLGA

### *3.3.2 Point Mutations in BRAF, RAF and RAS*

MAPK signaling can also sometimes be activated in PLGA by point mutations in various pathway members. Indeed, prior to the discovery of *BRAF* gene duplications, rare oncogenic mutations in *KRAS* had been described (Sharma, Zehnbauer et al. 2005; Janzarik, Kratz et al. 2007). Subsequent studies have confirmed the presence of occasional *KRAS* mutations in PA. Forshew and colleagues sequenced *HRAS*, *KRAS* and

*NRAS* in 50 PLGA and found an activating *KRAS* G12A mutation in one cerebellar PA which lacked *BRAF* and *RAF1* fusions (Forshew, Tatevossian et al. 2009). Cin and colleagues examined *HRAS*, *KRAS*, *NRAS*, *PTP11*, and *RAF1* in 125 primary PA samples and identified oncogenic *KRAS* mutations in 2 tumors (Cin, Meyer et al. 2011). Thus approximately 2% of PA have mutations activating *KRAS*. Point mutations in *RAF1* may not be selected for due to its lower basal activity as compared to *BRAF* (Emuss, Garnett et al. 2005; Jones, Kocialkowski et al. 2009), but it is not clear why mutations in *HRAS* and *NRAS* are not present in PLGA.

The commonest point mutation in PLGA occurs in *BRAF* itself at codon 600, and results in substitution of valine by glutamic acid. The $BRAF^{V600E}$ mutation was first described in tumor cell lines; it is most frequent in melanoma, but can also be found in a range of other neoplasms (Davies, Bignell et al. 2002). In PLGA, $BRAF^{V600E}$ mutations were identified in 4/66 (6%) of the tumors examined by Pfister et al. (Pfister, Janzarik et al. 2008), including 3 PA and 1 diffuse astrocytoma. Subsequent studies have also readily identified $BRAF^{V600E}$ mutations in PLGA (Forshew, Tatevossian et al. 2009; Sievert, Jackson et al. 2009; Yu, Deshmukh et al. 2009; Eisenhardt, Olbrich et al. 2010; Cin, Meyer et al. 2011; Schindler, Capper et al. 2011; Tian, Rich et al. 2011; Lin, Rodriguez et al. 2012), although as discussed below these are most common in tumors other than PA.

*BRAF* and *RAF1* fusions are generally mutually exclusive with other genetic alterations activating MAPK signaling, but some exceptions to this have been reported. Cin and colleagues identified 2 PA patients with concomitant $BRAF^{V600E}$ mutation and *BRAF* fusion, one of whom also had NF1 syndrome (Cin, Meyer et al. 2011). In another

study, 6 tumors (out of 198) had both *BRAF* fusion and $BRAF^{V600E}$ mutation (Horbinski, Nikiforova et al. 2012).

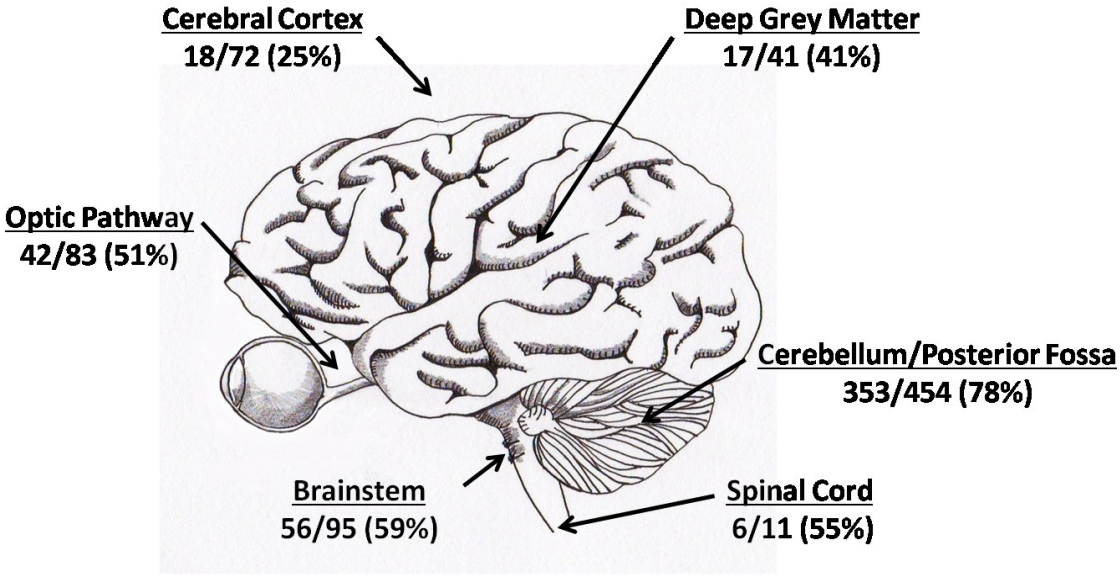


**Figure 3-6** – Localization of *BRAF* duplication/fusion in PA. Summary of tumor localization from published cases, including patients with NF1.

### *3.3.3 Genetic Alterations and Tumor Site*

Tandem duplications involving *BRAF* do not occur uniformly in PLGA at all sites in the CNS (Figure 6). The percentage of cerebellar/posterior fossa PA with molecular alterations at 7q34 is particularly high, ranging from 63% to 94% in various reports (Bar, Lin et al. 2008; Forshew, Tatevossian et al. 2009; Jacob, Albrecht et al. 2009; Sievert, Jackson et al. 2009; Cin, Meyer et al. 2011; Rodriguez, Scheithauer et al. 2011). In one study of 32 posterior fossa PAs, 30 had *KIAA1549:BRAF* fusions, 1 had a *SRGAP3:RAF1* fusion, and 1 had a mutation in *KRAS* (Forshew, Tatevossian et al. 2009). In contrast, the frequency of *BRAF* duplication/fusion in PA arising in the cerebral cortex is quite low,

ranging from 0% to 50% (Bar, Lin et al. 2008; Jones, Kocialkowski et al. 2008; Jacob, Albrecht et al. 2009; Korshunov, Meyer et al. 2009; Yu, Deshmukh et al. 2009; Schiffman, Hodgson et al. 2010; Cin, Meyer et al. 2011; Hawkins, Walker et al. 2011; Rodriguez, Scheithauer et al. 2011). A total of 72 cerebral cases were reported in these studies, with 18 (25%) showing *BRAF* duplication or fusion (Figure 6). Our review of published cases yielded percentages of *BRAF* duplications at other sites higher than cerebral cortex but lower than posterior fossa. This included the optic pathways (42/83, 51%), deep grey matter (17/41, 41%), brainstem (56/95, 59%) and spinal cord (6/11, 55%).

The limited number of other molecular changes in PA makes it harder to definitively assess their spatial distribution. However, it seems that $BRAF^{V600E}$ and *KRAS* mutations are more common in PA arising outside the posterior fossa. In one series, 10/49 (20%) of non-cerebellar PA had point mutations in one of these two oncogenes, as compared to 3/76 (4%) of cerebellar lesions, a statistically significant difference (Cin, Meyer et al. 2011). Schindler and colleagues also found a statistically significant association between $BRAF^{V600E}$ and extracerebellar location of PA ($p = 0.009$) (Schindler, Capper et al. 2011). In contrast, the handful of *SRGAP3:RAF1* and *FAM131B:BRAF* fusions reported to date have largely been in PA arising in the cerebellum(Forshew, Tatevossian et al. 2009; Cin, Meyer et al. 2011).

The cause of the increased incidence of *BRAF* duplication in the posterior fossa is not clear, but it may reflect increased susceptibility of the cell(s) of origin at this site. It has also been suggested that BRAF rearrangements in PA are less common in adult patients (Hasselblatt, Riesmeier et al. 2011), which could reflect changes in tumor

histogenesis as patients' age. Regional differences in expression of the fusions could also play a role. While the *KIAA1549*, *SRGAP3* and *FAM131B* genes are expressed in the CNS, little is known regarding their precise patterns. It has recently been demonstrated that *KIAA1549:BRAF* fusions are expressed at roughly equivalent levels in PA as the endogenous *KIAA1549* gene (Lin, Rodriguez et al. 2012).

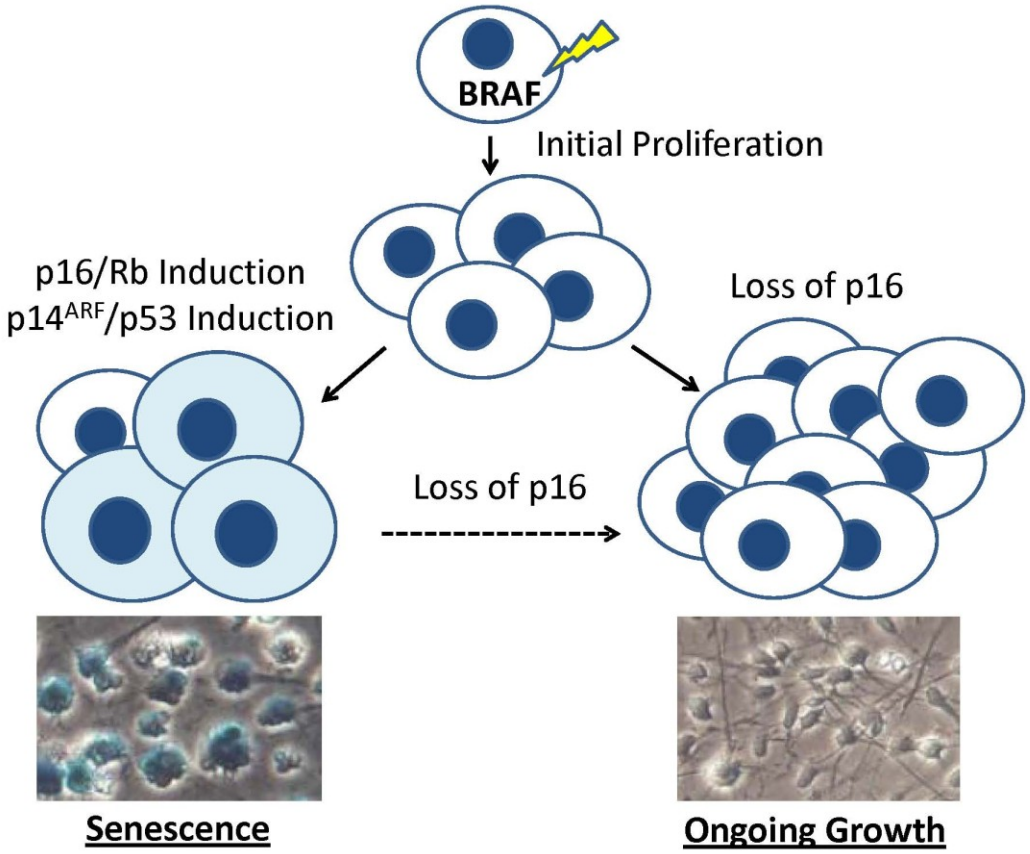


**Figure 3-7** – Oncogene induced senescence in PA. Senescence-associated -galactosidase stains of $BRAF^{V600E}$ and vector transduced human neural stem cells are shown in the bottom panels.

### *3.3.4 Senescence in PLGA*

One interesting feature of PLGA is the propensity of some tumors, particularly PA, to occasionally spontaneously stop growing or even regress (Gunny, Hayward et al. 2005; Sakai, Miyahara et al. 2011). A similar pattern of initial neoplastic proliferation followed by growth arrest is often seen in benign melanocytic nevi of the skin, which also commonly contain genetic alterations in BRAF (Michaloglou, Vredeveld et al. 2005). This process has been termed oncogene induced senescence (OIS), with senescence defined as an irreversible growth arrest. OIS has been shown to result from induction of the $p16^{INK4a}$ /Rb, $p14^{ARF}$/p53 and/or DNA damage response pathways by BRAF and other oncogenes (Larsson 2011; McDuff and Turner 2011). Markers of OIS include enlargement and flattening of cells, expression of $p16^{INK4a}$ and p53, and activation of acidic senescence-associated β-galactosidase (SA-β-Gal). These are frequently found in premalignant lesions, but are essentially absent in malignant tumor cells, suggesting they have found ways to bypass or escape senescence. One such mechanism is deletion of $p16^{INK4a}$, which is frequently identified in malignant melanoma (Larsson 2011; McDuff and Turner 2011).

Given the importance of BRAF activation in PA, and their often indolent growth pattern, it is not surprising that several groups have examined the potential role of OIS. In Raabe et al. and Jacob et al., the investigators show that OIS markers including $p16^{INK4a}$, p53 and SA-β-Gal are expressed in both primary PA samples and low passage tumor cultures (Jacob, Quang-Khuong et al. 2011; Raabe, Lim et al. 2011). The groups also found that introducing $BRAF^{V600E}$ into either human neural stem cells, hTERT-immortalized astrocytes or fetal astrocytes results in growth arrest and the induction of

$p16^{INK4a}$ and SA-β-Gal. OIS has also been documented in benign cutaneous neurofibromas driven by NF1 loss (Courtois-Cox, Genther Williams et al. 2006).

The role of $p16^{INK4a}$ in escape from OIS and aggressive tumor growth has attracted particular attention. Jacob and colleagues found that loss of $p16^{INK4a}$ was required for isolation of astrocyte clones stably expressing $BRAF^{V600E}$. Raabe and colleagues examined $p16^{INK4a}$ expression in 66 PA cases using immunohistochemistry, and found that the 9 patients whose tumors were $p16^{INK4a}$ negative had significantly shorter overall survival. Additional support for a prognostic clinical role comes from FISH studies by two groups. Homozygous $p16^{INK4a}$ deletions were selectively identified in more aggressive anaplastic PA in Rodriguez et al. (Rodriguez, Scheithauer et al. 2011). Horbinski and colleagues examined a large cohort of 198 PLGA, and found that $p16^{INK4a}$ deletion was the second strongest predictor of adverse outcome (after midline location) in the group overall, and also correlated with significantly shorter progression-free survival in tumors with BRAF rearrangement (Horbinski, Nikiforova et al. 2012). Taken together, these data strongly support the concept that OIS contributes to the sometimes indolent behavior of PA, and that $p16^{INK4a}$ loss can contribute to escape from senescence and clinically aggressive tumor growth (Figure 7). It remains to be seen if OIS also plays a role in the pathobiology of other PLGA.

Another potential contributor to the slowing or arrest of growth in PLGA is replicative senescence mediated by shortening of telomeres. In the study done by Chong et al., PCR-based telomeric repeat amplification assay was used to document telomerase activity in many high grade gliomas but not in the 16 PA and 2 PXA examined (Chong, Lam et al. 1998). Tabori and colleagues subsequently confirmed a lack of telomerase activity in 11

pediatric low grade gliomas (Tabori, Vukovic et al. 2006), as well as a significant decrease in telomere length over time leading them to propose that lack of telomere maintenance may contribute to growth arrest or regression of PLGA. Additionally, they found that longer telomere length is inversely correlated with survival, confirming the importance of telomeres in PLGAs (Tabori, Vukovic et al. 2006; Tabori and Dome 2007). A telomerase-independent process known as alternative lengthening of telomeres (ALT) has recently been shown to be active in almost half of pediatric glioblastoma (Heaphy, Subhawong et al. 2011). However ALT is very rare or absent in PA (Tabori, Vukovic et al. 2006; Heaphy, Subhawong et al. 2011), although ALT-associated promyelocytic leukemia bodies have been identified in some cases (Slatter, Gifford-Garner et al. 2010).

### *3.3.5 Neurofibromatosis type 1 (NF1)*

NF1 is caused by germline mutations in the gene at 17q11.2 encoding for neurofibromin, a tumor suppressor that works as a GTPase activating protein to deactivate RAS (Louis, Ohgaki et al. 2007). PA are the most frequent NF1-associated CNS tumors, and it is estimated that approximately 15% of pediatric NF1 patients develop optic pathway gliomas (Listernick, Charrow et al. 1989; Rodriguez, Giannini et al. 2008). Most molecular studies have demonstrated *BRAF* alterations to be mutually exclusive with NF1 clinical status (Jones, Kocialkowski et al. 2008; Yu, Deshmukh et al. 2009; Hawkins, Walker et al. 2011; Lin, Rodriguez et al. 2012). Conversely, the neurofibromin gene is almost never altered in sporadic PA (Kluwe, Hagel et al. 2001; Wimmer, Eckart et al. 2002), and NF1-associated and sporadic PA have distinct global gene expression patterns (Sharma, Mansur et al. 2007; Rodriguez, Giannini et al. 2008).

However, in rare instances NF1-associated tumors have been reported with additional activating mutations in *BRAF*. Such cases reported include *KIAA1549:BRAF* fusion in a NF1-associated pilomyxoid astrocytoma (Forshew, Tatevossian et al. 2009), a $BRAF^{V600E}$ point mutation in a NF1-associated PA(Eisenhardt, Olbrich et al. 2010), and an interesting "triple hit" with concomitant NF1 syndrome, $BRAF^{V600E}$, and *KIAA1549-BRAF* fusion (Cin, Meyer et al. 2011).

While a major molecular consequence of neurofibromin loss is MAPK pathway activation, additional signaling nodes contribute to tumorigenesis in NF1, including mTOR pathway activation (Banerjee, Gianino et al. 2011). Indeed, activation of the PI3K/AKT/mTOR signaling axis is a prominent feature of the rare PA that develop anaplastic change (Rodriguez, Scheithauer et al. 2011), 24% of which are NF1-associated. Recent studies have also highlighted a role for the non-neoplastic stromal microenvironment in optic glioma development in NF1 model systems. *Nf1* heterozygous microglia are required for glioma formation in these models, in addition to *Nf1* homozygous loss in neoplastic astrocytes. Recent evidence suggests that stromal derived factors (e.g. CXCL12) lead to altered cAMP levels and facilitate tumor formation in this setting (Warrington, Woerner et al. 2007).

### *3.3.6 AKT/mTOR*

Another important signaling pathway operating downstream from neurofibromin and RAS is AKT/mTOR, which leads to increased protein translation, cell growth and survival through two multiprotein complexes (mTORC1 and mTORC2) that vary in their sensitivity to rapamycin (Babcock and Quilliam 2011; Mendoza, Er et al. 2011; Magnuson, Ekim et al. 2012). The prototypical low grade glioma in which mTOR

activation is an intrinsic molecular property is the tuberous sclerosis-associated SEGA (Chan, Zhang et al. 2004). Tuberous sclerosis is characterized by germline mutations in the tumor suppressor genes *TSC1* or *TSC2*, which regulate AKT activation through RHEB, and recent clinical success has been described with mTOR pathway inhibitors (Krueger, Care et al. 2010). Some studies have also highlighted a role for mTOR signaling in NF1-associated tumors, in particular PA (Dasgupta, Yi et al. 2005). Examination of NF1 deficient mouse models has suggested anatomical variation in neuroglial progenitor proliferation through AKT activation (Lee da, Yeh et al. 2010). Recent studies have also suggested a possible role for differential mTOR activation in subsets of NF1 associated low grade gliomas difficult to classify by traditional criteria (Jentoft, Giannini et al. 2010).

Outside of the syndrome-associated low grade gliomas, little is known at the present time regarding mTOR pathway activation in tumorigenesis or progression in PLGA. However, immunohistochemical studies suggest the pathway is active in at least some tumors. Of interest, mutations in *PIK3CA* have been reported in 3 (of 4) rosette-forming glioneuronal tumors, a rare low grade neoplasm with a frequent pilocytic astrocytoma-like component (Ellezam, Theeler et al. 2012).

### *3.3.7 Gene Expression Analysis*

Early studies suggested that PA have expression profiles distinct from those of high grade gliomas (Rickman, Bobek et al. 2001; Hunter, Young et al. 2002; Colin, Baeza et al. 2006), and that PA could also be differentiated from diffuse astrocytoma (Rorive, Maris et al. 2006) oligodendroglioma and normal white matter (Gutmann, Hedrick et al. 2002). Additional studies identified MBP and Matrilin as potential markers

of poor outcome (Wong, Chang et al. 2005; Sharma, Watson et al. 2006). Gene expression analysis has also been used to suggest potential cells of origin for PA, which may be region-specific (Sharma, Mansur et al. 2007; Tchoghandjian, Fernandez et al. 2009). However, unlike other childhood brain tumors such as medulloblastoma and ependymoma, large-scale studies integrating pathology, clinical factors, and mutations/copy number change with mRNA and miRNA expression have not yet been published. For pediatric medulloblastoma and adult glioblastoma, such correlations have been critical for parsing clinically and genetically meaningful tumor subgroups, potential cells of origin, and generating molecularly relevant classification schemes. Hopefully similar integrated data will soon be available for PLGA.

## 3.4 CLINICAL AND THERAPEUTIC IMPLICATIONS

### *3.4.1 Diagnostic Utility of BRAF Alterations*

Distinguishing between the various types of PLGA can sometimes be difficult, thus testing for *BRAF* alterations could potentially be of great use diagnostically. In the first report in which *KIAA1549:BRAF* fusions were identified, Jones and colleagues noted that almost all cases were PA (Jones, Kocialkowski et al. 2008). A few PLGA not originally diagnosed as PA contained the alteration, but because they were all cerebellar and associated with survival of greater than 12 years the authors suggested that they might represent PA which had been misclassified. A number of subsequent investigations have confirmed a strong association between PA histology and *BRAF* duplication/fusion (Jacob, Albrecht et al. 2009; Lawson, Tatevossian et al. 2010; Schiffman, Hodgson et al. 2010), but some exceptions exist. In a study including 27 pediatric diffuse astrocytoma,

Jacob and colleagues did not detect duplication of 7q34 (Jacob, Albrecht et al. 2009), but the same group later found some diffuse astrocytoma with *KIAA1549:BRAF* fusions (Hawkins, Walker et al. 2011). Forshew and colleagues reported a *KIAA1549:BRAF* fusion in 1 of 11 pediatric diffuse astrocytoma in their study (Forshew, Tatevossian et al. 2009), while Sievert and colleagues identified the duplication in 3 of 6 of these tumors (Sievert, Jackson et al. 2009).

*BRAF* duplication/fusion events occur fairly frequently in pilomyxoid astrocytoma (Forshew, Tatevossian et al. 2009; Hawkins, Walker et al. 2011; Lin, Rodriguez et al. 2012) supporting a recent study suggesting that pilocytic and pilomyxoid astrocytoma may be part of a single disease spectrum (Johnson, Eberhart et al. 2010). However, the few PXA examined to date have not shown these alterations (Forshew, Tatevossian et al. 2009; Lin, Rodriguez et al. 2012). *BRAF* fusions have also not been identified in high grade pediatric gliomas. Finally, *BRAF* fusions were recently reported in a few pediatric low grade glioneuronal tumors (Lin, Rodriguez et al. 2012). Taken together, these reports of rare fusions in diffuse astrocytoma and other non-pilocytic lesions suggests that such molecular changes involving *BRAF* are not absolutely specific for PA.

In contrast to *BRAF* duplication/fusion, point mutations in *BRAF* are most common in low grade pediatric brain tumors other than PA, and are also found in higher grade gliomas (Schiffman, Hodgson et al. 2010). Dougherty and colleagues identified $BRAF^{V600E}$ mutations in 9/18 (50%) of gangliogliomas as well as several PXA (Dougherty, Santi et al. 2010). A study of 1,320 nervous system tumors found that $BRAF^{V600E}$ was most common in PXA (57/87, 66%) and WHO grade I ganglioglioma

(14/77, 18%) (Schindler, Capper et al. 2011). Another group also identified common $BRAF^{V600E}$ mutations in PXA (12/20, 60%) (Dias-Santagata, Lam et al. 2011).

### *3.4.2 Prognostic Utility of BRAF Alterations in PLGA*

Another potential clinical application of molecular testing for alterations in *BRAF* and other MAPK pathway members is to determine which PLGA are more aggressive, allowing more precise delivery of therapy. Neither our group nor Cin and colleagues found better outcomes in PLGA patients whose tumors contained *BRAF* fusions (Cin, Meyer et al. 2011; Lin, Rodriguez et al. 2012). Hawkins and colleagues focused on a "clinically relevant" subgroup of PLGA cases defined as non-NF1 patients with non-cerebellar tumor location and subtotal resection. They reported that *KIAA1549:BRAF* fusions were significantly associated with better outcome in a cohort of 70 PLGA patients meeting these criteria (Hawkins, Walker et al. 2011). However, when we examined an analogous subgroup within our cohort we did not identify any trend towards better outcome with *BRAF* fusion (Lin, Rodriguez et al. 2012).

Horbinski and colleagues examined *BRAF* status in 118 unselected PA with outcome data, but did not identify significantly different outcomes in cases with and without the duplication in their initial study (Horbinski, Hamilton et al. 2010). In a subsequent larger study of 198 cases by this group, of which 143 were PA, they found a trend towards improved progression free survival in patients with low grade gliomas whose tumors had *BRAF* rearrangements ($p = 0.06$)(Horbinski, Nikiforova et al. 2012). They also noted that the only patients with *BRAF* rearrangements who died had midline tumors. In contrast, patients in their cohort with $BRAF^{V600E}$ had a trend towards increased risk of progression ($p = 0.07$) (Horbinski, Nikiforova et al. 2012). Given the somewhat

conflicting data in these various studies, it seems that examination of a larger cohort, preferably from a controlled clinical trial, will be necessary to determine the prognostic role of *BRAF* alterations.

### *3.4.3 Clinical Testing for BRAF Alterations*

To date, no standard approach to testing for the various alterations affecting MAPK signaling in PLGA has been developed. Because fresh tissue is not always available, assays which can work with formalin fixed, paraffin-embedded (FFPE) specimens will be of greatest utility. Given the frequent presence of $BRAF^{V600E}$ point mutations in cutaneous melanoma and other common neoplasms arising outside the CNS, many clinical labs have standard tests for this alteration based on sequencing or hybridization (Sharma and Gulley 2010). A monoclonal antibody specific for the $BRAF^{V600E}$ protein has also recently been developed, and will be useful in small specimens (Capper, Preusser et al. 2011).

A range of approaches to identification of BRAF fusions have also been reported. Many laboratories have used duplication of the 7q34 region as a marker for this change. This can be assessed by FISH, which has the advantages of working well in FFPE tissues, spatially localizing the change, and detecting it in small groups of cells. As costs have dropped, array CGH is increasingly being used in a diagnostic capacity in both fresh and FFPE samples, and this technology can detect changes across the genome rather than only those at 7q34, including for example loss of the $p16^{INK4a}$ locus. Direct identification of fusion transcripts using reverse transcription polymerase chain reaction (RT PCR) is highly specific and yields information on fusion breakpoints, but only pre-determined regions can be assessed (Lin, Rodriguez et al. 2012). While this method has traditionally

been performed using RNA extracted from frozen tumors, it has recently been shown that 97% sensitivity and 91% specificity can be achieved using fusion transcripts isolated from FFPE tissue (Tian, Rich et al. 2011). Finally, pyrosequencing has been used to detect fusions and changes in *BRAF* gene dosage in FFPE specimens, and may identify some alterations not found using PCR primers specific for various fusions (Setty, Gessi et al. 2011).

### *3.4.4 Preclinical Testing Models*

The development of effective new therapies for PLGA would be greatly assisted by cell or animal based models which accurately reflect their molecular biology and pathology. Unfortunately, these are not as advanced overall as is true for high grade gliomas, although murine transgenic models of NF1-associated optic gliomas have been generated and used for preclinical testing (Bajenaru, Garbow et al. 2005; Hegedus, Banerjee et al. 2008). Another genetically engineered mouse model which may prove useful in preclinical PLGA testing was recently reported by Gronych and colleagues (Gronych, Korshunov et al. 2011). They found that BRAF activation alone in nestin-positive murine neural progenitors was sufficient to induce the formation of cerebral low grade gliomas, but was achieved by a combination of V600E mutation and deletion of the negative regulatory region. It therefore still remains to be seen if fusions of the *BRAF* kinase domain with KIAA1549 or other partners analogous to those in humans will be sufficient to drive tumorigenesis.

Cultures of human PLGA represent an additional potential platform for preclinical testing. It has been difficult to develop useful lines from PA and other indolent PLGA, but some have been reported (Pfister, Janzarik et al. 2008; Bax, Little et al. 2009). The

recent description of OIS in low passage cultures may account at least in part for these problems (Jacob, Quang-Khuong et al. 2011; Raabe, Lim et al. 2011). It may be possible to develop more robust cultures by maintaining them as neurospheres in serum-free media, or by manipulating expression of $p16^{INK4a}$ and other OIS factors. Now that signature genetic defects have been discovered it will be critical to demonstrate that any cell lines developed carry the molecular markers of the tumors from which they are derived.

Some preclinical testing has been done with the models currently available. Using their NF1 mutant optic glioma model, Banerjee and colleagues have explored various rapamycin doses affecting mTOR signaling, and shown that not all pathway biomarkers accurately reflect effective pathway response or changes in tumor growth (Banerjee, Gianino et al. 2011). Proliferation of one human PA culture was inhibited by pharmacological MAPK blockade (Pfister, Janzarik et al. 2008). Finally, murine neurospheres transduced with active BRAF are responsive to Sorafenib (Gronych, Korshunov et al. 2011), and engineered human neural stem and progenitor cell systems (Jacob, Quang-Khuong et al. 2011; Raabe, Lim et al. 2011) could also be used in this fashion.

### *3.4.5 Therapeutic Possibilities*

Given the high frequency of BRAF activation via duplication/fusion and mutation among pilocytic and pilomyxoid astrocytomas, there is considerable interest in targeted inhibition of the MAPK pathway as therapy for these tumors (Figure 8). Sorafenib (Nexavar, Bayer and Onyx Pharmacuticals) is an inhibitor of BRAF which has less potency against $BRAF^{V600E}$. Currently, Sorafenib is in phase II studies against recurrent

and chemotherapy-refractory PLGA (NCT01338857 ClinicalTrials.gov). AZD6244 (Selumetinib, AstraZeneca and Array BioPharma) is a potent inhibitor of MEK also currently in phase I trials against PLGA (NCT01386450, NCT01089101 ClinicalTrials.gov).

*BRAF*$^{V600E}$ mutations are rare among PLGA overall, but are relatively common among PXA, gangliogliomas and a subset of extra-cerebellar pilocytic astrocytomas (Dougherty, Santi et al. 2010; Schiffman, Hodgson et al. 2010; Dias-Santagata, Lam et al. 2011; Schindler, Capper et al. 2011). Vemurafenib is a competitive small molecule that was designed to bind to and inhibit the ATP binding domain of the *BRAF*$^{V600E}$mutant, but not other forms of BRAF (Shahabi, Whitney et al. ; Chapman, Hauschild et al. 2011). Following impressive albeit transient responses of recurrent melanoma to Vemurafenib (Chapman, Hauschild et al. 2011), the United States Food and Drug Administration (FDA) has approved it for the treatment of *BRAF*$^{V600E}$ mutation positive, inoperable, or metastatic melanoma. It is anticipated that there will be a clinical trial of Vemurafenib against *BRAF*$^{V600E}$ mutant low-grade gliomas in the near future.

The AKT/mTOR pathway has been implicated in several types of PLGA, including SEGA and PA. Clinical trials have demonstrated that mTOR inhibitors including Sirolimus and Everolimus (RAD-001 or Afinitor; Novartis Pharmaceuticals) have activity against SEGA (Franz, Leonard et al. 2006), and Everolimus has received approval by the FDA for the treatment of SEGA that cannot be surgically resected. A recent reported phase I/II study of Sirolimus (Rapamune, Pfizer) and Erlotinib (Tarceva, Genentech) examined 16 patients with recurrent PLGA (Packer, Yalon et al. 2010). Of the 7 children with NF-1 in this clinical trial, all patients had either stable disease or

tumor responses. A phase II study of Everolimus against recurrent and chemotherapy-refractory PLGA has recently been completed (NCT00782626); results of this study are pending. As agents targeting the MAPK and AKT/mTOR pathways are tested, it will be critical to search for molecular markers which are predictive of response.

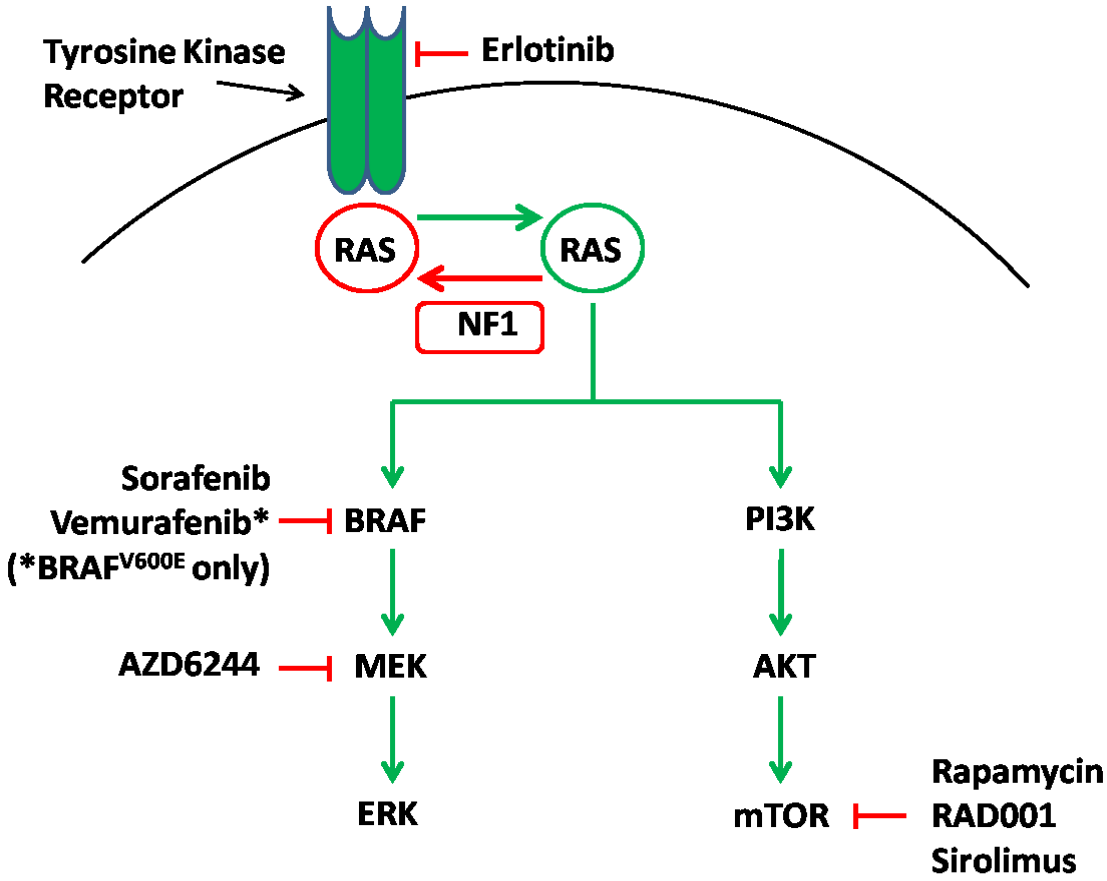


**Figure 3-8** – Therapeutic agents targeting BRAF/RAF1 and AKT/mTOR pathways

## 3.5 CONCLUSIONS

It is now clear that alterations affecting the *BRAF* oncogene and other members of the MAPK cascade represent the main genetic defects in PLGA. Segmental duplications resulting in fusions between *KIAA1549* and *BRAF* are most common, and result in a novel protein with constitutive kinase activity. Tumors lacking *KIAA1549:BRAF* fusions often have other changes with similar functional effects, including *SRGAP3:RAF1* and *FAM131B:BRAF* fusions and mutations and insertions activating *BRAF*. These findings link syndromic and sporadic PA, and suggest a dominant signaling pathway to target therapeutically. The detection of BRAF activation as a cardinal feature of PLGA has also led to the discovery that oncogenic induction of senescence may account for the spontaneous growth arrest or regression of some tumors.

The challenge now is to translate these new discoveries in improved diagnostic, prognostic and predictive markers, and to develop targeted therapies for patients with clinically aggressive tumors. PLGA are a heterogeneous group of lesions, and while BRAF fusions are not entirely specific for one entity they are almost always encountered in PA, thus molecular BRAF testing may help us to distinguish these tumors from other pediatric gliomas. The prognostic role of BRAF alteration is still not clear, and analysis of large, uniformly treated cohorts will likely be required to definitively assess associations with outcome. Finally, it will be critical to determine if specific genetic changes predict response to therapies targeting BRAF or other pathway members. The recent initiation of several clinical trials of MAPK inhibitors in PLGA patients should provide some initial insights into this key question.

**ACKNOWLEDGMENTS**

The work of CGE has been supported by the Children's Cancer Foundation and the PLGA foundation. The Childhood Brain Tumor Foundation provided support to FR.

# Chapter 4: Inhibition of Monocarboxylate Transporter-4 Depletes Stem-Like Glioblastoma Cells in a Lactate Independent Fashion

Kah Suan Lim[2] , Kah Jing Lim[2], Antionette C. Price[2], Brent A. Orr, MD, PhD[5], Charles G. Eberhart, MD, PhD[2,3,4] and Eli E. Bar, PhD[1,2]

[1]Department of Neurosurgery, Case Western Reserve University School of Medicine, Cleveland, OH 44106, USA

[2]Department of Pathology, Johns Hopkins University School of Medicine, Baltimore, MD 21205, USA

[3]Department of Ophthalmology, Johns Hopkins University School of Medicine, Baltimore, MD 21205, USA

[4]Department of Oncology, Johns Hopkins University School of Medicine, Baltimore, MD 21205, USA

[5]Department of Pathology, St. Jude Children's Research Hospital, Memphis, TN 38105, USA

**Correspondence to:**

Eli E. Bar, PhD

Assistant Professor, Department of Neurological Surgery

School of Medicine, Case Western Reserve University

Adjunct Assistant Professor, Johns Hopkins University School of Medicine

Mailing Address:

Case Western Reserve University

Department of Neurology

Robbins Building, Room E750A

10900 Euclid Avenue

Cleveland OH, 44106-4938

Office (216) 368-0933

Fax (216) 368-1144

E-mail: eli.bar@case.edu

**Running Title**: MCT4 inhibition depletes stem-like cells in GBM

**Keywords**: Hypoxia, Monocarboxylate Transporter 4, Stem Cells, Glioma

**Grant Support:** This work was supported by the Brain Tumor Funders Collaborative and R01 NS55089

**Pages**: 25

**Figures**: 5

**ABSTRACT**

Hypoxic regions are frequent in glioblastoma (GBM), the most common type of malignant adult brain tumor, and increased levels of tumor hypoxia have been associated with worse clinical outcomes. To unmask genes important in hypoxia, we treated GBM neurospheres in hypoxia and identified Monocarboxylate transporter-4 (MCT4) as one of the most upregulated genes. To investigate the clinical importance of MCT4 in GBM, we examined clinical outcomes and found that patients with at least two-fold upregulation of MCT4 have a significantly shorter survival than those with intermediate expression. Consistent with this, MCT4 upregulation correlated with the aggressive mesenchymal subset of GBM and MCT4 downregulation correlated with the less aggressive CIMP subset of GBM. Immunohistochemical analysis of tissue microarrays, confirmed that MCT4 protein levels were increased in high-grade as compared to lower grade astrocytomas, further suggesting that MCT4 is a clinically relevant target. To test the requirement for MCT4 in vitro, we transduced neurospheres with lentiviruses encoding shRNAs against MCT4, resulting in growth inhibition of 50-80% in hypoxia in two lines. Interestingly, while MCT4 was expressed at lower levels in normoxia, silencing in 21% oxygen also inhibited growth to a similar extent. MCT4 knockdown was associated with a decreased percentage of cells expressing the stem-cell marker CD133, and increased apoptotic fraction. We also found that flow-sorted CD133-positive cells had almost six-fold higher MCT4 levels than CD133-negative cells, suggesting that the stem-like population might have a greater requirement for MCT4. Most importantly, MCT4 silencing also slowed GBM intracranial xenograft growth in vivo. Interestingly, while MCT4 is a well-characterized lactate exporter, we found that both intracellular and

extracellular lactate levels did not change following MCT4 silencing, suggesting a novel lactate export-independent mechanism for growth inhibition in GBMs. To identify this potential mechanism, we performed microarray analysis on control and shMCT4 expressing HSR-GBM1 neurospheres, and found a dramatic reduction in expression of multiple HIF1alpha regulated genes following MCT4 knockdown, including Vascular Endothelial Growth Factor (VEGF), lysyl-oxidase (LOX), and Carbonic Anhydrase IX (CAIX). The overall reduction in HIF transcriptional response was further validated using an HRE-dependent GFP reporter line.

## 4.1 INTRODUCTION

Glioblastoma (GBM) are the most frequent malignant brain tumors in adults, but are still incurable, thus new therapeutic targets and improved treatments are needed. These neoplasms frequently exhibit tumor hypoxia and high glycolytic rate (Zhou, Shingu et al. 2011). Signaling pathways such as Hedgehog, Notch, and WNT have been discovered to play major roles in the proliferation and survival of primitive, stem-like GBM cells (Purow, Haque et al. 2005; Bar, Chaudhry et al. 2007; Clement, Sanchez et al. 2007; Ehtesham, Sarangi et al. 2007; Zhang, Zheng et al. 2008; Fan, Khaki et al. 2010; Hu, Zheng et al. 2011; Gong and Huang 2012; Zhang, Zhang et al. 2012). Work done by our group and others has established that stem-like GBM cells favor low oxygen levels and are typically found in the hypoxic tumor core (Heddleston, Li et al. 2009; Li, Bao et al. 2009; Pistollato, Chen et al. 2009; Soeda, Park et al. 2009; Bar, Lin et al. 2010; Seidel, Garvalov et al. 2010) (and reviewed in (Heddleston, Li et al. 2010; Bar 2011). However, while it is clear that Hypoxia Inducible Factor -1 and -2 alphas (HIF1alpha and

HIF2alpha) are intimately involved in the induction of stem-like phenotype under hypoxia, factors facilitating this critical phenotypic change are still unknown.

We investigated the role of the Monocarboxylate Transporter 4 (MCT4) in malignant gliomas for several reasons. First, MCT4 levels are greatly induced in the stem cell rich hypoxic microenvironment of GBMs. Second, MCTs have been linked to the regulation of glycolytic metabolism (Le Floch, Chiche et al. 2011), and glycolytic metabolism is crucial for the expansion of neoplastic as well as non-neoplastic stem cells (Collins, Nielsen et al. 1998; Pistollato, Chen et al. 2007; Lin, Kim et al. 2008; Westfall, Sachdev et al. 2008; Heddleston, Li et al. 2009; Pistollato, Chen et al. 2009; Bar, Lin et al. 2010; Heddleston, Li et al. 2010; Bar 2011; Zhu, Zhao et al. 2011; Estrada, Albo et al. 2012). MCT4 is one of four proton-linked monocarboxylate transporters. Expression patterns of MCTs vary with cell type. For example, while MCT1 is expressed primarily in endothelial cells, MCT4 is expressed mainly in astrocytes. Neurons, on the other hand, express primarily MCT2.

Because MCT4 is a critical component in glycolytic metabolism, and such metabolism is utilized in non-neoplastic neural stem cells (Zhu, Zhao et al. 2011), we hypothesized that neoplastic stem-like cells may be susceptible to MCT4 inhibition. The potential utilization of MCT1 inhibition as an anti GBM therapeutic approach has been explored using adherent, high serum propagated cells (Froberg, Gerhart et al. 2001; Mathupala, Parajuli et al. 2004; Fang, Quinones et al. 2006; Li, Pang et al. 2009; Colen, Shen et al. 2011; Miranda-Goncalves, Honavar et al. 2012). However, the role of HIF1alpha-regulated (Ullah, Davies et al. 2006) MCT4 in GBMs, including stem-like tumor cells has yet to be investigated.

In this study, we demonstrate that MCT4 expression is associated with increased world health organization (WHO) glioma grade, and inversely correlate with overall survival of GBM patients. In addition, based on the recent subgroup classification of GBMs, tumors which are classified as "mesenchymal" are more aggressive and express higher levels of MCT4. MCT4 appears to regulate proliferation, survival, and xenograft implantation/growth of some GBM neurosphere lines. Furthermore, we found that suppression of MCT4, using shRNAs, results in a dramatic downregulation of multiple HIF1alpha transcriptional targets. These effects appear to be independent of lactate homeostasis and provide a potential mechanism by which MCT4 may regulate stem-like phenotype and the hypoxic response in GBM. Overall, our data suggest that MCT4 represents a novel therapeutic target in GBMs, and links its expression to regulation of the hypoxic response driven by HIF.

## 4.2 MATERIALS AND METHODS

GBM Neurosphere Lines and Hypoxic Conditions

HSR-GBM1 (020913) was a kind gift from Dr. Angelo Vescovi and JHH-GBM10 was established from a freshly resected glioblastoma tumor and passaged as previously described (Galli, Binda et al. 2004). The lines were maintained in culture as originally described, and their identities confirmed at least once each year using tandem repeat analysis. A hypoxic chamber maintained at 37°C, 1% $O_2$, 5% $CO_2$ and 94% $N_2$ (COY laboratory equipment, Grass Lake, MI) was used to conduct *in vitro* hypoxic experiments. All hypoxic experiments were conducted on cells that were plated and allowed to recover overnight before hypoxic induction.

Lentivirus Preparation, Concentration and Transduction

Lentiviruses were produced using previously established method (Westerman, Ao et al. 2007). Briefly, MCT4 shRNA plasmids were purchased from Open Biosystems (Thermo Fisher Scientific, Huntsville, AL) and packaged into lentiviral vectors by co-transfection into 293T cells with plasmids containing Gag/Pol, REV and VSV-G. Viral supernatant was harvested 24h, 48h, 72h, and 96h post transfection and filtered through 0.45μm low protein-binding syringe filters. Glioblastoma neurosphere cultures were plated and transduced with viruses and then incubated at 37°C and 5% $CO_2$ for a week. After 1 week, cells were put under selection with 1-5μg/ml of puromycin (Sigma, St. Louis, MO) for at least a week until there were enough healthy cells to be used for experiments. Silencing of MCT4 was verified by both quantitative real-time PCR and western blot.

RNA and Protein Analyses

RNA analyses were performed by reverse transcription into cDNA then quantitative real-time PCR analysis in triplicates using SYBR Green reagents (Applied Biosystems, Foster City, CA; Bio-Rad, Hercules, CA). To prevent amplification of genomic DNA, on-column DNase digest was performed (Qiagen RNase-free DNase kit) during RNA extraction prior to reverse transcription. Standard curve analyses were used to determine RNA levels and beta-actin was used as a housekeeping gene for normalization. Primer sequences were as follows: MCT4 Forward – 5'-GAGTTTGGGATCGGCTACAG-3' and Reverse – 5'-CGGTTCACGCACACACTG-3'. ′; CAIX Forward – 5'-CTTGGAAGAAATCGCTGAGG-3'; and CAIX Reverse – 5'-TGGAAGTAGCGGCTGAAGTC-3'; Human actin-β Forward – 5'-

CCCAGCACAATGAAGATCAA-3′; and human actin-β Reverse: 5′-GATCCACACGGAGTACTTG- 3′. Additional primer sequences are available upon request.

Protein analyses were performed via immunoblot assays using antibodies against human MCT4 (sc-50329, Santa Cruz Biotechnology, Santa Cruz, CA), HIF1alpha (Catalog number 610959, 1:250, BD Biosciences, Franklin Lakes, NJ) and β-Tubulin (Catalog number mAB5564, 1:10000, Millipore, Billerica, MA)

Flow Cytometric Analysis

Cells were exposed to 24h normoxia or hypoxia and stained for CD133, then flow cytometry was performed as previously (Fan, Matsui et al. 2006). For experiments utilizing the HSR-GBM1 G6D hypoxia reporter line, cells were treated as described above, and following dispersal to single cell suspensions were immediately analyzed by flow cytometry without further manipulation.

Cell Growth, Annexin and Cell Cycle Analyses

Cell viability was assessed with an MTS assay. Cells were plated in 96-well plates and read using a plate reader 1 h after the addition of MTS reagent. Cell counts were performed using the Guava PCA machine and Guava Viacount reagent (Millipore, Billerica, MA). Annexin assays and cell cycle analyses were performed using the Guava PCA machine and Guava Cell Cycle and Nexin reagents.

Lactate Assays

Cells were plated in phenol-red free medium and allowed to recover overnight before being placed in either hypoxic or normoxic culture conditions for 24h. For extracellular lactate measurement, conditioned media was collected. For intracellular lactate measurement, cells were pelleted and 500ul of sterile distilled water was used to lyse each sample. Lactate assays were performed according to the manufacturer's instruction (Eton Bioscience Inc. L-Lactate Assay Kit).

Orthotopic Xenograft Transplantation

$1x10^5$ shRNA transduced HSR-GBM1 cells were stereotactically xenografted into each nude mouse: 7 mice for control, 8 mice for sh1 and 5 mice for sh2. Mice were sacrificed after approximately 2 and a half months and brains were taken out and sectioned. Sections were stained with hematoxylin and eosin and tumor area was measured by Dr. Charles Eberhart in microscopic images taken from coronal sections taken at the level of the injection site.

Immunofluorescence

Immunofluorescence staining was performed using standard technique on GBM neurospheres incubated for 24h either in normoxia or hypoxia then cytospun onto slides, probed with MCT4 antibody (sc-50329, Santa Cruz Biotechnology, Santa Cruz, CA) and counterstained with DAPI (4',6-diamidino-2-phenylindole).

Immunohistochemistry

Immunohistochemical staining was performed using standard technique on formalin-fixed paraffin-embedded tissue sections, probed with MCT4 antibody (sc-50329, Santa Cruz Biotechnology, Santa Cruz, CA) and counterstained with hematoxylin.

Statistical Methods

Unless otherwise noted, *in vitro* and quantitative PCR data are shown as mean values with error bars representing standard error of the mean for (at a minimum) three replicates, and experiments were repeated at least twice. Comparison of mean values between groups was evaluated by unpaired, two-tailed t-test or one-way Anova. For all statistical methods, a p-value less than 0.05 was considered significant. All tests were performed by using GraphPad Prism 5 (GraphPad Software, La Jolla, CA).

Microarray analysis

Neurospheres were transduced with shMCT4 (Sh1 and Sh2) or control and selected for one week with puromycin. Then, after removal of puromycin, cells were exposed to normoxia or hypoxia for 24 hours. RNA samples were processed and analyzed using Agilent Human single color 4x44k arrays according to the manufacturer protocols. GeneSpring GX (Agilent Technologies, Santa Clara, CA) software package was used to determine expression levels using standard parameters.

Hypoxia Reporter - HSR-GBM1 G6D

HSR-GBM1 cells were transfected with an HRE-GFP-d2 construct which was a kind gift from Dr. Brown Martin (Vordermark, Shibata et al. 2001). Following clonogenic selection of positive GFP-clones, we introduced the pLenti-UbC-dsRed-Express construct and a single clone (G6D) was selected on the basis of its ability to initiate infiltrative orthotopic xenografts in nude mice (data not shown).

## 4.3 RESULTS

### *4.3.1 MCT4 is overexpressed in hypoxic GBMs and associated with poor clinical outcome*

Our group and others have previously shown that hypoxia induces stem-like characteristics in GBM neurospheres, and that inhibition of HIF1alpha a master transcriptional regulator of the hypoxic response, reversed the effects of hypoxia and led to decreased clonogenicity and growth *in vitro* and tumor formation *in vivo* (Heddleston, Li et al. 2009; Li, Bao et al. 2009; Soeda, Park et al. 2009; Bar, Lin et al. 2010). Microarray analysis was subsequently performed on HSR-GBM1 and JHH-GBM10 glioblastoma neurosphere lines grown in normoxia (21% oxygen) or hypoxia (1% oxygen) for 24 hours. We identified monocarboxylate transporter 4, MCT4 (also known as SLC16A3), as one of the top 10 most upregulated genes in response to hypoxia (Figure 1A, SLC16A3 highlighted in green). We hypothesized that as the only monocarboxylate transporter (MCT) transcriptionally up-regulated in hypoxia (transcription of other MCTs were either unchanged or even downregulated, data not shown), it might play a critical role in therapy-resistant stem-like cell survival and that inhibition of MCT4 would target GBM tumor growth.

We first examined the levels of MCT4 in GBM patients. Figure 1B shows gene expression data collected from the gene expression omnibus (GEO) database of various glioma grades. We found that MCT4 mRNA is significantly overexpressed in Grade IV gliomas compared to normal brain, Grade II and Grade III gliomas (Figure 1B). To determine if this difference in expression is also present at the protein level, we

performed immunohistochemical analysis on tissue microarrays of grades II, III and IV gliomas. Semi-quantitative analysis of MCT4 immunoreactivity confirmed that MCT4 is overexpressed in GBM when compared to lower grade gliomas (Figure 1C). Indeed, overexpression of MCT4 may be a GBM-specific phenomenon as normal brain cores were always negative (data not shown).

We also found that MCT4 was most highly expressed in GBM tumors distal to blood vessels in regions generally associated with hypoxia. This latter finding is in agreement with our *in vitro* data that MCT4 is overexpressed in hypoxia (representative core shown in Figure 1C). Since increased intratumoral hypoxia has been linked to decreased survival in GBM patients (Szeto, Chakraborty et al. 2009) we hypothesized that as a surrogate marker of hypoxia, MCT4 may also predict survival. Examination of GBM patient survival data in REMBRANDT (https://caintegrator.nci.nih.gov/rembrandt/) revealed that MCT4 level is inversely correlated with survival of GBM patients (Figure 1E, log rank survival test, $p<0.05$). Furthermore, examination of MCT4 expression levels within the GBM subgroups described by Verhaak et al (Verhaak, Hoadley et al. 2010) strongly suggested that MCT4 is overexpressed primarily in the most aggressive mesenchymal subclass (Supplementary Figure S1). Finally, using the same TCGA (The Cancer Genome Atlas) dataset, we found that MCT4 is overexpressed primarily in the non-G-CIMP (Glioma CpG Island Methylator Phenotype) tumors, which have traditionally been associated with worse outcome than the G-CIMP subgroup (Supplementary Figure S2). Taken together, these data indicate that MCT4 is overexpressed in hypoxic GBMs and is associated with aggressive tumor behavior.

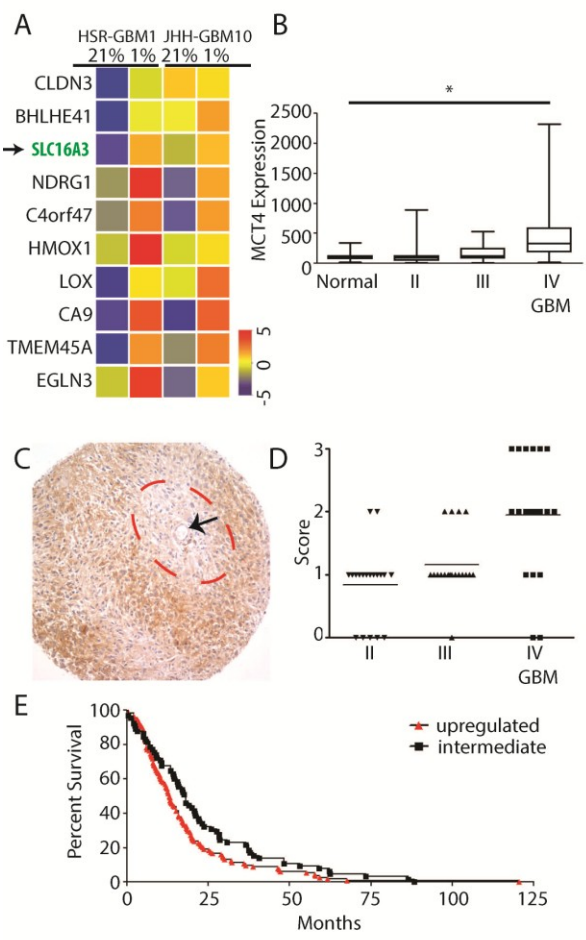


**Figure 4-1:** MCT4 expression is upregulated in hypoxic GBM neurospheres, increase with tumor grade, and is associated with poor survival

(A) Microarray data showing MCT4 (SLC16A3, highlighted in green) is one of the top ten upregulated genes in HSR-GBM1 and JHH-GBM10 in response to hypoxia (1% Oxygen). (B) Gene expression data from GEO (Gene Expression Omnibus) database of MCT4 in normal brain, Grade II, Grade III, and grade IV (GBM) gliomas. (C) Representative GBM tumor core immunostained for MCT4 showing blood vessel (arrow) and presumably normoxic (within dotted circle) and hypoxic areas (outside dotted circle). (D) Graph of scored tissue microarray of brain tumors comparing MCT4 protein expression in GBM tumors and Grade II and Grade III gliomas. (E) Kaplan-Meier survival curve comparing survival of GBM patients with upregulation of MCT4 (red triangles) and GBM patients with intermediate levels of MCT4 (black squares) (log rank survival test, $p<0.05$).

### *4.3.2 MCT4 levels increase in hypoxic GBM neurospheres*

To confirm induction of MCT4 in hypoxia, we exposed HSR-GBM1, JHH-GBM10, and JHH-GBM14 neurospheres to normoxia and hypoxia *in vitro* and quantitated MCT4 mRNA levels using quantitative Real Time PCR. We found that MCT4 mRNA levels increased over time, reaching maximal levels after 20 hours in HSR-GBM1 and 48 hours post exposure to hypoxia in JHH-GBM10 and JHH-GBM14 (Figure 2A-C, dark grey bars). These data are consistent with an earlier report showing that MCT4 is under direct HIF1alpha transcriptional regulation (Ullah, Davies et al. 2006). Interestingly, the increase in MCT4 mRNA levels over time was not limited to hypoxia. We measured significant increases even in normoxia, with maximal induction seen 48 hours after plating cells in fresh medium, suggesting that cell density may also play a role in MCT4 induction (Figure 2A-C, clear bars). To measure MCT4 protein levels we performed western blot analysis on neurospheres exposed to normoxia or hypoxia for 0, 2, 4, and 5 days. Consistent with the mRNA data, MCT4 protein levels increased rapidly, reaching maximal levels 48 hours and 96 hours in HSR-GBM1 neurospheres exposed to hypoxia and normoxia , respectively (Figure 2D). Thus MCT4 protein and mRNA levels increase in response to hypoxia, but also in normoxia as cultures become more confluent. In two additional lines, JHH-GBM10 and JHH-GBM14, we found significant increases in MCT4 levels following 48 hours of hypoxic treatment (Figure 2E). Interestingly, JHH-GBM10 had high baseline MCT4 mRNA and protein levels even in normoxia, which further increased under hypoxia, suggesting that normoxic expression of MCT4 vary with cell line and may potentially indicate difference in dependency. U87-MG protein lysate was used as a loading control as this line expresses MCT4 constitutively.

MCT4 plasma membrane localization is tightly regulated by its association with the plasma membrane glycoprotein CD147 (Basigin) (Kirk, Wilson et al. 2000), we therefore examined MCT4 subcellular localization in response to hypoxic treatment. To this end, we immunostained cytospun neurospheres pre-exposed to either normoxia or hypoxia for MCT4 (Figure 2F). In normoxia, MCT4 protein (red fluorescence) was barely detectable in HSR-GBM1 and JHH-GBM14 cells. Consistent with the western blot analysis (Figure 2E), we detected high basal level of MCT4 protein in normoxic JHH-GBM10, much of which was associated with the plasma membrane (Figure 2F). Additionally, the immunofluorescence staining suggests that MCT4 localization to the cell membrane increased under hypoxia (Figure 2F, lower panels). Taken together, these data suggest that MCT4 is induced at the mRNA and protein levels by hypoxia, but that it can also accumulate to a lesser degree in a time/cell density dependent fashion. Induction of MCT4 results in increased localization at the plasma membrane, the site it is expected to function as a monocarboxylate transporter.

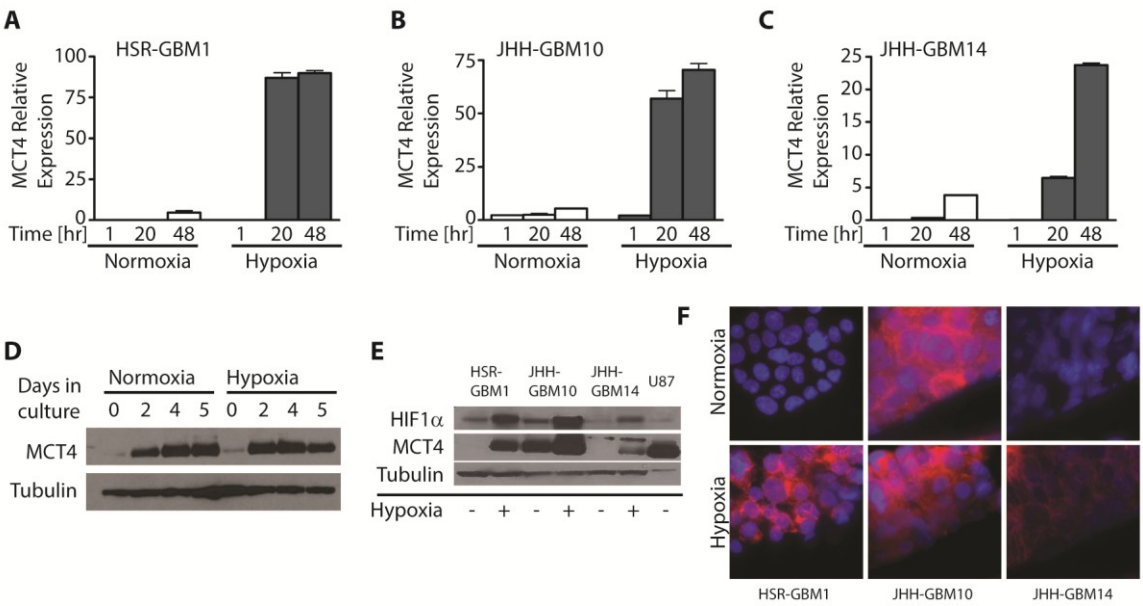


**Figure 4-2: MCT4 is upregulated in GBM neurospheres in response to both normoxia and hypoxia in a time-dependent manner**

(A-C) Quantitative real time PCR analysis showing MCT4 expression is upregulated in hypoxic (filled bars) HSR-GBM1 (A), JHH-GBM10 (B), and JHH-GBM14 (C) neurospheres after 20 hours of incubation in 1% oxygen. Normoxic neurospheres (clear bars) also induce MCT4 expression however with slower kinetics. With JHH-GBM10 and JHH-GBM14 showing higher MCT4 mRNA basal levels. (D) Western blot analysis of MCT4 levels in HSR-GBM1 at 0, 2, 4 and 5 days under normoxia, and hypoxia, with tubulin as loading control. (E) Western blot of HIF1alpha and MCT4 levels in HSR-GBM1, JHH-GBM10, and JHH-GBM14 under normoxia and hypoxia, with tubulin as loading control and U87 as positive control for MCT4. (F) Immunocytochemistry analysis for MCT4 in normoxic (top) and hypoxic (bottom) neurospheres: HSR-GBM1 (left), JHH-GBM10 (middle), and JHH-GBM14 (right). Nuclei were counterstained with DAPI.

### *4.3.3 Reduction in MCT4 levels result in induction of apoptosis and reduced cell proliferation*

The dramatic induction in most neurosphere lines of MCT4 in response to hypoxia suggests that it might be critical for proliferation and/or survival of GBM cells in reduced oxygen. Indeed, several reports have been recently published implicating another monocarboxylate transporter, MCT1, in the survival of adherent, high serum conditioned GBM cell lines (Froberg, Gerhart et al. 2001; Mathupala, Parajuli et al. 2004; Fang, Quinones et al. 2006; Li, Pang et al. 2009; Colen, Shen et al. 2011; Miranda-Goncalves, Honavar et al. 2012). To test the possibility that MCT4 may be required in stem-like GBM neurospheres, we transduced HSR-GBM1 (which has low levels of MCT4 in normoxia) and JHH-GBM10 (which has high levels of MCT4 in normoxia, Figure 2E) with viruses encoding shRNAs targeting MCT4. Two independent shRNAs constructs were used (sh1 and sh2) both of which resulted in significant reduction in MCT4 levels of up to 90% in HSR-GBM1 (Supplementary Figure S3A). Despite multiple rounds of transduction, we could not obtain a stable, proliferating culture of JHH-GBM10 expressing these same shRNA constructs suggesting more severe negative effects on growth in this line.

To circumvent this hurdle, we cloned a shRNA sequence against MCT4 (sh1) into conditional pLKO-Tet-ON inducible vector (Novartis Developmental and Molecular Pathways, Cambridge, MA, USA, through http://www.Addgene.org). Neurospheres were expanded in the absence of tetracycline to keep the levels of MCT4 high enough to allow cultures to be expanded. In all further experimentations using this inducible construct, we did not include tetracycline in the growth medium as we found this to be unnecessary.

The "leaky" shRNA cassette provided pronounced mRNA knockdown (an over 90%, statistically significant reduction by Student's t-test) and appeared to inhibit cell growth without completely killing the cultures (Figure S3B).

To quantify the effects of MCT4 knockdown on growth, we performed MTS assays on HSR-GBM1 and JHH-GBM10 neurospheres expressing either control or shMCT4 constructs. We found that MCT4 silencing resulted in significant growth inhibition in HSR-GBM1 (Figure 3A, B; normoxia, hypoxia) and JHH-GBM10 (Figure 3C, D; normoxia, hypoxia) under both normoxic and hypoxic conditions. One potential caveat to the MTS/MTT assay is its dependency on mitochondrial dehydrogenase activity, since oxygen is a major effector of mitochondrial activity. We therefore also performed viable cell counts using Guava-PCA flow cytometer. Consistent with the MTS assays, MCT4 inhibition using sh1 and sh2 resulted in a significant growth inhibition in HSR-GBM1 neurospheres grown for five days in normoxia and hypoxia (Supplementary Figure S4A-B). While both HSR-GBM1 and JHH-GBM10 showed clear growth inhibition following shMCT4 virus transduction, two additional neurosphere lines, HSR-040622 and HSR-040821, showed less pronounced growth effects following MCT4 inhibition (data not shown). We therefore focused our studies on HSR-GBM1 and JHH-GBM10.

We next attempted to elucidate the mechanism by which MCT4 inhibition affect proliferation. First, we performed cell cycle analysis of normoxic and hypoxic neurospheres. We could not detect any clear difference in cell cycle fractions in HSR-GBM1 under normoxic or hypoxic conditions (data not shown). However, we identified significant increases in sub-G1 (G0) fractions in normoxic (0.5% in control to 3.1% and 5.6% in sh1 and sh2 expressing cells) and hypoxic (1.2% in control to 11% and 6.4% in

sh1 and sh2 expressing cells) neurospheres (Figure 3E). These data suggest that reduced MCT4 levels may lead to induction of apoptosis. To further quantitate the apoptotic fraction we performed Annexin-V assays on normoxic and hypoxic neurospheres expressing either control or the sh1 or sh2 constructs. We found that in normoxia, MCT4 silencing by both shRNAs resulted in at least a 1.8-fold increase in the apoptotic fractions, from 9.6% in controls to 18% and 21% in sh1 and sh2, respectively. Under hypoxia, apoptotic fractions increased from 12.4% to 23% and 26% in sh1 and sh2, respectively. These inductions were statistically significant as determined by one-way Anova analysis ($p<0.0001$) (Figure 3F).

### *4.3.4 Stem-like CD133-positive cells are sensitive to MCT4 inhibition*

The dramatic induction of MCT4 in hypoxia and the significant growth inhibition we observed following MCT4 inhibition prompted us to investigate a potential requirement for MCT4 in stem-like GBM cells, as we have previously shown that hypoxia induces stem-like characteristics in GBM (Bar, Lin et al. 2010). HSR-GBM1 and JHH-GBM10 were FACS sorted into CD133-positive and -negative fractions followed immediately by quantitative Real Time PCR analysis (Figure 4A-B). We found that normoxic, stem-like CD133-positive fractions in both HSR-GBM1 and JHH-GBM10 cultures, expressed significantly higher levels of MCT4 mRNA compared to the CD133-negative fractions. The difference between fractions was greatest in HSR-GBM1, with an almost six fold induction (Student's t-test, $p=0.0016$ and $p=0.0019$ respectively) (Figure 4A-B). These results suggest that there might be a greater requirement for MCT4 in CD133-positive stem-like cells as compared to CD133-negative cells, and that this requirement may not be limited to growth under hypoxic conditions.

We next quantitated CD133-positive fractions by flow cytometry following MCT4 silencing in HSR-GBM1 and JHH-GBM10. Consistent with our previous report, the percentage of CD133-positive cells increased following hypoxic treatment of HSR-GBM1 (Figure 4C-D). In JHH-GBM10, the majority of cells expressed CD133 in normoxic conditions and these levels didn't change significantly upon hypoxic treatment (Figure 4E-F). Importantly, we found that CD133-positive fractions were sharply reduced following MCT4 silencing in both HSR-GBM1 and JHH-GBM10. CD133-positive fractions decreased from 49% in control to 40% in sh1 expressing normoxic and from 63% to 37% in hypoxic HSR-GBM1 cells, respectively (Figure 4C-D). In JHH-GBM10 we recorded the most dramatic reduction in CD133-positive fractions, from 82% to 1.4% and from 78% to 5.33% in normoxia and hypoxia respectively, for sh1 ($p<0.0001$ by one-way Anova and Student's t-test respectively).

Finally, we also examined the expression of Nestin, another marker routinely used to mark stem-like GBM cells. We found that similar to CD133, Nestin expression nearly halved in HSR-GBM1 following MCT4 silencing (Figure 4G). Additionally, Nestin expression was nearly extinguished (over 90% reduction) in JHH-GBM10 (Figure 4H), mirroring the dramatic reduction in CD133 fraction in this neurosphere line (Figure 4E, F).

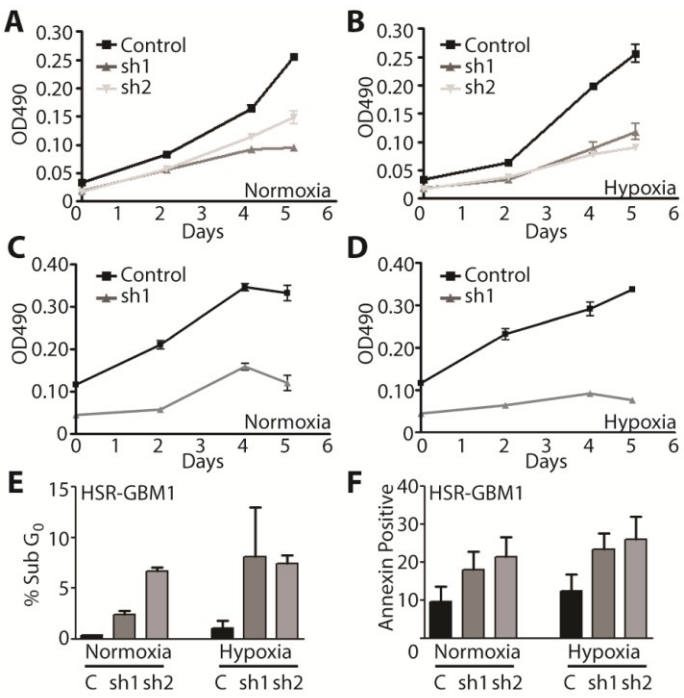


**Figure 4-3: Reduction in MCT4 levels result in induction of apoptosis and reduced cell proliferation**

(A-B) MTS assays for HSR-GBM1 (normoxia and hypoxia) and (C-D) JHH-GBM10 (normoxia and hypoxia) expressing either control shRNA or shRNA against MCT4 (sh1 or sh2). (E) Cell cycle analysis showing that hypoxia increases the percentage of Sub $G_0$ cells in HSR-GBM1 expressing sh1 or sh2 as compared with control. (F) Annexin assay confirming induction of apoptosis in HSR-GBM1 expressing sh1 or sh2 as compared with control under normoxia and hypoxia. (abbreviations: C=control shRNA)

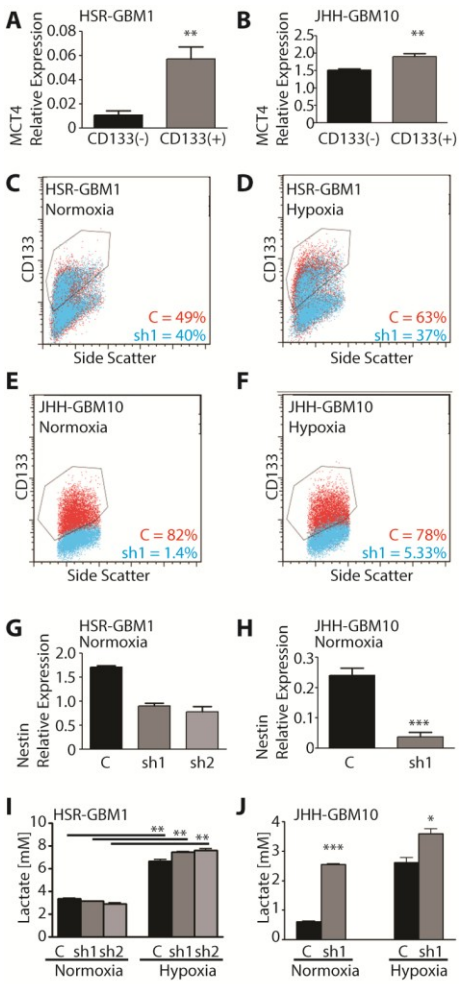


**Figure 4-4: MCT4 downregulation reduces stem-like GBM cell populations without affecting lactate homeostasis**

(A-B) MCT4 is overexpressed in stem-like CD133-positive cells as compared to CD133-negative cells in both HSR-GBM1 (A) and JHH-GBM10 (B). (C) MCT4 downregulation results in significant reduction in the stem-like CD133-positive cell population in both HSR-GBM1 (from 49% to 40%, normoxia (C), and from 63% to 37%, hypoxia (D)) and JHH-GBM10 (from 82% to 1.4%, normoxia (E), and from 78% to 5.33%, hypoxia (F)). (G) Reduction in MCT4 levels, using either sh1 or sh2 reduces Nestin expression as measured by quantitative Real-Time PCR in HSR-GBM1 (G) and JHH-GBM10 (H). (I) Extracellular lactate levels are induced under hypoxic conditions (compare filled to clear bars) in both HSR-GBM1 (I) and JHH-GBM10 (J). However, reduction in MCT4 levels using either sh1 or sh2 does not reduce lactate levels in either normoxia or hypoxia. (One-way Anova (I) and student t-test (J); *= $p<0.05$, ** = $p<0.01$, ***= $p<0.001$).

### *4.3.5 The effects of MCT4 inhibition are not associated with alterations in lactate levels*

As the most noted activity of MCT4 is passive exportation of lactate across the plasma membrane, we next explored the possibility that inhibition of growth and the reduction in the stem-like subpopulation may be due to reduced lactate secretion. To this end, we measured extracellular lactate levels in control and shMCT4 expressing HSR-GBM1 and JHH-GBM10 cells. As expected, extracellular lactate levels almost doubled when control HSR-GBM1 cells were grown under hypoxic conditions, increasing from 2.8 mM to 4.5 mM (Figure 4I). In JHH-GBM10, extracellular lactate levels more than doubled, increasing from 0.6 mM to 2.6 mM (Figure 4J). Surprisingly, we found no significant reduction in extracellular lactate levels following MCT4 inhibition (Figure 4I-J, grey bars). To further investigate the lack of lactate level changes, we also examined intracellular lactate levels and found no significant changes between control and shMCT4 expressing cells (not shown). In contrast, inhibition of pan-MCT transporter activity, using the natural small molecule Cinnamic Acid, did result in a significant reduction of extracellular lactate levels (not shown). These data strongly suggest that lactate homeostasis did not play a significant role mediating the various cell phenotypes noted above.

A

| Fold Change | Regulation | GeneSymbol | GeneName |
|---|---|---|---|
| 163.34 | down | RGL3 | ral guanine nucleotide dissociation stimulator-like 3 |
| 108.01 | down | PANX2 | pannexin 2 |
| 107.55 | down | TMEM184C | transmembrane protein 184C |
| 18.09 | down | TPSAB1 | tryptase alpha/beta 1 |
| 9.91 | down | LY6K | lymphocyte antigen 6 complex, locus K |
| 8.88 | down | PADI2 | peptidyl arginine deiminase, type II |
| 5.39 | down | NKX6-2 | NK6 homeobox 2 |
| 5.11 | down | SPHKAP | SPHK1 interactor, AKAP domain containing |
| 4.20 | down | LMO2 | LIM domain only 2 (rhombotin-like 1) |
| 3.38 | down | WISP2 | WNT1 inducible signaling pathway protein 2 |
| 3.26 | down | C1orf170 | chromosome 1 open reading frame 170 |
| 2.88 | down | DDIT4L | DNA-damage-inducible transcript 4-like |
| 2.68 | down | NDRG1 | N-myc downstream regulated 1 |
| 2.15 | down | LOX | lysyl oxidase |
| 2.08 | down | C8orf22 | chromosome 8 open reading frame 22 |
| 2.07 | down | NDUFA4L2 | NADH dehydrogenase (ubiquinone) 1 alpha subcomplex, 4-like 2 |
| 2.03 | down | CA9 | carbonic anhydrase IX |
| 1.82 | down | BHLHE41 | basic helix-loop-helix family, member e41 |
| 1.81 | down | STC2 | stanniocalcin 2 |
| 1.63 | down | KIAA1244 | KIAA1244 |
| 1.54 | down | TMEM45A | transmembrane protein 45A |

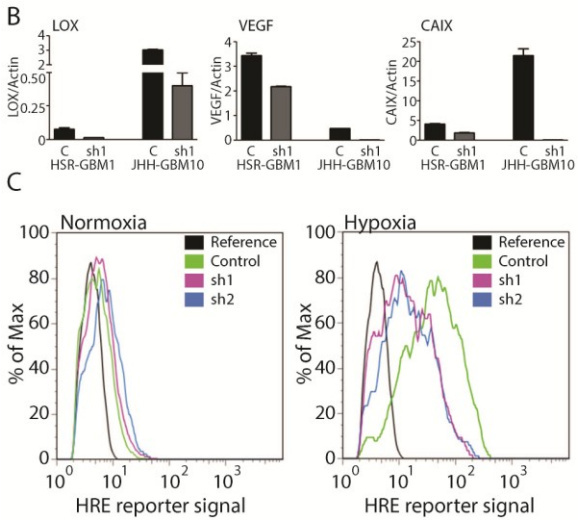


**Figure 4-5: Expression of hypoxia inducible genes is repressed in HSR-GBM1 expressing shRNAs targeting MCT4.**

Examination of the top 20 genes which are most differentially regulated in HSR-GBM1 expressing shRNAs against MCT4 as compared to control in hypoxia, revealed that many of these genes are direct HIF1alpha targets (A). Quantitative real time PCR analysis of selected HIF1alpha transcriptional targets: LOX, VEGF, and CAIX confirming significant downregulation in HSR-GBM1 (left portion of graphs) and JHH-GBM10 (right side of each graph) cells expressing shRNA against MCT4 (sh1) and treated with hypoxia (B). Flow Cytometric analysis of normoxic (left) and hypoxic (right) HSR-GBM1 expressing HRE-GFP (G6D) and either control or shRNAs against MCT4 (sh1 and sh2) (reference HSR-GBM1 cells are unlabeled and were used to set up the gates – black line).

### *4.3.6 MCT4 inhibition suppresses HIF transcriptional activity*

To get further insight into the potential mechanism by which MCT4 downregulation may inhibit cell proliferation and stem cell properties, we performed microarray analysis on HSR-GBM1 cells expressing control or shRNA against MCT4 (sh1 and sh2). Excitingly, we found that multiple known HIF1alpha transcriptional targets, such as NDRG1, STC2, CAIX and LOX(Kita, Mimori et al. ; Schietke, Warnecke et al. ; Wang, Li et al. ; Grabmaier, MC et al. 2004), were dramatically downregulated in HSR-GBM1 expressing shMCT4 as compared with control HSR-GBM1 cells (Figure 5A). In addition, we found that WISP2, a known HIF2alpha target, is greatly downregulated as well, suggesting that HIF2alpha transcriptional activity might also be inhibited(Stiehl, Bordoli et al.). We found that additional known HIF1alpha targets such as PLOD1, VEGFA, ENO1, PGK1, and ALDOA were also significantly downregulated but to a lesser degree (data not shown). Next, we validated these results by directly measuring relative expression levels of several known direct HIF1alpha transcriptional-targets by quantitative real time PCR analysis in HSR-GBM1 and JHH-GBM10 neurospheres expressing shRNA against MCT4 (sh1) or control. We found that VEGFA was inhibited by 36% in HSR-GBM1 sh1 and by 95% in JHH-GBM10 sh1. Similarly, LOX was inhibited by 81% in HSR-GBM1 sh1 and by 87% in JHH-GBM10 sh1, and CAIX was inhibited by 55% in HSR-GBM1 sh1 and almost completely extinguished in JHH-GBM10 sh1 (Figure 5B). Significant reduction in these genes was also observed with a second shRNA construct against MCT4 (sh2) in HSR-GBM1 (data not shown).

The reduction in the transcript levels of individual HIF1alpha targets (Figure 5A) prompted us to examine the overall effects of silencing MCT4 on HIF transcriptional

activity. To this end, we generated HSR-GBM1 neurospheres expressing an integrated hypoxia response element (HRE) – destabilized green fluorescent protein construct in addition to a constitutive dsRed driven by the UbC promoter (named HSR-GBM1 G6D). Following transduction with shRNAs targeting MCT4, we exposed cells to either normoxia or hypoxia for 48 hours and evaluated overall HIF transcriptional activity by flow cytometry. As seen in Figure 5C, hypoxia increases the percentage of GFP positive cells from 13.2% to 81.5% in control. In contrast, the percentage of GFP positive cells was significantly reduced to 62.4% and 59.5% in sh1 and sh2 expressing HSR-GBM1 G6D reporter cells, respectively (one way ANOVA, $p<0.001$ ***). These data represent a 70% and 50% reduction in the relative HIF transcriptional reporter activity in hypoxia for sh1 and sh2, respectively. Importantly, these dramatic changes in HIF1alpha activity are most likely due to reduced transcriptional activity as overall HIF1alpha protein levels remained unchanged (not shown). Taken together, these data strongly suggest that MCT4 downregulation significantly inhibits HIF transcriptional activity.

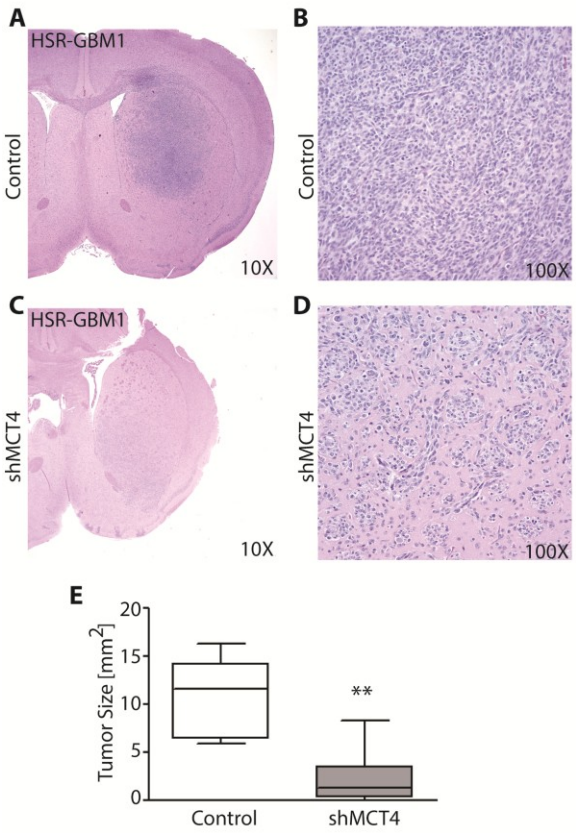


**Figure 4-6: MCT4 silencing results in growth inhibition in vivo.**

Representative images of intracranial xenografts of HSR-GBM1 expressing control shRNA (A-B, magnification - 10X and 100X, respectively) and shMCT4 (C-D, magnification - 10X and 100X, respectively). (E) HSR-GBM1 transduced with either sh1 or sh2 form significantly smaller tumors as compared to cells transduced with control virus (p=0.0013)

### *4.3.7 MCT4 silencing results in growth inhibition in vivo*

We have previously shown that in glioma, hypoxia induces expansion of the stem-like population (Bar, Lin et al. 2010) and that therapies which target stem-like cells prevent tumor engraftment and long-term growth (Fan, Matsui et al. 2006; Bar, Chaudhry et al. 2007; Bar, Lin et al. 2010; Fan, Khaki et al. 2010). The dramatic reduction in the

expression of HIF1alpha target genes and the stem-like population in HSR-GBM1 and JHH-GBM10 following MCT4 inhibition *in vitro* prompted us to evaluate the potential effects of MCT4 downregulation *in vivo*. HSR-GBM1 neurospheres were transduced with either control or shMCT4 viruses before intracerebral implantation of 1 x $10^5$ viable cells (7 animals in control, 8 animals in sh1, and 5 animals in sh2). Xenografts were allowed to grow for approximately four months followed by histological analysis of the resulting tumors (Figure 6A-D). We found that sh1 MCT4 and sh2 MCT4 expressing cells formed significantly smaller tumors as compared to cells transduced with control virus (Student's t-test, p=0.0013) (Figure 6E). In addition, it appeared that shMCT4 expressing cells formed tumors which were less invasive (Figure 6A, C).

## 4.4 DISCUSSION

In this study, we have shown that the proliferation and survival of GBM stem-like cells are dependent on the monocarboxylate transporter-4 (MCT4). We first demonstrated that hypoxia dramatically induces MCT4 expression in all neurosphere cultures we tested. In addition, MCT4 overexpression is correlated with increased aggressiveness and decreased survival in glioblastoma patients. Reducing MCT4 expression by short hairpin RNA-mediated silencing resulted in dramatic reduction in the stem-like CD133-positive population. This gave rise to cultures with significantly reduced capacity to proliferate *in vitro* and to form intracranial xenografts *in vivo*.

We demonstrated that some GBM neurospheres cultures are extremely sensitive to MCT4 inhibition while others are less affected by reduced levels of this monocarboxylate-transporter. This heterogeneity underscores the notion that no single target is likely to control growth of all gliomas. It also indicates that while most GBMs

share similar histological characteristics (vascular proliferation, hypoxic core, often surrounded by pseudo palisading cells), they are likely to exhibit a range of monocarboxylate and thus metabolic dependencies. Indeed, the vast wealth of data generated by the Cancer Genome Atlas Project (TCGA) has confirmed that subtypes with distinct pathological molecular events and therapeutic responses exist in GBM. Our findings point to a significantly increased expression of MCT4 in the mesenchymal subtype of GBMs. These data may explain the metabolic requirement as well as drug resistance of GBMs with heightened MCT4 levels.

Finally, we examined the role of lactate in an attempt to explain the phenotypes we observed. Recent literature suggest that MCT4, with its relative low affinity for lactate (Km of ~30 mM) and extremely low affinity for pyruvate (Km of ~150 mM), appears to be exclusively designed for lactate efflux (Dimmer, Friedrich et al. 2000; Manning Fox, Meredith et al. 2000). Our results suggest that while growth of numerous neurosphere lines was inhibited by reduced MCT4 levels, intracellular and extracellular lactate levels remained unchanged. These results are not necessarily surprising considering the fact that monocarboxylate transporters are passive transporters with redundancy between multiple MCTs. Chiche *et al.* showed that reduced MCT4 levels resulted in intracellular acidification (Chiche, Le Fur et al. 2012). This discrepancy may be explained by the fact that while our studies focused on glioblastomas, Chiche et al studied RAS-transformed fibroblasts which may differ not only by their cell of origin but also by their metabolic requirement and mechanisms of pH homeostasis. In addition, MCT4 is known to transport numerous monocarboxylates across the plasma membrane and therefore while our results clearly suggest that lactate homeostasis is unaffected by MCT4 silencing, it is

possible that the levels of other, yet to be characterized, monocarboxylates is more strictly dependent on MCT4 levels. Alternatively, it is possible that MCT4's catalytic activity is dispensable and that the effects we documented are mediated by yet an unidentified activity of MCT4. Support for the latter comes from our examination of the effects of MCT4 knockdown on global gene expression profiles of normoxic and hypoxic neurospheres. The identification of multiple direct HIF1alpha transcriptional targets in cells expressing reduced levels of MCT4 (Figure 5A) strongly suggest that MCT4 feeds back on HIF1alpha activity. These results were confirmed by quantitative real time PCR (Figure 5B) as well as by examination of global HIF transcription using HSR-GBM1 G6D hypoxia-dependent HRE-reporter model (Figure 5C).

Taken together, our studies suggest that MCT4 plays a role in the response of stem-like GBM cells to hypoxia, and that some of these effects may be independent of its role as a lactate transporter. Inhibiting MCT4 shows promise as a new therapy for GBM, particularly in stem-like and hypoxic cells. Small molecule inhibitors of various MCT family members are being developed, and our data provide a rationale for testing MCT4 inhibitors in patients with malignant gliomas. We speculate that inhibitors which will target MCT4 plasma membrane localization, via inhibition of its association with its chaperon, CD147 (Kirk, Wilson et al. 2000), may prove more useful than inhibitors simply targeting its transporter activity.

**Supplementary Figures:**

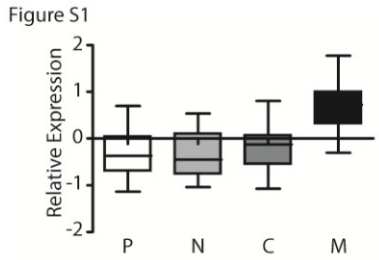


**Figure 4-S1:** The aggressive mesenchymal GBM subgroup (based on the TCGA classification scheme) express significantly higher levels of MCT4 compared to the other subgroups. Graph showing relative MCT4 expression levels in the four different GBM subgroups (P = proneural, N = Neural, C = Classical, M = Mesenchymal).

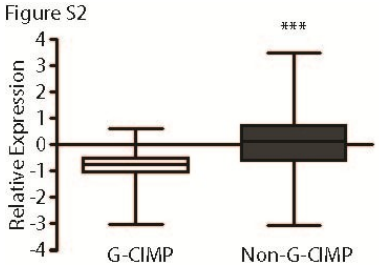


**Figure 4-S2:** The less aggressive G-CIMP (Glioma CpG Island Methylator Phenotype) GBM subgroup (based on the TCGA classification scheme) expresses significantly lower levels of MCT4 compared to the non-G-CIMP subgroup.

Figure S3

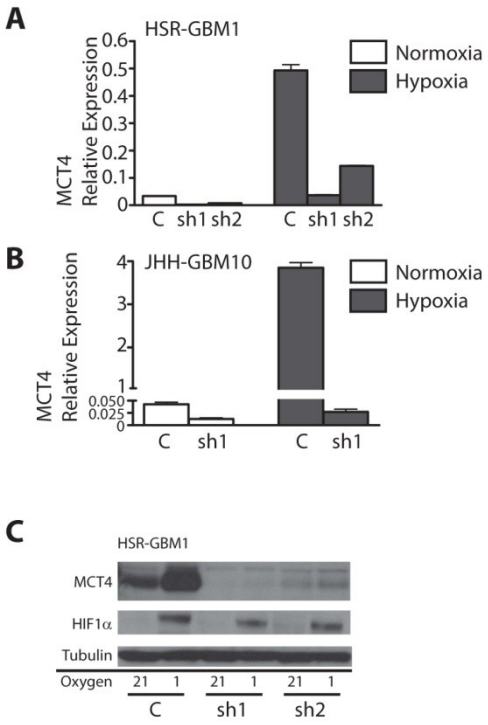


**Figure 4-S3:** Expression knockdown confirmation for shRNA MCT4 constructs (sh1 and sh2). (A) Quantitative Real-Time PCR analysis showing relative MCT4 expression of HSR-GBM1 transduced with either Control or shMCT4 viruses (sh1 and sh2) in normoxia and hypoxia. (B) Quantitative Real-Time PCR analysis showing relative MCT4 expression in JHH-GBM10 transduced with control or sh1 viruses in normoxia and hypoxia. (C) Western blot analysis for MCT4 and HIF1alpha in control or shMCT4 (sh1 and sh2) transduced HSR-GBM1 neurospheres cultured in 21% (normoxia) or 1% oxygen (hypoxia). Tubulin was used as a loading control.

Figure S4

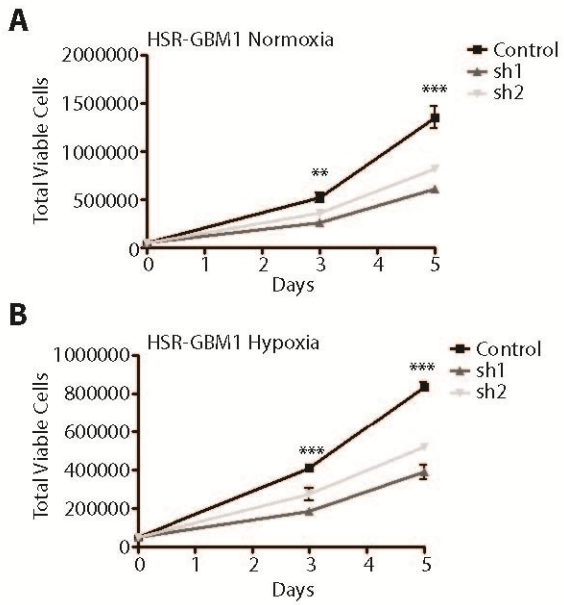


**Figure 4-S4:** MCT4 knockdown results in significant growth inhibition in HSR-GBM1 neurospheres as assessed by flow cytometry. The total number of viable cells in HSR-GBM1 transduced with shMCT4 (sh1 and sh2) as compared with controls is significantly reduced in normoxia (A) and hypoxia (B) over five days in culture (Student t-test; ** = $p<0.01$, ***= $p<0.001$).

# Chapter 5: Arsenic Trioxide Inhibits Hedgehog, Notch And Stem Cell Properties In Glioblastoma Neurospheres

Dacheng Ding[1,5], Kah Suan Lim[2,5], Charles G. Eberhart[2,3,4,*]

[1]Department of Neurosurgery, Xiangya Hospital of Central South University, 87 Xiangya Road, Changsha, Hunan 410078, China, [2]Departments of Pathology, [3]Oncology and [4]Ophthalmology, Johns Hopkins University School of Medicine, Baltimore, MD 21287, USA, [5]These authors contributed equally to this work, *To whom correspondence should be addressed <ceberha@jhmi.edu>

**Abstract**

Background: Notch and Hedgehog signaling have been implicated in the pathogenesis and stem-like characteristics of glioblastomas, and inhibitors of the pathways have been suggested as new therapies for these aggressive tumors. It has also been reported that targeting both pathways simultaneously can be advantageous in treating glioblastoma neurospheres, but this is difficult to achieve *in vivo* using multiple agents. Since arsenic trioxide has been shown to inhibit both Notch and Hedgehog in some solid tumors, we examined its effects on these pathways and on stem cell phenotype in glioblastoma.
Results: We found that arsenic trioxide suppresses proliferation and promotes apoptosis in three stem-like glioblastoma neurospheres lines, while inhibiting Notch and Hedgehog target genes. Importantly, arsenic trioxide markedly reduced clonogenic capacity of the tumor neurospheres, and the stem-like CD133-positive fraction was also diminished along with expression of the stem cell markers SOX2 and CD133.
Conclusions: Our results suggest that arsenic trioxide may be effective in targeting stem-like glioblastoma cells in patients by inhibiting Notch and Hedgehog activity.

## 5.1 Background

Glioblastoma (GBM) are the most common primary adult brain malignancy, and despite some advances in therapeutic options survival remains dismal. One reason suggested for the deadliness of this disease is the presence of treatment-resistant stem-like cancer cells(Reya, Morrison et al. 2001; Dean, Fojo et al. 2005; Wicha, Liu et al. 2006; Eyler and Rich 2008; Visvader and Lindeman 2008; O'Brien, Kreso et al. 2009). While conventional therapies are thought to target much of the tumor, it is believed that stem-like neoplastic cells survive and go on to regenerate the lesion. We therefore need new therapies targeting these cancer stem cells (CSC) in glioma.

Notch and Hedgehog signaling have been implicated in the survival of CSC in GBM by our group and others, and single agent therapies targeting either pathway have yielded promising results(Fan, Khaki et al. ; Hu, Zheng et al. ; Wang, Wakeman et al. ; Purow, Haque et al. 2005; Shih and Holland 2006; Bar, Chaudhry et al. 2007; Clement, Sanchez et al. 2007; Ehtesham, Sarangi et al. 2007; Kanamori, Kawaguchi et al. 2007; Zhang, Zheng et al. 2008; Sarangi, Valadez et al. 2009). However, single therapies often allow resistance to develop in tumor cells, suggesting that several pathways will need to be targeted simultaneously if we are to eradicate GBM in patients.. Our group recently identified one mechanism of cellular resistance to Notch pathway inhibition in GBM: direct upregulation of the Hedgehog pathway through a novel cross talk mechanism. This involved constitutive suppression of Hedgehog activity by direct binding of the Notch mediator Hes1 to the Gli promoter(Schreck, Taylor et al.). While dual agent therapy with separate compounds targeting both Notch and Hedgehog was able to overcome this problematic therapeutic resistance, toxicity and other issues limit the *in vivo* use of the

specific agents tested in our prior study. We have therefore now investigated the potential of a single compound, arsenic trioxide (ATO), to target both Notch and Hedgehog signaling in stem-like glioma cells.

Arsenic trioxide was first used in the treatment of acute promyelocytic leukemia (APL) in China, where one of the potential mechanisms of action involved induction of differentiation of leukemic cells(Chen, Zhu et al. 1996; Shen, Chen et al. 1997). ATO has since been FDA approved for treatment of APL patients for which ATRA failed to work(Cohen, Hirschfeld et al. 2001). The effects of ATO were subsequently examined in other tumor types, including multiple myeloma, glioma, neuroblastoma, esophageal carcinoma and prostate cancer, and it has been found to be efficacious in many of these as well(Akao, Nakagawa et al. 1999; Rousselot, Labaume et al. 1999; Park, Seol et al. 2000; Shen, Shen et al. 2000; Maeda, Hori et al. 2001; Kanzawa, Kondo et al. 2003). The mechanism of action of ATO is not entirely clear, but in many tumors it is thought to function via regulation of various developmental pathways important in cancer. In APL for example, ATO inhibits the oncogenic fusion protein promyelocytic leukemia-retinoic acid receptor α (PML-RAR)(Nasr, Guillemin et al. 2008). In other tumors such as basal cell carcinoma, ATO is believed to exert its effects by inhibiting the Hedgehog signaling pathway(Kim, Aftab et al.). Finally, in one report using glioma cells grown adherently, ATO was shown to target Notch signaling(Zhen, Zhao et al.).

A number of studies have looked at the anti-growth effects of ATO in gliomas, however all but one were done using adherent glioma lines grown in high serum (Zhen, Zhao et al. ; Kanzawa, Kondo et al. 2003; Kim, Lew et al. 2003; Ning and Knox 2004; Haga, Fujita et al. 2005; Kanzawa, Zhang et al. 2005; Wei, Liu et al. 2008; Chiu, Ho et al. 2009;

Pucer, Castino et al. 2010; Song, Chen et al. 2010; Chiu, Ho et al. 2011; Sun and Zhang 2011). It has been suggested that glioma cells grown under these conditions are poor models in which to address CSC related issues(Lee, Kotliarova et al. 2006). We therefore used several serum-free glioblastoma neurosphere cultures to examine the effects of ATO on the growth and survival of stem-like tumors cells, as well as its effects on key developmental pathways such as Notch and Hedgehog. We found that ATO inhibits both of these pathways, along with growth, clonogenicity and stem-cell characteristics in the GBM neurospheres.

## 5.2 Material and Methods

Cell culture condition and drug preparation

HSR-GBM1, 040622 and 040821 neurosphere lines were kind gifts from Dr. Angelo Vescovi. GBM neurospheres were maintained in Neurocult Complete Medium supplemented with human epidermal growth factor and human fibroblast growth factor (Peprotech, Rocky Hill, NJ). Arsenic Trioxide (ATO) powder (Sigma, St Louis, Mo-Aldrich) was dissolved in 1 mM sodium hydroxide. Cell number and viability were assessed using the hemocytometer and trypan blue.

Determination of cell growth

We performed MTS assays to determine growth in viable cell mass. Cells were seeded into 96-well plates at a density of 5000 per well in 100µl of medium. Cells were then treated with concentrations of arsenic trioxide (ATO) ranging from 0µM to 5µM and incubated in 5% CO2 at 37°C. For the MTS readings, 20µl of MTS solution was added to each well at 24, 48 and 72 hours post plating and incubated for 1 hour. After that optical

density was measured by spectrophotometer. The experiments were repeated at least three times for each cell line.

Cell proliferation assay

BrdU assay was performed to determine proliferation. Cells were treated with concentrations of ATO ranging from 0μM to 5μM for 72 hours, and then cytospun onto slides. They were then fixed with 4% formaldehyde in PBS for 15 minutes, and permeabilized with 0.1% Triton/PBST for 15 minutes. Cellular proteins were then denatured with 2N HCL, washed with PBST (PBS Tween-20), blocked with 5%NGS/PBST for 15 minutes and then incubated in primary antibody against BrdU (Sigma, B2531). Anti-BrdU antibody was used per the manufacturer's instruction at 1:500 dilution. After washing 3 times with PBST, cells were incubated for 45 minutes in the dark with the appropriate cy-3 conjugated secondary antibody. Cells were then counterstained with 4',6-diamidino-2-phenylindole (DAPI), mounted with Vectashield (Vector Laboratories), and visualized and pictures taken by fluorescence microscopy.

Western blot analysis

Proteins were extracted from HSR-GBM1, 040622 and 040821 treated with ATO for 72 hours. The cells were lysed, sonicated until clear, and then centrifuged at 4°C and 15000rpm for 10 min to remove cell debris. Subsequently, protein separation was performed on a 4-12% SDS-polyacrylamide gel by electrophoresis, and then transferred onto PVDF membranes. Membranes were probed with antibodies against Cleaved

Caspase-3 (1:1000, Cell Signaling Technology, Danvers, MA) and GAPDH (1:5000, Sigma, St. Louis, MO).

Cell cycle analyses

Cells were plated in 6-well plates at a density of 1.5×105-2.5×105 cells per well and treated with ATO ranging from 0μM to 5μM for 72 hours. Cells were then fixed with 70% ethanol for at least 12 hours and stained with Guava Cell Cycle Reagent (Millipore, Billerica, MA). Cell cycle analyses were performed using the Guava PCA machine.

Clonogenic assays

HSR-GBM1, 040622 and 040821 neurospheres were treated with concentrations of ATO ranging between 0μM and 5μM for 72 hours. Neurospheres were then mechanically dissociated into single cells. 20000 viable cells were counted and plated in methylcellulose in 6-well plates. Pictures of colonies were taken after 10-12 days. 2-3 wells were plated per cell line and 3-4 separate fields were taken per well. Measurements were taken of the widest diameter of each colony and its corresponding right angle diameter and the measurements averaged. The number of colonies that have an average diameter above 100μM were then counted for each field and graphed.

Flow cytometric analyses

For CD133 flow cytometric analyses, neurospheres were treated with 0μM-5μM ATO for 24 hours and then collected, dissociated, and stained for CD133. Flow cytometry was then performed as previously described(Fan, Matsui et al. 2006).

Quantitative real-time PCR analyses

HSR-GBM1, 040622 and 040821 were collected after treatment with 0μM-5μM ATO for 24 hours. RNA was then extracted, reversed transcribed, and cDNA levels analyzed by quantitative real-time PCR analysis performed in triplicate with SYBR Green reagents (Bio-Rad, Hercules, CA). Standard curves were used to determine expression levels and all values were normalized to beta-actin. Statistical comparisons are between multiple experiments each with triplicate technical replicates. Primer sequences were as follows: Hes1 forward 5'-GTC AAG CAC CTC CGGAAC-3'; Hes1 reverse 5'-CGT TCA TGC ACT CGC TGA-3'; Hey1 forward 5'-TCT GAG CTG AGA AGG CTG GT-3'; Hey1 reverse 5'-CGA AAT CCC AAACTC CGA TA-3'; Ptch1B forward 5'-GAC GCC GCC TTC GCT CTG-3'; Ptch1B reverse 5'-GCC CAC AAC CAA GAA CTT GCC-3'; N-Myc forward 5'-CGACCACAAGGCCCTCAGTA -3'; N-Myc reverse 5'-CAGCCTTGGTGTTGGAGGAG-3'(Bordow, Haber et al. 1994); Human actin- β forward – 5'-CCCAGCACAATGAAGATCAA-3′; and human actin-β feverse: 5′-GATCCACACGGAGTACTTG- 3′.

Statistical analyses

Statistical significance was evaluated using unpaired, two-tailed Student's t-test. P-values $<0.05$ were considered statistically significant. Unless otherwise noted, error bars represent standard error of the mean. All statistical tests were performed using the GraphPad Prism 5 software (GraphPad Software, La Jolla, CA).

## 5.3 Results

### *5.3.1 ATO inhibits growth and promotes apoptosis in glioblastoma neurospheres*

We first examined the effects of ATO on the growth of three glioblastoma neurosphere lines using the MTS assay. In all three lines, we saw a dose dependent reduction in growth over five days (Figure 1a). These studies were performed in technical triplicates at least 4 separate times for each cell line with similar results, and a bar graph containing all data points for the multiple experiments is shown in the lower right panel of Figure 1a. Mean growth inhibition of between 33-86% was seen after treatment at the 2.5 μM ATO levels, and statistically significant 65-92% inhibition of growth was achieved by 5 μM ATO in all three neurosphere lines. To directly determine the effects of ATO on the proliferation of glioblastoma neurospheres, we assessed the number of BRDU positive tumor cells after 72 hours of treatment in the three lines. We identified statistically significant reductions in proliferation of up to 90% using 2.5 uM ATO, and even more pronounced effects with 5 μM ATO (Figure 1B). These data suggest that decreased proliferation accounts for much of the slower growth we observed.
Induction of apoptosis may also mediate some of the anti-tumor effects of ATO. Cleaved caspase 3 levels were increased after ATO treatment in all three lines tested (Figure 2A). In addition, flow cytometric analysis revealed an increase in the sub-G1 fraction of all three lines which was significant at higher levels of the compound (Figure 2B). We also measured GFAP mRNA levels by quantitative RT PCR, but did not detect increases suggesting enhanced glial differentiation of tumor cells after therapy (data not shown).

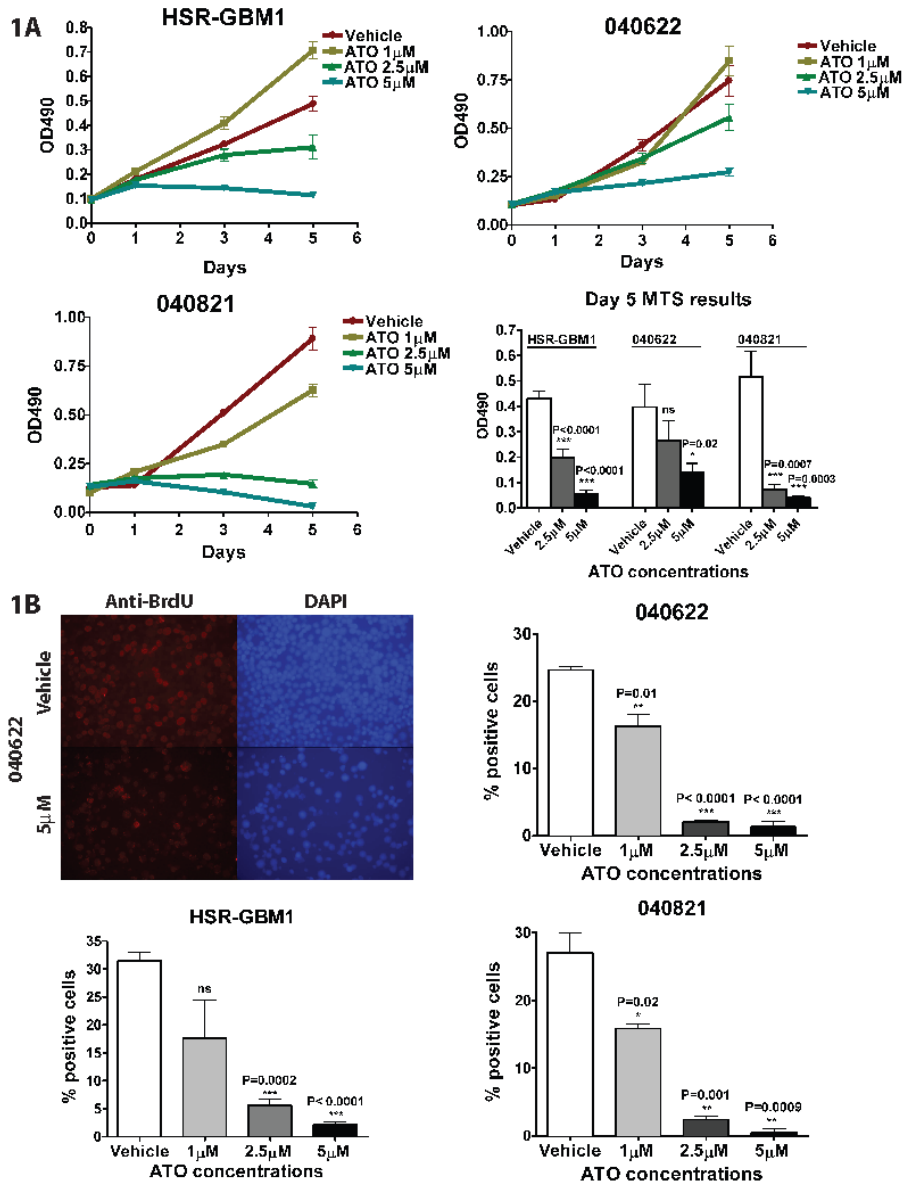


**Figure 5-1. Arsenic trioxide inhibits glioblastoma neurosphere growth and proliferation.**

A) MTS assays showing growth inhibition following ATO treatment in the 040821, HSR-GBM1 and 040622 glioblastoma neurosphere lines, with a bar graph highlighting the significance compared to vehicle. B) Representative BRDU staining images showing anti-BRDU staining (red) and DAPI counterstaining (blue) in vehicle and 5μM ATO-treated 040622 neurosphere cells are shown in the top left panel. The percentage of BRDU positive cells in 040622, 040821 and HSR-GBM1 neurospheres was significantly decreased in all three lines after treatment with either 2.5μM or 5μM ATO.

### *5.3.2 ATO inhibits Notch and Hedgehog pathway targets*

Because ATO has been reported to suppress Hedgehog and Notch activity in other tumor types, we examined effects on the two pathways after 24 hour treatment of GBM neurosphere lines. Pathway activity was assessed using quantitative RT PCR to measure levels of the canonical pathway transcriptional targets PTCH1b and N-Myc (Hedgehog) as well as Hes1, Hes5 and Hey1 (Notch). At least two experimental replicates were performed, each with triplicate technical measurements, and all data points are combined in Figure 3. A statistically significant 40 – 89 % inhibition of PTCH1b was noted at the highest ATO dose in all three lines, while the lesser 2.5 μM dose resulted in significant inhibition in two of the three lines (Figure 3A). 2.5μM ATO also resulted in significant inhibition of another direct Hedgehog target N-Myc in all three GBM lines, while the highest ATO dose resulted in significant inhibition of two of the three lines (Figure 3A).

We also observed inhibition of Notch target expression in GBM neurospheres treated with ATO. These changes were not dose dependent in all the lines, but the 2.5 μM level of ATO significantly suppressed Hes5 and Hey1 in all three cultures, while the suppression of Hes1 was significant in two of three (Figure 3B). Interestingly, the highest levels of ATO (5 μM) resulted in an increase in the mRNA levels of Hes5 and Hey1 in several lines. While the cause of this is not clear, we have previously observed paradoxical increases in the mRNA levels of Notch targets when treating brain tumor cells with high levels of gamma-secretase inhibitors that target Notch, and this may represent a feedback or resistance mechanism of some sort in cells surviving maximal therapy (CGE, unpublished data).

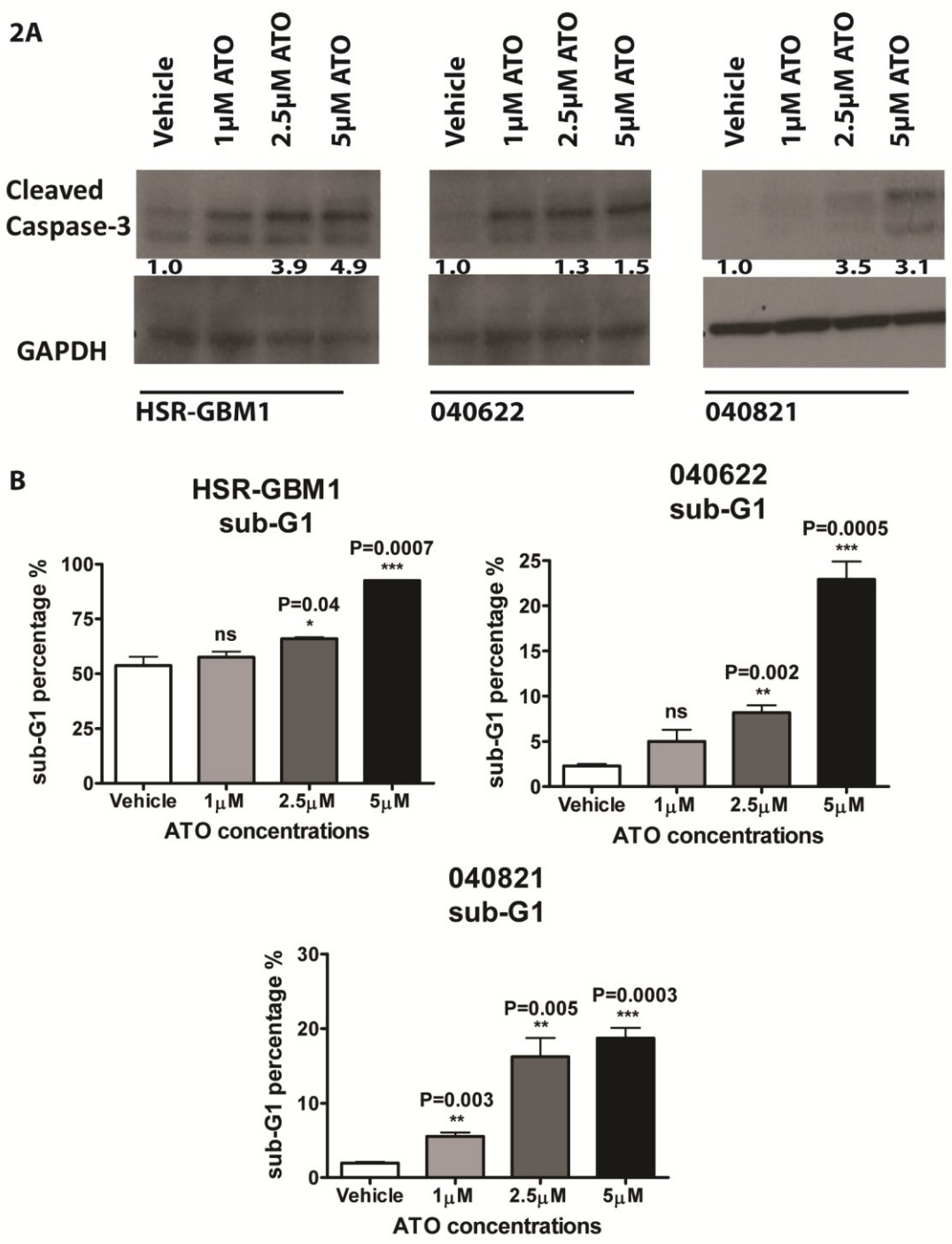


**Figure 5-2. Arsenic trioxide induces apoptosis in glioblastoma neurosphere cells.**

A) Western blots show induction of caspase-3 cleavage in HSR-GBM1, 040622 and 040821 cells following treatment with 2.5μM or 5μM ATO. B) Cell cycle analysis by flow cytometry performed on neurosphere lines after ATO treatment reveal a significant increase in the sub-G1 population.

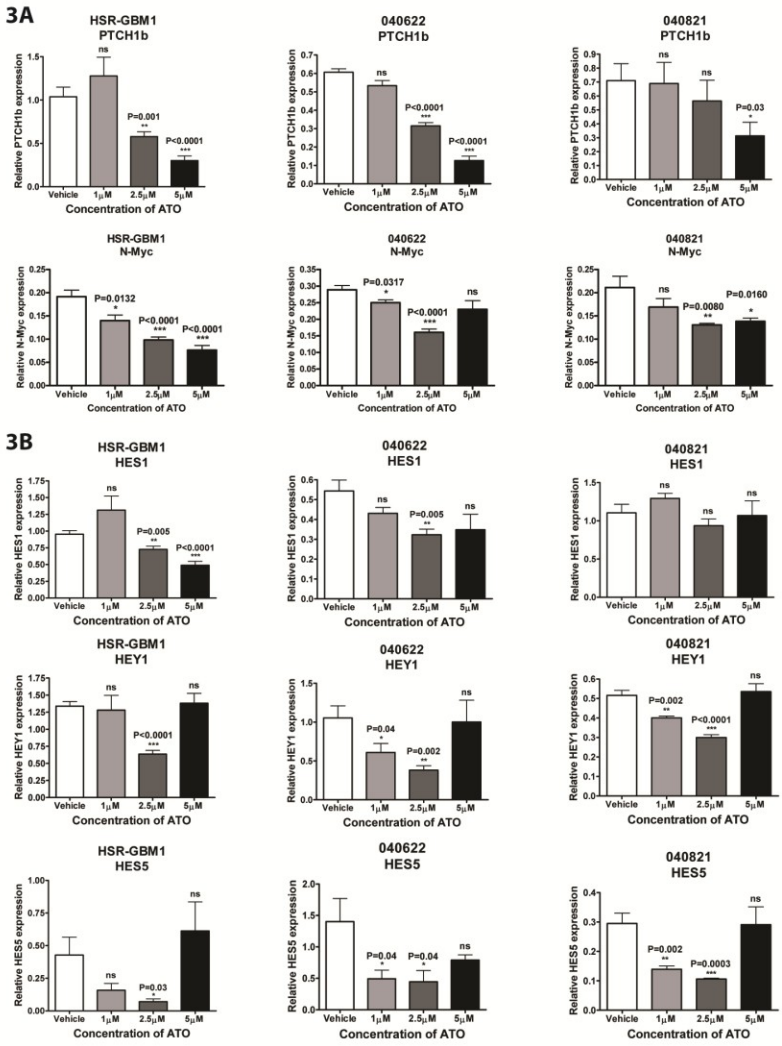


**Figure 5-3. Arsenic trioxide inhibits Hedgehog and Notch pathway target gene expression.**

A) Quantitative PCR analysis revealed that ATO significantly inhibited transcript levels of the Hedgehog pathway target gene PTCH1b at 5μM in all 3 glioblastoma neurosphere lines compared to vehicle treatment, and in 2 lines after 2.5μM ATO. ATO also significantly inhibited another Hedgehog pathway target N-Myc in 2 lines at 5μM, in all 3 glioblastoma neurosphere lines at 2.5μM, and in 2 lines at 1μM. B) ATO also significantly inhibited expression of the Notch target HES1 as compared to vehicle treatment in HSR-GBM1 and 040622 cells, but not in 040821. HES5 and HEY1 transcript levels were also reduced in all 3 glioblastoma neurosphere lines following 2.5μM ATO treatment, but a non-significant paradoxical increase was seen at the higher 5 μM dose.

### *5.3.3 Clonogenic capacity and stem cell markers are reduced following ATO treatment*

We next evaluated the effects of ATO treatment on the clonogenic capacity of glioblastoma cells. Neurosphere lines were treated for three days with ATO, triturated, and counted. Equal numbers of surviving cells were then seeded into methylcellulose and allowed to grow into colonies with no additional treatment. We have previously shown that only large glioblastoma spheres grown in methylcellulose can be serially passaged(Bar, Lin et al.). The number of spheres over 100 uM in size was significantly reduced following ATO treatment in HSR-GBM1 and 040821 cells (Figure 4), while a modest non-significant reduction was seen in 040622 cells (data not shown). This suggested that the stem-like clonogenic fraction is depleted by ATO treatment.

To more directly examine the effects of ATO on stem cell markers, we measured levels of SOX2 and CD133 mRNA after 24 hours of treatment. For the HSR-GBM1 and 040622 lines, a dose-dependent significant inhibition in CD133 mRNA expression was seen (Figure 5A,B). Pronounced reductions in SOX2 mRNA levels were also noted in all three lines, and were significant in 040622 (Figure 5B).

We also used flow cytometric analysis to measure the fraction of cells expressing the marker CD133 on their surface. Triplicate analyses showed significant reductions in this stem-like cell fraction at both 2.5 uM and 5 uM levels of ATO in all three lines (Figure 5C). The changes were most pronounced in the HSR-GBM1 and 040821 lines, and relatively modest in the 040622 cells. This experiment was repeated twice with similar results.

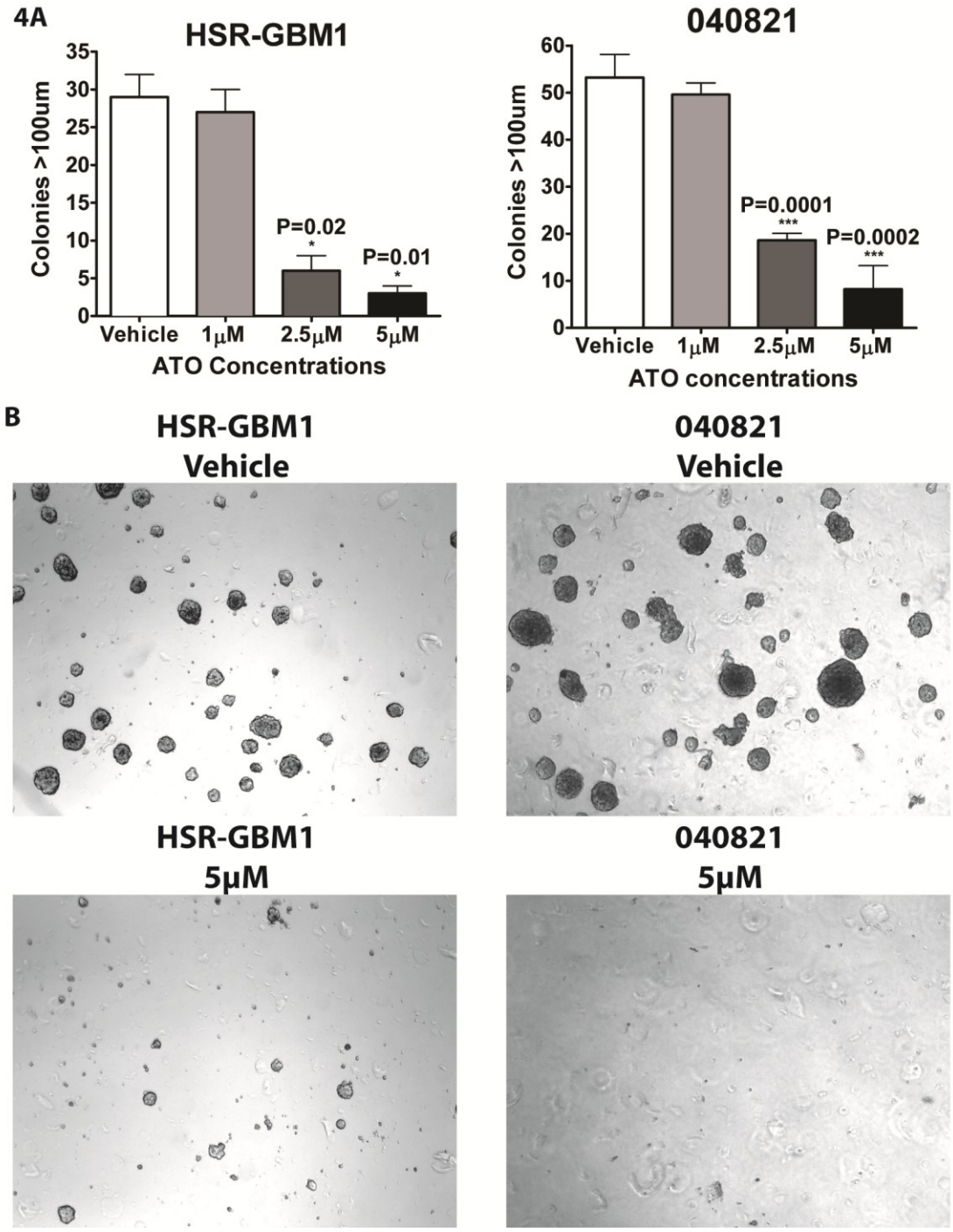


**Figure 5-4. Arsenic trioxide treatment inhibits clonogenicity in glioblastoma neurosphere cells.**

A) Quantification of clonogenicity in equal numbers of single viable HSR-GBM1 and 040821 cells seeded in methylcellulose following 3 days of ATO treatment showed significantly fewer colonies over 100μM in size. B) Representative images of colonies.

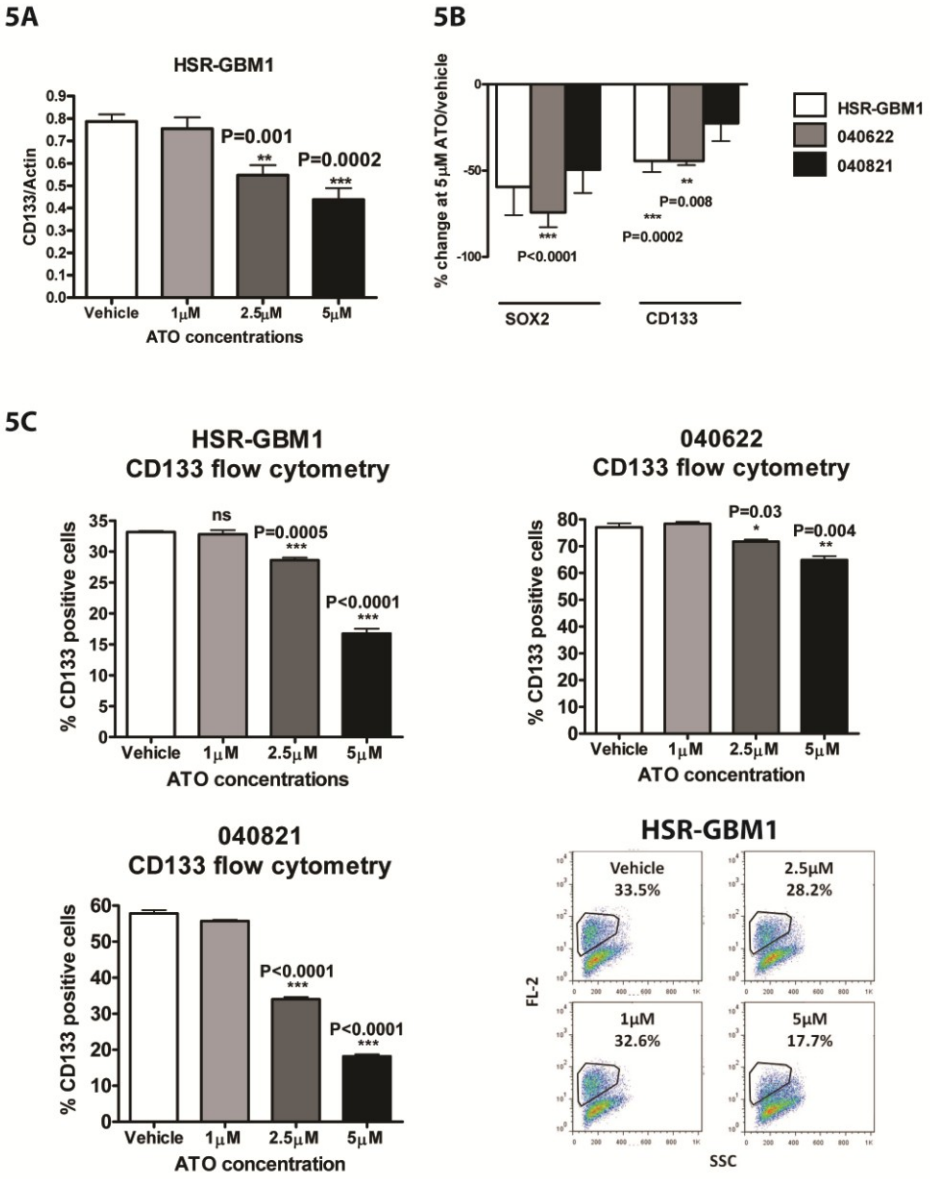


**Figure 5-5. Arsenic trioxide treatment inhibits the expression of stem-cell markers in glioblastoma neurosphere cells.**

A) A representative experiment showing decreased transcript levels of the stem-cell marker CD133 in HSR-GBM1 cells following ATO treatment measured using quantitative real-time PCR. B) mRNA expression of the stem-cell markers CD133 and SOX2 was suppressed by ATO. C) Flow cytometric analysis of the CD133 positive fraction also revealed variable reductions in this stem-like subpopulation following ATO treatment. Representative flow cytometry plots of CD133-positive cells in vehicle and ATO treated HSR-GBM1 cultures are shown in the lower right panel.

## 5.4 Discussion

Standard GBM treatment includes surgical resection followed by radiotherapy and temozolomide (TMZ) chemotherapy, but rarely results in long term survival(Clarke, Penas et al.). In this study, we focused on the potential of ATO as a therapeutic agent for GBM patients, particularly its ability to inhibit the Notch and Hedgehog pathways which have been shown to play key roles in stem-like glioma cells. While both of these pathways have been shown to be inhibited by ATO in some tumor types(Wu, Ji et al. ; Yang, Cao et al.), the ability of this compound to affect them in gliomas is less clear. Zhen and colleagues treated three adherent GBM lines (U87MG, U251MG and U373MG) with ATO and reported decreased protein levels of the Notch1 receptor and Hes1 target, as well as reductions in growth *in vitro* and *in vivo*(Zhen, Zhao et al.). They also identified lower levels of the stem/progenitor marker Nestin after treatment, although as noted above high serum lines are not thought to be good models of cancer stem cells in glioma. To our knowledge, no data addressing the effects of ATO on Hedgehog activity in glioma has been published.

We examined the effects of ATO inhibition on Notch and Hedgehog pathways in three GBM neurosphere lines which we have previously shown to contain stem-like fractions that require one or both of these signaling cascades(Fan, Khaki et al. ; Schreck, Taylor et al. ; Bar, Chaudhry et al. 2007). We found that ATO inhibits growth and clonogenicity with induction of apoptosis in all three lines. CD133 percentage, as assessed by flow and quantitative real-time PCR, as well as the levels of other stem cell transcripts, were also reduced following ATO treatment. Finally, we found significant reductions in the expression of both Notch and Hedgehog pathway targets.

A recently published study by Wu et al(Wu, Ji et al.) also examined the effects of ATO on Notch signaling and clonogenic growth in several adherent GBM lines as well as what appeared to be a single neurosphere culture(Wu, Ji et al.). Like us, they found reductions in stem cell markers and phenotype in the glioma cells following ATO treatment, which they suggest were at least partially due to effects on Notch. They did not examine Hedgehog pathway inhibition.

In summary, ATO has been previously shown to inhibit the growth of high serum GBM cultures, but little was known about its effects on glioma stem cells or the pathways thought to promote their specification and survival. We found that ATO depletes stem-like cancer cells as defined by surface CD133 expression in all three GBM neurosphere lines tested, with negative effects on overall growth and clonogenicity. We also noted inhibition of both Notch and Hedgehog signaling by ATO, suggesting a potential mechanism for the effects on cancer stem cells and tumor growth. Our findings are consistent with another recent study of ATO and Notch signaling in GBM neurospheres, and together these and prior reports support the development of ATO as a clinical therapeutic agent capable of inhibiting multiple signaling pathways important in stem like glioma cells.

# Chapter 6: Conclusion and Future Directions

## 6.1 Advances in Our Knowledge of Pilocytic Astrocytoma Biology

Since the publication of our work on oncogene-induced senescence in pilocytic astrocytoma (Chapter 2), there had been significant advances in our knowledge of pilocytic astrocytoma biology. New mutations had been identified, including mutations novel BRAF mutations and activating mutations in FGFR1, PTPN11 and NTRK2(Dahiya, Yu et al. ; Jones, Hutter et al. ; Lin, Rodriguez et al.). Additionally, the mTOR pathway, found to be activated in the majority of pediatric low-grade gliomas, had been identified as another potential therapeutic target (Hutt-Cabezas, Karajannis et al.). This is due in part to availability of better model systems, including the short-term pilocytic astrocytoma cultures that groups including ours generated, stable pilocytic astrocytoma cell lines for example Res186, established by Dr. Michael Bobola (University of Washington, Seattle, WA) and mouse models with fusion BRAF-transduced neural stem cells(Kaul, Chen et al. ; Bobola, Silber et al. 2005).

Using these model systems, targeted therapies against pathways found to be hyperactivated in pilocytic astrocytomas have also been studied. For example, mTOR pathway inhibition had been found to be a viable therapeutic strategy in pediatric low-grade gliomas with mTOR hyperactivation (Hutt-Cabezas, Karajannis et al.). Interestingly, molecular targeting of pilocytic astrocytomas containing the KIAA1549-BRAF fusion might prove to be trickier than anticipated, as specific $BRAF^{V600E}$ inhibitor Vemurafenib had been found to paradoxically activate the MAPK pathway rather than inhibit it. This suggests that thoroughly understanding the pathobiology of molecular

pathways driving pilocytic astrocytomagenesis might be important for tailoring therapies and a one-size-fits-all approach might not be viable. In conclusion, while our understanding of pilocytic astrocytoma biology has increased tremendously since the identification of the first genetic abnormality characterizing the majority of pilocytic astrocytoma, the KIAA1549-BRAF fusion gene, we are still a long way from achieving maximal therapeutic efficacy with minimal long-term side effects in children suffering from this disease.

### 6.2 Advances in our knowledge of metabolic targeting in glioblastomas

Aberrant metabolic signaling is one of the major hallmarks of cancer and is widely studied. In addition to the aerobic glycolytic phenomenon commonly seen in cancer cells, known as the "Warburg Effect", many aggressive tumors also contain highly hypoxic regions, resulting in a primarily glycolytic metabolism in tumors. Glioblastoma tumors are a classic example of aggressive, highly hypoxic tumors, where intratumoral hypoxic pseudopalisading necrosis is one of the key diagnosing criteria. There are many ways aberrant metabolic signaling can be targeted, and our work in Chapter 4 demonstrated that one of the ways to target glycolytic metabolism in glioblastoma is by inhibiting a gene, MCT4 that is specifically required for survival under highly glycolytic or hypoxic conditions.

In addition to targeting hypoxic metabolism, driving carbon-containing glycolytic byproducts towards oxidative phosphorylation has proven to be quite a successful therapeutic strategy. For example, Michelakis *et al.* used dichloroacetate to inhibit pyruvate dehydrogenase kinase II, driving pyruvate through the TCA cycle and oxidative phosphorylation rather than producing lactate, resulting in apoptosis induction in primary

glioblastoma cells(Michelakis, Sutendra et al.). As oxidative phosphorylation is more energetically efficient, this might appear to be counter-intuitive. However, shunting carbon towards oxidative phosphorylation also starves tumor cells of important cellular building blocks that can be produced using by-products of glycolysis. As a result, tumor cells do not favor it.

It is important to note that in addition to glucose metabolism and glycolysis, glutamine metabolism and the TCA cycle is equally important to glioblastoma tumor survival. DeBerardinis, Thompson and colleagues first demonstrated that intermediates from the TCA cycle are important for anaplerosis and glutamine conversion to oxaloacetate helps drive this process(DeBerardinis, Mancuso et al. 2007). A study by Marin-Valencia *et al.* utilizing human GBM orthotopic tumor xenografts to investigate GBM metabolism in cells that had never been cultured *in vitro*, also found that GBM tumors are distinct from the surrounding brain and are very metabolically diverse. They undergo aerobic glycolysis, the TCA cycle, anaplerosis, and importantly have a large pool of glutamine that are important for their growth and survival(Marin-Valencia, Yang et al.). This addiction to glutamine for anaplerosis might be mutation-dependent. Seltzer, Riggins and colleague found that glioblastoma cell lines carrying mutant IDH1 were significantly more sensitive to glutaminase inhibitors compared to isogenic IDH wild type lines. As this growth inhibition can be rescued by exogenous alpha-ketoglutarate, it suggests that mutant IDH1 might shunt the majority of available alpha-ketoglutarate into 2-hydroxyglutarate production, leading to a shortfall of alpha-ketoglutarate that glutaminase will have to make up for(Seltzer, Bennett et al.).

With the advances in our knowledge of the aberrant metabolism in glioblastoma, there are also advances in metabolic targeting of glioblastoma tumors. Our work in Chapter 4 is just one of the many ways in which this can be done. It is important to understand that glioblastoma tumors are highly aggressive malignant brain tumors that have a very low 5-year survival rate. Overall survival has increased just a few months following decades of research. Realistically, novel single agent therapy is unlikely to improve survival much compared to available therapeutic agents. Increasingly, novel therapeutic agents are being used in conjunction with existing therapy to target tumors simultaneously. For example, the most common therapeutic options for glioblastoma involve both surgical resection and radiation. A study by Tamura *et al.* found that patients who had undergone these treatments have increased expression of stem-cell markers, including Nestin and CD133, by immunohistochemistry performed on histological sections, suggesting that stem-like glioblastoma cells are giving rise to tumor resistance(Tamura, Aoyagi et al.). One potential way MCT4 inhibitors can be used in glioblastomas is together with radiotherapy, where radiotherapy would kill the bulk of the tumor, and MCT4 inhibitors would target the radiotherapy resistant stem-like cells. Since one of the major therapeutic challenges of glioblastoma is resistance, our work in Chapter 4 also demonstrated that MCT4 inhibitors might be useful for preventing tumors from recurring by getting rid of stem-like cells in glioblastoma.

### 6.3 Advances in stem-cell targeting in glioblastoma

Indeed, since glioblastoma stem-like cells are causing recurrence and therapeutic resistance, targeting glioblastoma stem-like cells is becoming an attractive therapeutic strategy. In addition to having a unique metabolic phenotype, glioblastoma stem cells

also have aberrant activation of proteins such as telomerase and developmental pathways usually only turned on in normal stem cells, for example TGF-beta, Wnt, Hedgehog and Notch(Clarke, Dick et al. 2006; Clement, Sanchez et al. 2007). As a result, therapeutic targeting of these proteins and pathways had been an attractive therapeutic strategy(Marian, Cho et al. ; Bar, Chaudhry et al. 2007; Ikushima, Todo et al. 2009). In fact, it had been shown that Notch silencing sensitizes glioma stem cells to radiation therapy(Wang, Wakeman et al. 2010). However, single pathway targeting has not always been successful in inhibiting glioblastoma stem-like cell growth. In fact, our group had shown that targeting the Notch pathway in glioblastoma stem-like cells led to the upregulation of the Hedgehog pathway, a potential source of therapeutic resistance(Schreck, Taylor et al.). Therefore, in Chapter 5, we explored co-targeting 2 stem-cell pathways, the Hedgehog and Notch signaling pathways using arsenic trioxide as a potential therapeutic option in glioblastoma. We found that, as a single agent, arsenic trioxide inhibited both Notch and Hedgehog pathways and also led to suppression of growth, clonogenicity and stem-like phenotype. This suggests that arsenic trioxide might be a useful therapeutic agent to target glioblastoma stem-like cells with aberrant activation of both Notch and Hedgehog pathways, and in fact, it is currently being used in phase I clinical trials against childhood infiltration astrocytomas, another indicator of its efficacy(Cohen, Gibbs et al.).

Another method researchers have used to target these tumor stem cells is by attempting to differentiate them. For example, Piccirillo *et al.* have used bone morphogenic proteins (BMPs) to differentiate CD133+ glioblastoma stem-like cells, and this led to decreased tumor-formation capacity(Piccirillo, Reynolds et al. 2006). It is important to note that not

all glioblastoma stem-like cells were differentiated with BMP treatment. While increasing the dosage and timing of BMP treatment might ameliorate this, Lee and colleagues have also found that epigenetic silencing of the BMP pathway abrogated the pro-differentiation effect of BMP in glioblastoma stem-like cells and led to resistance(Lee, Son et al. 2008).

Interestingly, it had been shown that some commonly used chemotherapeutic agents work surprisingly well on glioblastoma stem-like cells. For example, temozolomide had been shown to selectively inhibit growth of glioblastoma stem-like cells(Beier, Rohrl et al. 2008). This suggests that simply tweaking the treatment regiment of patients to adjust the dosage and timing of temozolomide administration and radiation might be sufficient lead to improved therapeutic efficacy. Alternatively, inhibitors of DNA repair pathway genes such as Chk1 and Chk2 kinases also seem to act synergistically with radiation to target glioblastoma stem-like cells(Bao, Wu et al. 2006).

Last but not least, it is important to consider microenvironmental factors and their contribution in the stem-like potential of glioblastoma cells. Piccirillo *et al.* compared cells from glioblastoma tumor core and periphery and found that only cells from tumor core formed xenografts in SCID mice(Piccirillo, Combi et al. 2009). Increased hypoxia within the tumor core might contribute to increased stem-like potential of the cells, leading to increased tumorigenicity. It is also possible that other microenvironmental factors in the different regions of the tumor contributed to this difference in tumorigenicity. Interestingly, Calabrese and colleagues found that glioblastoma stem-like cells seem to preferentially home to perivascular regions of the tumor, which would likely be well-oxygenated(Calabrese, Poppleton et al. 2007). This is in contrast to our

group's finding that glioblastoma stem-like cells appear to be preferentially located around the hypoxic regions of the tumor. It is possible that this dichotomy exist due to different factors that are produced both during hypoxic induction and in perivascular regions, that are beneficial for stem-cells or induce stem-like behaviour in tumor cells. This also highlights the complexity of glioblastoma stem-like cells, and the difficulty in therapeutically targeting them. While significant advances had been made in the past few years, more work needs to be done before we can fully understand glioblastoma stem-like cell behaviour in order to achieve therapeutic advancement.

### 6.4 Concluding remarks

We have investigated 3 different hallmarks of cancer - evading growth suppressors, deregulated energetic and sustained proliferative signaling. We had found that downregulation of tumor suppressor $p16^{INK4a}$ led to pilocytic astrocytoma patients having poorer survival, presumably due to bypassing senescence regulation. We had also found that in glioblastoma, inhibiting tumor metabolism by inhibiting MCT4 led to decreased cell growth. In addition, inhibiting stem cell pathways Notch and Hedgehog led to decreased cell growth and stem-ness. However, while we have achieved, as many others had, great success in our preclinical models of glioblastoma, it is important to note that this might not translate to clinical efficacy. As had often been seen, single agent or single target therapy almost invariably leads to resistance. Therefore, it might be worthwhile to consider targeting genes and pathways like MCT4, Notch and Hedgehog, as complimentary to current therapeutic regiments. For example, MCT4 is important for hypoxic stem-like cell survival, and these are the same cells that are resistant to

radiotherapy. If MCT4 inhibition can be achieved concurrently with radiotherapy, both tumor bulk and radioresistant cell population might be eradicated.

Cancer is a devastating disease, and glioblastoma is one of the deadliest malignant tumors, with 5-year survivals of less than 10%. While 5-year survival is still relatively low, it is important to note that newer drugs have significantly improved overall survival. For example, Temodar has more than doubled glioblastoma 2-year survival to 26.5%, as compared to radiotherapy alone (10.4%)(Stupp, Mason et al. 2005). With continued research and identification of novel therapeutic targets, improved clinical regiment and clinical care, glioblastoma might one day become a manageable disease like many breast cancers and prostate cancers now are.

References


Akao, Y., Y. Nakagawa, et al. (1999). "Arsenic trioxide induces apoptosis in neuroblastoma cell lines through the activation of caspase 3 in vitro." FEBS Lett 455(1-2): 59-62.

Babcock, J. T. and L. A. Quilliam (2011). "Rheb/mTOR activation and regulation in cancer: novel treatment strategies beyond rapamycin." Curr Drug Targets 12(8): 1223-31.

Bajenaru, M. L., J. R. Garbow, et al. (2005). "Natural history of neurofibromatosis 1-associated optic nerve glioma in mice." Ann Neurol 57(1): 119-27.

Banerjee, S., S. M. Gianino, et al. (2011). "Interpreting mammalian target of rapamycin and cell growth inhibition in a genetically engineered mouse model of Nf1-deficient astrocytes." Mol Cancer Ther 10(2): 279-91.

Bao, S., Q. Wu, et al. (2006). "Glioma stem cells promote radioresistance by preferential activation of the DNA damage response." Nature 444(7120): 756-60.

Bar, E. E. (2011). "Glioblastoma, cancer stem cells and hypoxia." Brain Pathol 21(2): 119-29.

Bar, E. E., A. Chaudhry, et al. (2007). "Cyclopamine-mediated hedgehog pathway inhibition depletes stem-like cancer cells in glioblastoma." Stem Cells 25(10): 2524-33.

Bar, E. E., A. Lin, et al. "Hypoxia increases the expression of stem-cell markers and promotes clonogenicity in glioblastoma neurospheres." Am J Pathol 177(3): 1491-502.

Bar, E. E., A. Lin, et al. (2010). "Hypoxia increases the expression of stem-cell markers and promotes clonogenicity in glioblastoma neurospheres." Am J Pathol 177(3): 1491-502.

Bar, E. E., A. Lin, et al. (2008). "Frequent gains at chromosome 7q34 involving BRAF in pilocytic astrocytoma." J Neuropathol Exp Neurol 67(9): 878-87.

Bax, D. A., S. E. Little, et al. (2009). "Molecular and phenotypic characterisation of paediatric glioma cell lines as models for preclinical drug development." PLoS One 4(4): e5209.

Beier, D., S. Rohrl, et al. (2008). "Temozolomide preferentially depletes cancer stem cells in glioblastoma." Cancer Res 68(14): 5706-15.

Berman, D. M., S. S. Karhadkar, et al. (2003). "Widespread requirement for Hedgehog ligand stimulation in growth of digestive tract tumours." Nature 425(6960): 846-51.

Bobola, M. S., J. R. Silber, et al. (2005). "O6-methylguanine-DNA methyltransferase, O6-benzylguanine, and resistance to clinical alkylators in pediatric primary brain tumor cell lines." Clin Cancer Res 11(7): 2747-55.

Bordow, S. B., M. Haber, et al. (1994). "Expression of the multidrug resistance-associated protein (MRP) gene correlates with amplification and overexpression of the N-myc oncogene in childhood neuroblastoma." Cancer Res 54(19): 5036-40.

Bowers, D. C., L. Gargan, et al. (2003). "Study of the MIB-1 labeling index as a predictor of tumor progression in pilocytic astrocytomas in children and adolescents." J Clin Oncol 21(15): 2968-73.

Buccoliero, A. M., F. Castiglione, et al. (2012). "IDH1 Mutation in Pediatric Gliomas: Has it a Diagnostic and Prognostic Value?" Fetal Pediatr Pathol.
Buccoliero, A. M., A. Franchi, et al. (2009). "Subependymal giant cell astrocytoma (SEGA): Is it an astrocytoma? Morphological, immunohistochemical and ultrastructural study." Neuropathology 29(1): 25-30.
Calabrese, C., H. Poppleton, et al. (2007). "A perivascular niche for brain tumor stem cells." Cancer Cell 11(1): 69-82.
Capper, D., M. Preusser, et al. (2011). "Assessment of BRAF V600E mutation status by immunohistochemistry with a mutation-specific monoclonal antibody." Acta Neuropathol 122(1): 11-9.
Chan, J. A., H. Zhang, et al. (2004). "Pathogenesis of tuberous sclerosis subependymal giant cell astrocytomas: biallelic inactivation of TSC1 or TSC2 leads to mTOR activation." J Neuropathol Exp Neurol 63(12): 1236-42.
Chapman, P. B., A. Hauschild, et al. (2011). "Improved Survival with Vemurafenib in Melanoma with BRAF V600E Mutation." New England Journal of Medicine 364(26): 2507-2516.
Chen, G. Q., J. Zhu, et al. (1996). "In vitro studies on cellular and molecular mechanisms of arsenic trioxide (As2O3) in the treatment of acute promyelocytic leukemia: As2O3 induces NB4 cell apoptosis with downregulation of Bcl-2 expression and modulation of PML-RAR alpha/PML proteins." Blood 88(3): 1052-61.
Cheng, Y., J. C. Pang, et al. (2000). "Pilocytic astrocytomas do not show most of the genetic changes commonly seen in diffuse astrocytomas." Histopathology 37(5): 437-44.
Chiche, J., Y. Le Fur, et al. (2012). "In vivo pH in metabolic-defective Ras-transformed fibroblast tumors: key role of the monocarboxylate transporter, MCT4, for inducing an alkaline intracellular pH." Int J Cancer 130(7): 1511-20.
Chiu, H. W., S. Y. Ho, et al. (2009). "Combination treatment with arsenic trioxide and irradiation enhances autophagic effects in U118-MG cells through increased mitotic arrest and regulation of PI3K/Akt and ERK1/2 signaling pathways." Autophagy 5(4): 472-83.
Chiu, H. W., Y. S. Ho, et al. (2011). "Arsenic trioxide induces autophagy and apoptosis in human glioma cells in vitro and in vivo through downregulation of survivin." J Mol Med (Berl) 89(9): 927-41.
Chong, E. Y., P. Y. Lam, et al. (1998). "Telomerase expression in gliomas including the nonastrocytic tumors." Hum Pathol 29(6): 599-603.
Cin, H., C. Meyer, et al. (2011). "Oncogenic FAM131B-BRAF fusion resulting from 7q34 deletion comprises an alternative mechanism of MAPK pathway activation in pilocytic astrocytoma." Acta Neuropathol 121(6): 763-74.
Clarke, J., C. Penas, et al. "Epigenetic pathways and glioblastoma treatment." Epigenetics 8(8).
Clarke, M. F., J. E. Dick, et al. (2006). "Cancer stem cells--perspectives on current status and future directions: AACR Workshop on cancer stem cells." Cancer Res 66(19): 9339-44.
Clement, V., P. Sanchez, et al. (2007). "HEDGEHOG-GLI1 signaling regulates human glioma growth, cancer stem cell self-renewal, and tumorigenicity." Curr Biol 17(2): 165-72.

Cohen, K. J., I. C. Gibbs, et al. "A phase I trial of arsenic trioxide chemoradiotherapy for infiltrating astrocytomas of childhood." Neuro Oncol 15(6): 783-7.
Cohen, M. H., S. Hirschfeld, et al. (2001). "Drug approval summaries: arsenic trioxide, tamoxifen citrate, anastrazole, paclitaxel, bexarotene." Oncologist 6(1): 4-11.
Colen, C. B., Y. Shen, et al. (2011). "Metabolic targeting of lactate efflux by malignant glioma inhibits invasiveness and induces necrosis: an in vivo study." Neoplasia 13(7): 620-32.
Colin, C., N. Baeza, et al. (2006). "Identification of genes differentially expressed in glioblastoma versus pilocytic astrocytoma using Suppression Subtractive Hybridization." Oncogene 25(19): 2818-26.
Collins, P. C., L. K. Nielsen, et al. (1998). "Characterization of hematopoietic cell expansion, oxygen uptake, and glycolysis in a controlled, stirred-tank bioreactor system." Biotechnol Prog 14(3): 466-72.
Conley, S. J., E. Gheordunescu, et al. "Antiangiogenic agents increase breast cancer stem cells via the generation of tumor hypoxia." Proc Natl Acad Sci U S A 109(8): 2784-9.
Courtois-Cox, S., S. M. Genther Williams, et al. (2006). "A negative feedback signaling network underlies oncogene-induced senescence." Cancer Cell 10(6): 459-72.
Dahiya, S., J. Yu, et al. "Novel BRAF Alteration in a Sporadic Pilocytic Astrocytoma." Case Rep Med 2012: 418672.
Dasgupta, B., Y. Yi, et al. (2005). "Proteomic analysis reveals hyperactivation of the mammalian target of rapamycin pathway in neurofibromatosis 1-associated human and mouse brain tumors." Cancer Res 65(7): 2755-60.
Davies, H., G. R. Bignell, et al. (2002). "Mutations of the BRAF gene in human cancer." Nature 417(6892): 949-54.
Dean, M., T. Fojo, et al. (2005). "Tumour stem cells and drug resistance." Nat Rev Cancer 5(4): 275-84.
DeBerardinis, R. J., A. Mancuso, et al. (2007). "Beyond aerobic glycolysis: transformed cells can engage in glutamine metabolism that exceeds the requirement for protein and nucleotide synthesis." Proc Natl Acad Sci U S A 104(49): 19345-50.
Deshmukh, H., T. H. Yeh, et al. (2008). "High-resolution, dual-platform aCGH analysis reveals frequent HIPK2 amplification and increased expression in pilocytic astrocytomas." Oncogene 27(34): 4745-51.
Dias-Santagata, D., Q. Lam, et al. (2011). "BRAF V600E mutations are common in pleomorphic xanthoastrocytoma: diagnostic and therapeutic implications." PLoS One 6(3): e17948.
Dimmer, K. S., B. Friedrich, et al. (2000). "The low-affinity monocarboxylate transporter MCT4 is adapted to the export of lactate in highly glycolytic cells." Biochem J 350 Pt 1: 219-27.
Dirven, C. M., J. Koudstaal, et al. (1998). "The proliferative potential of the pilocytic astrocytoma: the relation between MIB-1 labeling and clinical and neuro-radiological follow-up." J Neurooncol 37(1): 9-16.
Dougherty, M. J., M. Santi, et al. (2010). "Activating mutations in BRAF characterize a spectrum of pediatric low-grade gliomas." Neuro Oncol 12(7): 621-30.
Ehtesham, M., A. Sarangi, et al. (2007). "Ligand-dependent activation of the hedgehog pathway in glioma progenitor cells." Oncogene 26(39): 5752-61.

Eisenhardt, A. E., H. Olbrich, et al. (2010). "Functional characterization of a BRAF insertion mutant associated with pilocytic astrocytoma." Int J Cancer.
Ellezam, B., B. J. Theeler, et al. (2012). "Recurrent PIK3CA mutations in rosette-forming glioneuronal tumor." Acta Neuropathol 123(2): 285-7.
Emuss, V., M. Garnett, et al. (2005). "Mutations of C-RAF are rare in human cancer because C-RAF has a low basal kinase activity compared with B-RAF." Cancer Res 65(21): 9719-26.
Estrada, J. C., C. Albo, et al. (2012). "Culture of human mesenchymal stem cells at low oxygen tension improves growth and genetic stability by activating glycolysis." Cell Death Differ 19(5): 743-55.
Eyler, C. E. and J. N. Rich (2008). "Survival of the fittest: cancer stem cells in therapeutic resistance and angiogenesis." J Clin Oncol 26(17): 2839-45.
Fan, X., L. Khaki, et al. "NOTCH pathway blockade depletes CD133-positive glioblastoma cells and inhibits growth of tumor neurospheres and xenografts." Stem Cells 28(1): 5-16.
Fan, X., L. Khaki, et al. (2010). "NOTCH pathway blockade depletes CD133-positive glioblastoma cells and inhibits growth of tumor neurospheres and xenografts." Stem Cells 28(1): 5-16.
Fan, X., W. Matsui, et al. (2006). "Notch pathway inhibition depletes stem-like cells and blocks engraftment in embryonal brain tumors." Cancer Res 66(15): 7445-52.
Fang, J., Q. J. Quinones, et al. (2006). "The H+-linked monocarboxylate transporter (MCT1/SLC16A1): a potential therapeutic target for high-risk neuroblastoma." Mol Pharmacol 70(6): 2108-15.
Fernandez, C., D. Figarella-Branger, et al. (2003). "Pilocytic astrocytomas in children: prognostic factors--a retrospective study of 80 cases." Neurosurgery 53(3): 544-53; discussion 554-5.
Fisher, B. J., E. Naumova, et al. (2002). "Ki-67: a prognostic factor for low-grade glioma?" Int J Radiat Oncol Biol Phys 52(4): 996-1001.
Fisher, P. G., T. Tihan, et al. (2008). "Outcome analysis of childhood low-grade astrocytomas." Pediatr Blood Cancer 51(2): 245-50.
Forshew, T., R. G. Tatevossian, et al. (2009). "Activation of the ERK/MAPK pathway: a signature genetic defect in posterior fossa pilocytic astrocytomas." J Pathol 218(2): 172-81.
Franz, D. N., J. Leonard, et al. (2006). "Rapamycin causes regression of astrocytomas in tuberous sclerosis complex." Annals of Neurology 59(3): 490-498.
Froberg, M. K., D. Z. Gerhart, et al. (2001). "Expression of monocarboxylate transporter MCT1 in normal and neoplastic human CNS tissues." Neuroreport 12(4): 761-5.
Fryssira, H., G. Leventopoulos, et al. (2008). "Tumor development in three patients with Noonan syndrome." Eur J Pediatr 167(9): 1025-31.
Galli, R., E. Binda, et al. (2004). "Isolation and characterization of tumorigenic, stem-like neural precursors from human glioblastoma." Cancer Res 64(19): 7011-21.
Gong, A. and S. Huang (2012). "FoxM1 and Wnt/beta-catenin signaling in glioma stem cells." Cancer Res 72(22): 5658-62.
Grabmaier, K., A. d. W. MC, et al. (2004). "Strict regulation of CAIX(G250/MN) by HIF-1alpha in clear cell renal cell carcinoma." Oncogene 23(33): 5624-31.

Gronych, J., A. Korshunov, et al. (2011). "An activated mutant BRAF kinase domain is sufficient to induce pilocytic astrocytoma in mice." J Clin Invest 121(4): 1344-8.
Gunny, R. S., R. D. Hayward, et al. (2005). "Spontaneous regression of residual low-grade cerebellar pilocytic astrocytomas in children." Pediatr Radiol 35(11): 1086-91.
Gutmann, D. H., N. M. Hedrick, et al. (2002). "Comparative gene expression profile analysis of neurofibromatosis 1-associated and sporadic pilocytic astrocytomas." Cancer Res 62(7): 2085-91.
Haga, N., N. Fujita, et al. (2005). "Involvement of mitochondrial aggregation in arsenic trioxide (As2O3)-induced apoptosis in human glioblastoma cells." Cancer Sci 96(11): 825-33.
Hanahan, D. and R. A. Weinberg "Hallmarks of cancer: the next generation." Cell 144(5): 646-74.
Hasselblatt, M., B. Riesmeier, et al. (2011). "BRAF-KIAA1549 fusion transcripts are less frequent in pilocytic astrocytomas diagnosed in adults." Neuropathol Appl Neurobiol 37(7): 803-6.
Hawkins, C., E. Walker, et al. (2011). "BRAF-KIAA1549 fusion predicts better clinical outcome in pediatric low-grade astrocytoma." Clin Cancer Res 17(14): 4790-8.
Heaphy, C. M., A. P. Subhawong, et al. (2011). "Prevalence of the alternative lengthening of telomeres telomere maintenance mechanism in human cancer subtypes." Am J Pathol 179(4): 1608-15.
Heddleston, J. M., Z. Li, et al. (2010). "Hypoxia inducible factors in cancer stem cells." Br J Cancer 102(5): 789-95.
Heddleston, J. M., Z. Li, et al. (2009). "The hypoxic microenvironment maintains glioblastoma stem cells and promotes reprogramming towards a cancer stem cell phenotype." Cell Cycle 8(20): 3274-84.
Hegedus, B., D. Banerjee, et al. (2008). "Preclinical cancer therapy in a mouse model of neurofibromatosis-1 optic glioma." Cancer Res 68(5): 1520-8.
Horbinski, C., R. L. Hamilton, et al. (2010). "Association of molecular alterations, including BRAF, with biology and outcome in pilocytic astrocytomas." Acta Neuropathol 119(5): 641-9.
Horbinski, C., M. N. Nikiforova, et al. (2012). "Interplay among BRAF, p16, p53, and MIB1 in pediatric low-grade gliomas." Neuro Oncol.
Hu, Y. L., M. DeLay, et al. "Hypoxia-induced autophagy promotes tumor cell survival and adaptation to antiangiogenic treatment in glioblastoma." Cancer Res 72(7): 1773-83.
Hu, Y. Y., M. H. Zheng, et al. "Notch signaling contributes to the maintenance of both normal neural stem cells and patient-derived glioma stem cells." BMC Cancer 11: 82.
Hu, Y. Y., M. H. Zheng, et al. (2011). "Notch signaling contributes to the maintenance of both normal neural stem cells and patient-derived glioma stem cells." BMC Cancer 11: 82.
Hunter, S., A. Young, et al. (2002). "Differential expression between pilocytic and anaplastic astrocytomas: identification of apolipoprotein D as a marker for low-grade, non-infiltrating primary CNS neoplasms." J Neuropathol Exp Neurol 61(3): 275-81.

Hutt-Cabezas, M., M. A. Karajannis, et al. "Activation of mTORC1/mTORC2 signaling in pediatric low-grade glioma and pilocytic astrocytoma reveals mTOR as a therapeutic target." Neuro Oncol 15(12): 1604-14.
Ikushima, H., T. Todo, et al. (2009). "Autocrine TGF-beta signaling maintains tumorigenicity of glioma-initiating cells through Sry-related HMG-box factors." Cell Stem Cell 5(5): 504-14.
Jacob, K., S. Albrecht, et al. (2009). "Duplication of 7q34 is specific to juvenile pilocytic astrocytomas and a hallmark of cerebellar and optic pathway tumours." Br J Cancer 101(4): 722-33.
Jacob, K., D. A. Quang-Khuong, et al. (2011). "Genetic aberrations leading to MAPK pathway activation mediate oncogene-induced senescence in sporadic pilocytic astrocytomas." Clin Cancer Res 17(14): 4650-60.
Janzarik, W. G., C. P. Kratz, et al. (2007). "Further evidence for a somatic KRAS mutation in a pilocytic astrocytoma." Neuropediatrics 38(2): 61-3.
Jentoft, M., C. Giannini, et al. (2010). "Phenotypic variations in NF1-associated low grade astrocytomas: possible role for increased mTOR activation in a subset." Int J Clin Exp Pathol 4(1): 43-57.
Johnson, M. W., C. G. Eberhart, et al. (2010). "Spectrum of pilomyxoid astrocytomas: intermediate pilomyxoid tumors." Am J Surg Pathol 34(12): 1783-91.
Jones, D. T., B. Hutter, et al. "Recurrent somatic alterations of FGFR1 and NTRK2 in pilocytic astrocytoma." Nat Genet 45(8): 927-32.
Jones, D. T., S. Kocialkowski, et al. (2008). "Tandem duplication producing a novel oncogenic BRAF fusion gene defines the majority of pilocytic astrocytomas." Cancer Res 68(21): 8673-7.
Jones, D. T., S. Kocialkowski, et al. (2009). "Oncogenic RAF1 rearrangement and a novel BRAF mutation as alternatives to KIAA1549:BRAF fusion in activating the MAPK pathway in pilocytic astrocytoma." Oncogene 28(20): 2119-23.
Jozwiak, J., S. Jozwiak, et al. (2005). "Immunohistochemical and microscopic studies on giant cells in tuberous sclerosis." Histol Histopathol 20(4): 1321-6.
Kanamori, M., T. Kawaguchi, et al. (2007). "Contribution of Notch signaling activation to human glioblastoma multiforme." J Neurosurg 106(3): 417-27.
Kanzawa, T., Y. Kondo, et al. (2003). "Induction of autophagic cell death in malignant glioma cells by arsenic trioxide." Cancer Res 63(9): 2103-8.
Kanzawa, T., L. Zhang, et al. (2005). "Arsenic trioxide induces autophagic cell death in malignant glioma cells by upregulation of mitochondrial cell death protein BNIP3." Oncogene 24(6): 980-91.
Karafin, M., G. I. Jallo, et al. (2011). "Rosette forming glioneuronal tumor in association with Noonan syndrome: pathobiological implications." Clin Neuropathol 30(6): 297-300.
Kaul, A., Y. H. Chen, et al. "Pediatric glioma-associated KIAA1549:BRAF expression regulates neuroglial cell growth in a cell type-specific and mTOR-dependent manner." Genes Dev 26(23): 2561-6.
Kim, J., B. T. Aftab, et al. "Itraconazole and arsenic trioxide inhibit Hedgehog pathway activation and tumor growth associated with acquired resistance to smoothened antagonists." Cancer Cell 23(1): 23-34.

Kim, J. H., Y. S. Lew, et al. (2003). "Arsenic trioxide enhances radiation response of 9L glioma in the rat brain." Radiat Res 160(6): 662-6.
Kirk, P., M. C. Wilson, et al. (2000). "CD147 is tightly associated with lactate transporters MCT1 and MCT4 and facilitates their cell surface expression." EMBO J 19(15): 3896-904.
Kita, Y., K. Mimori, et al. "STC2: a predictive marker for lymph node metastasis in esophageal squamous-cell carcinoma." Ann Surg Oncol 18(1): 261-72.
Kluwe, L., C. Hagel, et al. (2001). "Loss of NF1 alleles distinguish sporadic from NF1-associated pilocytic astrocytomas." Journal of neuropathology and experimental neurology 60(9): 917-20.
Korshunov, A., J. Meyer, et al. (2009). "Combined molecular analysis of BRAF and IDH1 distinguishes pilocytic astrocytoma from diffuse astrocytoma." Acta Neuropathol 118(3): 401-5.
Krueger, D. A., M. M. Care, et al. (2010). "Everolimus for subependymal giant-cell astrocytomas in tuberous sclerosis." N Engl J Med 363(19): 1801-11.
Larsson, L. G. (2011). "Oncogene- and tumor suppressor gene-mediated suppression of cellular senescence." Semin Cancer Biol 21(6): 367-76.
Lawson, A. R., G. F. Hindley, et al. (2011). "RAF gene fusion breakpoints in pediatric brain tumors are characterized by significant enrichment of sequence microhomology." Genome Res 21(4): 505-14.
Lawson, A. R., R. G. Tatevossian, et al. (2010). "RAF gene fusions are specific to pilocytic astrocytoma in a broad paediatric brain tumour cohort." Acta Neuropathol 120(2): 271-3.
Le Floch, R., J. Chiche, et al. (2011). "CD147 subunit of lactate/H+ symporters MCT1 and hypoxia-inducible MCT4 is critical for energetics and growth of glycolytic tumors." Proc Natl Acad Sci U S A 108(40): 16663-8.
Lee da, Y., T. H. Yeh, et al. (2010). "Neurofibromatosis-1 regulates neuroglial progenitor proliferation and glial differentiation in a brain region-specific manner." Genes Dev 24(20): 2317-29.
Lee, J., S. Kotliarova, et al. (2006). "Tumor stem cells derived from glioblastomas cultured in bFGF and EGF more closely mirror the phenotype and genotype of primary tumors than do serum-cultured cell lines." Cancer Cell 9(5): 391-403.
Lee, J., M. J. Son, et al. (2008). "Epigenetic-mediated dysfunction of the bone morphogenetic protein pathway inhibits differentiation of glioblastoma-initiating cells." Cancer Cell 13(1): 69-80.
Li, K. K., J. C. Pang, et al. (2009). "miR-124 is frequently down-regulated in medulloblastoma and is a negative regulator of SLC16A1." Hum Pathol 40(9): 1234-43.
Li, Z., S. Bao, et al. (2009). "Hypoxia-inducible factors regulate tumorigenic capacity of glioma stem cells." Cancer Cell 15(6): 501-13.
Lin, A., F. J. Rodriguez, et al. "BRAF alterations in primary glial and glioneuronal neoplasms of the central nervous system with identification of 2 novel KIAA1549:BRAF fusion variants." J Neuropathol Exp Neurol 71(1): 66-72.
Lin, A., F. J. Rodriguez, et al. (2012). "BRAF alterations in primary glial and glioneuronal neoplasms of the central nervous system with identification of 2 novel KIAA1549:BRAF fusion variants." J Neuropathol Exp Neurol 71(1): 66-72.

Lin, Q., Y. Kim, et al. (2008). "Oxygen and Cell Fate Decisions." Gene Regul Syst Bio 2: 43-51.
Listernick, R., J. Charrow, et al. (1989). "Optic gliomas in children with neurofibromatosis type 1." The Journal of pediatrics 114(5): 788-92.
Liu, S., G. Dontu, et al. (2006). "Hedgehog signaling and Bmi-1 regulate self-renewal of normal and malignant human mammary stem cells." Cancer Res 66(12): 6063-71.
Louis, D. N., H. Ohgaki, et al. (2007). WHO Classification of Tumours of the Central Nervous System. LYON, IARC Press.
Maeda, H., S. Hori, et al. (2001). "Tumor growth inhibition by arsenic trioxide (As2O3) in the orthotopic metastasis model of androgen-independent prostate cancer." Cancer Res 61(14): 5432-40.
Magnuson, B., B. Ekim, et al. (2012). "Regulation and function of ribosomal protein S6 kinase (S6K) within mTOR signalling networks." Biochem J 441(1): 1-21.
Manning Fox, J. E., D. Meredith, et al. (2000). "Characterisation of human monocarboxylate transporter 4 substantiates its role in lactic acid efflux from skeletal muscle." J Physiol 529 Pt 2: 285-93.
Marian, C. O., S. K. Cho, et al. "The telomerase antagonist, imetelstat, efficiently targets glioblastoma tumor-initiating cells leading to decreased proliferation and tumor growth." Clin Cancer Res 16(1): 154-63.
Marin-Valencia, I., C. Yang, et al. "Analysis of tumor metabolism reveals mitochondrial glucose oxidation in genetically diverse human glioblastomas in the mouse brain in vivo." Cell Metab 15(6): 827-37.
Mathupala, S. P., P. Parajuli, et al. (2004). "Silencing of monocarboxylate transporters via small interfering ribonucleic acid inhibits glycolysis and induces cell death in malignant glioma: an in vitro study." Neurosurgery 55(6): 1410-9; discussion 1419.
McDuff, F. K. and S. D. Turner (2011). "Jailbreak: oncogene-induced senescence and its evasion." Cell Signal 23(1): 6-13.
Mendoza, M. C., E. E. Er, et al. (2011). "The Ras-ERK and PI3K-mTOR pathways: cross-talk and compensation." Trends Biochem Sci 36(6): 320-8.
Michaloglou, C., L. C. Vredeveld, et al. (2005). "BRAFE600-associated senescence-like cell cycle arrest of human naevi." Nature 436(7051): 720-4.
Michelakis, E. D., G. Sutendra, et al. "Metabolic modulation of glioblastoma with dichloroacetate." Sci Transl Med 2(31): 31ra34.
Miranda-Goncalves, V., M. Honavar, et al. (2012). "Monocarboxylate transporters (MCTs) in gliomas: expression and exploitation as therapeutic targets." Neuro Oncol.
Nasr, R., M. C. Guillemin, et al. (2008). "Eradication of acute promyelocytic leukemia-initiating cells through PML-RARA degradation." Nat Med 14(12): 1333-42.
Ning, S. and S. J. Knox (2004). "Increased cure rate of glioblastoma using concurrent therapy with radiotherapy and arsenic trioxide." Int J Radiat Oncol Biol Phys 60(1): 197-203.
O'Brien, C. A., A. Kreso, et al. (2009). "Cancer stem cells in solid tumors: an overview." Semin Radiat Oncol 19(2): 71-7.
Packer, R. J., M. Yalon, et al. (2010). "Phase I/II Study of Tarceva/Rapamcin for Recurrent Pediatric Low-Grade Gliomas (LGG)." Neuro-Oncology 12(6): ii20.

Park, W. H., J. G. Seol, et al. (2000). "Arsenic trioxide-mediated growth inhibition in MC/CAR myeloma cells via cell cycle arrest in association with induction of cyclin-dependent kinase inhibitor, p21, and apoptosis." Cancer Res 60(11): 3065-71.

Pasca di Magliano, M. and M. Hebrok (2003). "Hedgehog signalling in cancer formation and maintenance." Nat Rev Cancer 3(12): 903-11.

Paugh, B. S., C. Qu, et al. (2010). "Integrated molecular genetic profiling of pediatric high-grade gliomas reveals key differences with the adult disease." J Clin Oncol 28(18): 3061-8.

Peacock, C. D., Q. Wang, et al. (2007). "Hedgehog signaling maintains a tumor stem cell compartment in multiple myeloma." Proc Natl Acad Sci U S A 104(10): 4048-53.

Pencalet, P., W. Maixner, et al. (1999). "Benign cerebellar astrocytomas in children." J Neurosurg 90(2): 265-73.

Pfister, S., W. G. Janzarik, et al. (2008). "BRAF gene duplication constitutes a mechanism of MAPK pathway activation in low-grade astrocytomas." J Clin Invest 118(5): 1739-49.

Piccirillo, S. G., R. Combi, et al. (2009). "Distinct pools of cancer stem-like cells coexist within human glioblastomas and display different tumorigenicity and independent genomic evolution." Oncogene 28(15): 1807-11.

Piccirillo, S. G., B. A. Reynolds, et al. (2006). "Bone morphogenetic proteins inhibit the tumorigenic potential of human brain tumour-initiating cells." Nature 444(7120): 761-5.

Pistollato, F., H. L. Chen, et al. (2009). "Hypoxia and HIF1alpha repress the differentiative effects of BMPs in high-grade glioma." Stem Cells 27(1): 7-17.

Pistollato, F., H. L. Chen, et al. (2007). "Oxygen tension controls the expansion of human CNS precursors and the generation of astrocytes and oligodendrocytes." Mol Cell Neurosci 35(3): 424-35.

Pollack, I. F., D. Claassen, et al. (1995). "Low-grade gliomas of the cerebral hemispheres in children: an analysis of 71 cases." J Neurosurg 82(4): 536-47.

Pollack, I. F., R. L. Hamilton, et al. (2011). "IDH1 mutations are common in malignant gliomas arising in adolescents: a report from the Children's Oncology Group." Childs Nerv Syst 27(1): 87-94.

Potter, V. R. (1958). "The biochemical approach to the cancer problem." Fed Proc 17(2): 691-7.

Pucer, A., R. Castino, et al. (2010). "Differential role of cathepsins B and L in autophagy-associated cell death induced by arsenic trioxide in U87 human glioblastoma cells." Biol Chem 391(5): 519-31.

Purow, B. W., R. M. Haque, et al. (2005). "Expression of Notch-1 and its ligands, Delta-like-1 and Jagged-1, is critical for glioma cell survival and proliferation." Cancer Res 65(6): 2353-63.

Raabe, E. H., K. S. Lim, et al. (2011). "BRAF activation induces transformation and then senescence in human neural stem cells: a pilocytic astrocytoma model." Clin Cancer Res 17(11): 3590-9.

Reya, T., S. J. Morrison, et al. (2001). "Stem cells, cancer, and cancer stem cells." Nature 414(6859): 105-11.

Rickman, D. S., M. P. Bobek, et al. (2001). "Distinctive molecular profiles of high-grade and low-grade gliomas based on oligonucleotide microarray analysis." Cancer Res 61(18): 6885-91.
Rodriguez, E. F., B. W. Scheithauer, et al. (2011). "PI3K/AKT pathway alterations are associated with clinically aggressive and histologically anaplastic subsets of pilocytic astrocytoma." Acta Neuropathol 121(3): 407-20.
Rodriguez, F. J., C. Giannini, et al. (2008). "Gene expression profiling of NF-1-associated and sporadic pilocytic astrocytoma identifies aldehyde dehydrogenase 1 family member L1 (ALDH1L1) as an underexpressed candidate biomarker in aggressive subtypes." J Neuropathol Exp Neurol 67(12): 1194-204.
Rodriguez, F. J., B. W. Scheithauer, et al. (2010). "Anaplasia in pilocytic astrocytoma predicts aggressive behavior." Am J Surg Pathol 34(2): 147-60.
Rorive, S., C. Maris, et al. (2006). "Exploring the distinctive biological characteristics of pilocytic and low-grade diffuse astrocytomas using microarray gene expression profiles." J Neuropathol Exp Neurol 65(8): 794-807.
Rousselot, P., S. Labaume, et al. (1999). "Arsenic trioxide and melarsoprol induce apoptosis in plasma cell lines and in plasma cells from myeloma patients." Cancer Res 59(5): 1041-8.
Sakai, K., T. Miyahara, et al. "Spontaneous regression of multicentric pilocytic astrocytoma with CSF dissemination in an adult." Brain Tumor Pathol 28(2): 151-6.
Sakai, K., T. Miyahara, et al. (2011). "Spontaneous regression of multicentric pilocytic astrocytoma with CSF dissemination in an adult." Brain Tumor Pathol 28(2): 151-6.
Sanford, R. A., R. Bowman, et al. (1999). "A 16-year-old male with Noonan's syndrome develops progressive scoliosis and deteriorating gait." Pediatr Neurosurg 30(1): 47-52.
Sarangi, A., J. G. Valadez, et al. (2009). "Targeted inhibition of the Hedgehog pathway in established malignant glioma xenografts enhances survival." Oncogene 28(39): 3468-76.
Schietke, R., C. Warnecke, et al. "The lysyl oxidases LOX and LOXL2 are necessary and sufficient to repress E-cadherin in hypoxia: insights into cellular transformation processes mediated by HIF-1." J Biol Chem 285(9): 6658-69.
Schiffman, J. D., J. G. Hodgson, et al. (2010). "Oncogenic BRAF mutation with CDKN2A inactivation is characteristic of a subset of pediatric malignant astrocytomas." Cancer Res 70(2): 512-9.
Schindler, G., D. Capper, et al. (2011). "Analysis of BRAF V600E mutation in 1,320 nervous system tumors reveals high mutation frequencies in pleomorphic xanthoastrocytoma, ganglioglioma and extra-cerebellar pilocytic astrocytoma." Acta Neuropathol 121(3): 397-405.
Schreck, K. C., P. Taylor, et al. "The Notch target Hes1 directly modulates Gli1 expression and Hedgehog signaling: a potential mechanism of therapeutic resistance." Clin Cancer Res 16(24): 6060-70.
Schuettpelz, L. G., S. McDonald, et al. (2009). "Pilocytic astrocytoma in a child with Noonan syndrome." Pediatr Blood Cancer 53(6): 1147-9.

Seidel, S., B. K. Garvalov, et al. (2010). "A hypoxic niche regulates glioblastoma stem cells through hypoxia inducible factor 2 alpha." Brain 133(Pt 4): 983-95.
Seltzer, M. J., B. D. Bennett, et al. "Inhibition of glutaminase preferentially slows growth of glioma cells with mutant IDH1." Cancer Res 70(22): 8981-7.
Serrano, M., A. W. Lin, et al. (1997). "Oncogenic ras provokes premature cell senescence associated with accumulation of p53 and p16INK4a." Cell 88(5): 593-602.
Setty, P., M. Gessi, et al. (2011). "Sensitive determination of BRAF copy number in clinical samples by pyrosequencing." Diagn Mol Pathol 20(3): 148-57.
Shahabi, V., G. Whitney, et al. "Assessment of association between BRAF-V600E mutation status in melanomas and clinical response to ipilimumab." Cancer Immunology, Immunotherapy: 1-5.
Sharma, M. C., A. M. Ralte, et al. (2004). "Subependymal giant cell astrocytoma--a clinicopathological study of 23 cases with special emphasis on histogenesis." Pathol Oncol Res 10(4): 219-24.
Sharma, M. K., D. B. Mansur, et al. (2007). "Distinct genetic signatures among pilocytic astrocytomas relate to their brain region origin." Cancer Res 67(3): 890-900.
Sharma, M. K., M. A. Watson, et al. (2006). "Matrilin-2 expression distinguishes clinically relevant subsets of pilocytic astrocytoma." Neurology 66(1): 127-30.
Sharma, M. K., B. A. Zehnbauer, et al. (2005). "RAS pathway activation and an oncogenic RAS mutation in sporadic pilocytic astrocytoma." Neurology 65(8): 1335-6.
Sharma, S. G. and M. L. Gulley (2010). "BRAF mutation testing in colorectal cancer." Arch Pathol Lab Med 134(8): 1225-8.
Shen, Z. X., G. Q. Chen, et al. (1997). "Use of arsenic trioxide (As2O3) in the treatment of acute promyelocytic leukemia (APL): II. Clinical efficacy and pharmacokinetics in relapsed patients." Blood 89(9): 3354-60.
Shen, Z. Y., J. Shen, et al. (2000). "The alteration of mitochondria is an early event of arsenic trioxide induced apoptosis in esophageal carcinoma cells." Int J Mol Med 5(2): 155-8.
Shih, A. H. and E. C. Holland (2006). "Notch signaling enhances nestin expression in gliomas." Neoplasia 8(12): 1072-82.
Shih Ie, M. and T. L. Wang (2007). "Notch signaling, gamma-secretase inhibitors, and cancer therapy." Cancer Res 67(5): 1879-82.
Sievert, A. J. and M. J. Fisher (2009). "Pediatric low-grade gliomas." J Child Neurol 24(11): 1397-408.
Sievert, A. J., E. M. Jackson, et al. (2009). "Duplication of 7q34 in pediatric low-grade astrocytomas detected by high-density single-nucleotide polymorphism-based genotype arrays results in a novel BRAF fusion gene." Brain Pathol 19(3): 449-58.
Slatter, T., J. Gifford-Garner, et al. (2010). "Pilocytic astrocytomas have telomere-associated promyelocytic leukemia bodies without alternatively lengthened telomeres." Am J Pathol 177(6): 2694-700.
Soeda, A., M. Park, et al. (2009). "Hypoxia promotes expansion of the CD133-positive glioma stem cells through activation of HIF-1alpha." Oncogene 28(45): 3949-59.
Song, X., Z. Chen, et al. (2010). "Abrogating HSP response augments cell death induced by As2O3 in glioma cell lines." Can J Neurol Sci 37(4): 504-11.

Stiehl, D. P., M. R. Bordoli, et al. "Non-canonical HIF-2alpha function drives autonomous breast cancer cell growth via an AREG-EGFR/ErbB4 autocrine loop." Oncogene 31(18): 2283-97.
Stuer, C., B. Vilz, et al. (2007). "Frequent recurrence and progression in pilocytic astrocytoma in adults." Cancer 110(12): 2799-808.
Stupp, R., W. P. Mason, et al. (2005). "Radiotherapy plus concomitant and adjuvant temozolomide for glioblastoma." N Engl J Med 352(10): 987-96.
Sun, H. and S. Zhang (2011). "Arsenic trioxide regulates the apoptosis of glioma cell and glioma stem cell via down-regulation of stem cell marker Sox2." Biochem Biophys Res Commun 410(3): 692-7.
Szeto, M. D., G. Chakraborty, et al. (2009). "Quantitative metrics of net proliferation and invasion link biological aggressiveness assessed by MRI with hypoxia assessed by FMISO-PET in newly diagnosed glioblastomas." Cancer Res 69(10): 4502-9.
Tabori, U. and J. S. Dome (2007). "Telomere biology of pediatric cancer." Cancer Invest 25(3): 197-208.
Tabori, U., B. Vukovic, et al. (2006). "The role of telomere maintenance in the spontaneous growth arrest of pediatric low-grade gliomas." Neoplasia 8(2): 136-42.
Takei, H., S. T. Yogeswaren, et al. (2008). "Expression of oligodendroglial differentiation markers in pilocytic astrocytomas identifies two clinical subsets and shows a significant correlation with proliferation index and progression free survival." J Neurooncol 86(2): 183-90.
Tamura, K., M. Aoyagi, et al. "Accumulation of CD133-positive glioma cells after high-dose irradiation by Gamma Knife surgery plus external beam radiation." J Neurosurg 113(2): 310-8.
Tchoghandjian, A., C. Fernandez, et al. (2009). "Pilocytic astrocytoma of the optic pathway: a tumour deriving from radial glia cells with a specific gene signature." Brain 132(Pt 6): 1523-35.
Thayer, S. P., M. P. di Magliano, et al. (2003). "Hedgehog is an early and late mediator of pancreatic cancer tumorigenesis." Nature 425(6960): 851-6.
Tian, Y., B. E. Rich, et al. (2011). "Detection of KIAA1549-BRAF fusion transcripts in formalin-fixed paraffin-embedded pediatric low-grade gliomas." J Mol Diagn 13(6): 669-77.
Tibbetts, K. M., R. J. Emnett, et al. (2009). "Histopathologic predictors of pilocytic astrocytoma event-free survival." Acta Neuropathol 117(6): 657-65.
Tihan, T., A. Ersen, et al. (2012). "Pathologic characteristics of pediatric intracranial pilocytic astrocytomas and their impact on outcome in 3 countries: a multi-institutional study." Am J Surg Pathol 36(1): 43-55.
Tihan, T., P. G. Fisher, et al. (1999). "Pediatric astrocytomas with monomorphous pilomyxoid features and a less favorable outcome." J Neuropathol Exp Neurol 58(10): 1061-8.
Ullah, M. S., A. J. Davies, et al. (2006). "The plasma membrane lactate transporter MCT4, but not MCT1, is up-regulated by hypoxia through a HIF-1alpha-dependent mechanism." J Biol Chem 281(14): 9030-7.
Vander Heiden, M. G., L. C. Cantley, et al. (2009). "Understanding the Warburg effect: the metabolic requirements of cell proliferation." Science 324(5930): 1029-33.

Verhaak, R. G., K. A. Hoadley, et al. (2010). "Integrated genomic analysis identifies clinically relevant subtypes of glioblastoma characterized by abnormalities in PDGFRA, IDH1, EGFR, and NF1." Cancer Cell 17(1): 98-110.
Visvader, J. E. and G. J. Lindeman (2008). "Cancer stem cells in solid tumours: accumulating evidence and unresolved questions." Nat Rev Cancer 8(10): 755-68.
Vordermark, D., T. Shibata, et al. (2001). "Green fluorescent protein is a suitable reporter of tumor hypoxia despite an oxygen requirement for chromophore formation." Neoplasia 3(6): 527-34.
Wang, J., T. P. Wakeman, et al. "Notch promotes radioresistance of glioma stem cells." Stem Cells 28(1): 17-28.
Wang, J., T. P. Wakeman, et al. (2010). "Notch promotes radioresistance of glioma stem cells." Stem Cells 28(1): 17-28.
Wang, Q., L. H. Li, et al. "HIF-1alpha up-regulates NDRG1 expression through binding to NDRG1 promoter, leading to proliferation of lung cancer A549 cells." Mol Biol Rep 40(5): 3723-9.
Warburg, O. (1956). "On respiratory impairment in cancer cells." Science 124(3215): 269-70.
Warburg, O. (1956). "On the origin of cancer cells." Science 123(3191): 309-14.
Warburg, O., F. Wind, et al. (1927). "The Metabolism of Tumors in the Body." J Gen Physiol 8(6): 519-30.
Warrington, N. M., B. M. Woerner, et al. (2007). "Spatiotemporal differences in CXCL12 expression and cyclic AMP underlie the unique pattern of optic glioma growth in neurofibromatosis type 1." Cancer research 67(18): 8588-95.
Wei, Y., D. Liu, et al. (2008). "Down-regulation of beta1,4GalT V at protein level contributes to arsenic trioxide-induced glioma cell apoptosis." Cancer Lett 267(1): 96-105.
Westerman, K. A., Z. Ao, et al. (2007). "Design of a trans protease lentiviral packaging system that produces high titer virus." Retrovirology 4: 96.
Westfall, S. D., S. Sachdev, et al. (2008). "Identification of oxygen-sensitive transcriptional programs in human embryonic stem cells." Stem Cells Dev 17(5): 869-81.
Wicha, M. S., S. Liu, et al. (2006). "Cancer stem cells: an old idea--a paradigm shift." Cancer Res 66(4): 1883-90; discussion 1895-6.
Wimmer, K., M. Eckart, et al. (2002). "Mutational and expression analysis of the NF1 gene argues against a role as tumor suppressor in sporadic pilocytic astrocytomas." Journal of neuropathology and experimental neurology 61(10): 896-902.
Wong, C. C., D. M. Gilkes, et al. "Hypoxia-inducible factor 1 is a master regulator of breast cancer metastatic niche formation." Proc Natl Acad Sci U S A 108(39): 16369-74.
Wong, C. C., H. Zhang, et al. "Inhibitors of hypoxia-inducible factor 1 block breast cancer metastatic niche formation and lung metastasis." J Mol Med (Berl) 90(7): 803-15.
Wong, K. K., Y. M. Chang, et al. (2005). "Expression analysis of juvenile pilocytic astrocytomas by oligonucleotide microarray reveals two potential subgroups." Cancer Res 65(1): 76-84.

Wu, J., Z. Ji, et al. "Arsenic trioxide depletes cancer stem-like cells and inhibits repopulation of neurosphere derived from glioblastoma by downregulation of Notch pathway." Toxicol Lett 220(1): 61-9.

Yang, D., F. Cao, et al. "Arsenic Trioxide Inhibits the Hedgehog Pathway Which Is Aberrantly Activated in Acute Promyelocytic Leukemia." Acta Haematol 130(4): 260-267.

Yu, J., H. Deshmukh, et al. (2009). "Alterations of BRAF and HIPK2 loci predominate in sporadic pilocytic astrocytoma." Neurology 73(19): 1526-31.

Zhang, K., J. Zhang, et al. (2012). "Wnt/beta-catenin signaling in glioma." J Neuroimmune Pharmacol 7(4): 740-9.

Zhang, X. P., G. Zheng, et al. (2008). "Notch activation promotes cell proliferation and the formation of neural stem cell-like colonies in human glioma cells." Mol Cell Biochem 307(1-2): 101-8.

Zhen, Y., S. Zhao, et al. "Arsenic trioxide-mediated Notch pathway inhibition depletes the cancer stem-like cell population in gliomas." Cancer Lett 292(1): 64-72.

Zhou, Y., T. Shingu, et al. (2011). "Metabolic alterations in highly tumorigenic glioblastoma cells: preference for hypoxia and high dependency on glycolysis." J Biol Chem 286(37): 32843-53.

Zhu, L. L., T. Zhao, et al. (2011). "Gene expression profiles and metabolic changes in embryonic neural progenitor cells under low oxygen." Cell Reprogram 13(2): 113-20.

**Kah Suan Lim**
101 East Mount Royal Avenue • Apt #305 • Baltimore, MD 21202
klim13@jhmi.edu • kahsuan.lim@gmail.com • 443-676-1646 **(C)**

## Education

**2008 – present:** **Ph.D candidate in Pathobiology, Johns Hopkins University School of Medicine, Baltimore, MD, USA**
**Laboratory of Dr. Charles G. Eberhart (MD, Ph.D)**

**2004 – 2008:** **Bachelor of Science (Honours) in Biological Sciences, Nanyang Technological University, Singapore. Honours Thesis Title: Profiling Liver Cancer Cell Lines for Sensitivity to Non-Selective FGFR Inhibitor, PD173074**

## Research Experience

**2008 – present:** **Ph.D candidate, Eberhart and Bar lab in the Department of Neuropathology, Johns Hopkins University School of Medicine, Baltimore, MD, USA**

- Role of novel KIAA1549-BRAF fusion in pediatric low-grade gliomas
- Role of oncogene-induced senescence in pediatric low-grade gliomas
- Study of tumor metabolism, specifically the role of MCT4 (monocarboxylate transporter 4) in glioblastoma

**2010:** **Translational Rotation 1** (short clinical rotation), shadowing neuropathologist Dr. Peter Burger and learning about how different brain tumors are diagnosed

**2011:** **Translational Rotation 2** (short clinical rotation), shadowing molecular pathologist Dr. James R. Eshleman, learning about how a clinical molecular diagnostics lab is run and how molecular biology is being used to diagnose different types of cancers

**2008 (June – Aug):** **Research assistant (intern) in the Singapore Oncogenome Project headed by Dr. Axel Ullrich, Institute of Medical Biology, A*Star, Singapore**

- Role of FGFR4 in hepatocellular carcinoma

**2007 (May – Aug):** **Research assistant (intern) in the LDX Lab, Institute of Molecular and Cellular Biology, A*STAR, Singapore**

- Role of DuSP1 in coronavirus infection by siRNA and shRNA knockdown studies

**2006 (Sept – Dec):** **Research assistant (intern) in the Rieseberg Lab, University of British Columbia, Vancouver, BC, Canada**

- Using molecular biology techniques to definitively prove hybridization between *Osmundas cinnamomea* and *Osmundas claytoniana*
- Possible oldest fern hybrid ever identified

**2006 (June – Aug): Research assistant (intern), Singapore Oncogenome Project headed by Dr. Axel Ullrich, Centre of Molecular Medicine, A*Star, Singapore**

- Gene sequencing and mutational analysis on clinical liver cancer samples

**Manuscripts and Publications**

- "Hypoxia-inducible factor 1α (HIF1α) promotes Notch activation and cellular invasion in uveal melanoma"
  (Submitted to Pigment Cell & Melanoma Research)
  Laura Asnaghi, Michael H. Lin, **Kah Suan Lim**, Kah Jing Lim, Murilo Wendeborn, Shannath L. Merbs, James T. Handa, Akrit Sodhi, Eli E. Bar, and Charles G. Eberhart

- "Inhibition Of Hedgehog, Notch And Stem Cell Properties In Glioblastoma Neurospheres By Arsenic Trioxide"
  (Under revision, Acta Neuropathologica Communications)
  Dacheng Ding*, **Kah Suan Lim***, Charles G. Eberhart (*equal contribution)

- "Inhibition of monocarboxylate transporter-4 depletes stem-like glioblastoma cells and inhibits HIF transcriptional response in a lactate-independent manner"
  (Accepted for publication in Oncogene)
  **Kah Suan Lim**, Kah Jing Lim, Brent A. Orr, Antoinette C. Price, Charles G. Eberhart, Eli E. Bar
  *Oncogene, in press, 2013*

- "Molecular Advances in Pediatric Low Grade Astrocytoma"
  Fausto Rodriguez, **Kah Suan Lim**, Daniel Bowers, Charles G. Eberhart
  *Annu. Rev. Pathol. Mech. Dis*. 2013. 8:361–79

- "BRAF Activation Induces Transformation and Then Senescence in Human Neural Stem Cells: A Pilocytic Astrocytoma Model"
  Eric H. Raabe, **Kah Suan Lim**, Julia M. Kim, Alan Meeker, Xing-gang Mao, Guido Nikkhah, Jarek Maciaczyk, Ulf Kahlert, Deepali Jain, Eli Bar, Kenneth J. Cohen, and Charles G. Eberhart
  *Clin Cancer Res* June 1, 2011 17(11):3590–3599

- "Fibroblast growth factor receptor 4 regulates proliferation, anti-apoptosis and alpha-fetoprotein secretion during hepatocellular carcinoma progression and represents a potential target for therapeutic intervention"
  Han Kiat Ho, Sharon Pok, Sylvia Streit, Jens E. Ruhe, Stefan Hart, **Kah Suan Lim**, Hooi Linn Loo, Myat Oo Aung, Seng Gee Lim, Axel Ullrich
  *J Hepatol* 2009;50:118–27

## Research Presentation

- "The Role of Senescence in Pilocytic Astrocytoma Pathogenesis"
  Short talk at Pathology Grand Rounds, June 2010
- "Novel KIAA1549-BRAF Fusion Involved in the Pathogenesis of Pilocytic Astrocytoma"
  Poster presentation at Pathology Young Investigators' Day 2010
- "Expression of Oncogene-Induced Senescence Markers in Pilocytic Astrocytoma is Associated with Longer Survival"
  Poster presentation at AACR 2011
- "Inhibition of MCT4 Preferentially Targets Stem-Like Cells in Glioblastoma"
  Poster presentation at Metabolism and Cancer conference 2011
- "Inhibition of MCT4 Targets Stem-Like Cells in Glioblastoma"
  Poster presentation at Pathology Young Investigators' Day 2012; Poster presentation at AACR 2012
- "Inhibition of MCT4 Targets Stem-Like Cells in Glioblastoma" (updated)
  Poster presentation at SNO 2012 (Society of Neuro-Oncology)
- "Silencing MCT4 inhibits GBM growth, HIF response and CD133-positive fraction in a lactate-independent fashion"
  Poster presentation at AACR 2013

## Teaching and Mentorship

**2010:** Teaching assistant for ***Pathology for Graduate Students: Basic Mechanisms***

**2011:** Teaching assistant for ***Grant Writing 101*** (for writing the top-scoring assignment grant in 2010)

**2011 – 2013:** Supervision and mentorship of undergraduate, Masters and Ph.D students performing experiments and interpreting results

## Awards

- Johns Hopkins University Fourteenth Annual Pathology Young Investigators' Day Award (2012):
  **Excellence in Translational Research** for poster
  "Inhibition of MCT4 Targets Stem-Like Cells in Glioblastoma"
- Johns Hopkins University Fifteenth Annual Pathology Young Investigators' Day Award (2013):
  **Excellence in Translational Research** for poster
  "Silencing MCT4 inhibits the HIF response and CD133-positive stem-like GBM cells in a lactate-independent fashion"

## Technical Proficiency

**Cell Biology:** Cell culture of adherent cells obtained from ATCC such as HEK293T, HUH7, HepG2, U87; cell culture of primary pilocytic astrocytoma and primary suspension neurospheres lines; generation of primary pilocytic astrocytoma and primary suspension neurosphere lines; lentivirus production; pharmacological treatment of cell lines; cell viability analysis by trypan blue, Alamar Blue/MTT/MTS colorimetric/fluorimetric assays; flow cytometry; immunohistochemistry; immunofluorescence; methylcellulose-based clonogenic assay; transwell invasion assay; cell culture in the hypoxic chamber; cellular transfection; viral transduction; intra and extracellular lactate measurement; senescence-associated beta-galactosidase staining in fixed cells

**Molecular Biology:** RNA and genomic DNA extraction; cDNA synthesis; quantitative real-time PCR; regular PCR; primer design; bacterial transformation; cloning; western blotting

**Computer Literacy:** Windows software (Excel, Word, Powerpoint, Adobe Illustrator, Graphpad Prism); Primer3 web-based primer design software; UCSC Genome Browser; NCBI Pubmed; Image J

## Languages

**English:** Native speaker; **Mandarin:** Fluent

## Membership

**AACR (American Association of Cancer Research)** Associate Member since 2010
**ASCO (American Society of Clinical Oncology)** Member since 2012